ABSTRACT

Title of Dissertation: **CHARACTERIZATION OF THE TYPE II ACTIVATED MACROPHAGE AND THE REGULATION OF HEPARIN BINDING EGF-LIKE GROWTH FACTOR.**

Justin Philip Edwards, Doctor of Philosophy, 2008

Directed By: Professor David M. Mosser
Department of Cell Biology and Molecular Genetics

Three populations of activated macrophages were generated in vitro and characterized each. These include the classically (Ca-MΦ), alternatively (AA-MΦ), and type II activated (MΦ-II) macrophages. Here, a side-by-side comparison of the three cell types is presented, focusing primarily on differences between MΦ-II and AA-MΦ, because both have previously been classified as M2 macrophages, distinct from Ca-MΦ. I show that MΦ-II are similar to Ca-MΦ in that MΦ-II and Ca-MΦ, but not AA-MΦ, produce high levels of NO and have low arginase activity. MΦ-II and Ca-MΦ express relatively high levels of CD86, whereas AA-MΦ are virtually devoid of this co-stimulatory molecule. Ca-MΦ and MΦ-II are efficient antigen presenting cells (APCs), whereas AA-MΦ fail to stimulate efficient T-cell proliferation. The differences between Ca-MΦ and MΦ-II are more subtle. Ca-MΦ produce IL-12/23 and give rise to Th1 cells when used as APCs. MΦ-II produce high levels of IL-10 and low IL-12 and thus give rise to Th2 cells secreting IL-4 and IL-10. I identify two

new markers for the MΦ-II, sphingosine kinase and LIGHT. Thus, classically, type II, and alternatively activated macrophages represent three distinct populations of cells with different biological functions.

The expression of Heparin-Binding Epidermal Growth Factor-like Growth Factor (HB-EGF) by MΦ-II is then characterized. HB-EGF has previously been associated with a number of physiological and pathological conditions, including tumor growth and angiogenesis. MΦ-II exhibit increased HB-EGF mRNA levels and protein secretion relative to resting and Ca-MΦ. HB-EGF induction is dependent upon the activation of the MAPKs ERK1/2 and p38. The transcription factor, Sp1, was recruited to 3 sites within the first 2kb of the HB-EGF promoter following stimulation, and the site located at -83/-54 was required for HB-EGF promoter activity. These regions of the promoter became more accessible to endonuclease activity following activation, and this accessibility was contingent upon activation of ERK. We show that several conditions which enhanced macrophage IL-10 production also resulted in HB-EGF induction, suggesting that these two genes may be coordinately regulated. These observations indicate that in addition to the secretion of the anti-inflammatory IL-10, another characteristic of MΦ-II is their production of angiogenic HB-EGF.

CHARACTERIZATION OF THE TYPE II ACTIVATED MACROPHAGE AND THE REGULATION OF HEPARIN BINDING EGF-LIKE GROWTH FACTOR

By

Justin Philip Edwards

Dissertation submitted to the Faculty of the Graduate School of the
University of Maryland, College Park, in partial fulfillment
of the requirements for the degree of
Doctor of Philosophy
2008

Advisory Committee:
Professor David M. Mosser, Chair
Professor Philip DeShong, Dean's Representative
Professor Daniel C. Stein
Assistant Professor Kenneth Frauwirth
Assistant Professor Volker Briken

DEDICATION

This dissertation is dedicated to my parents who have always been there for me. I love you guys!

ACKNOWLEDGEMENTS

First of all, I have to thank my parents and my brothers Brenton and Gareth for giving me all the love and support that I have needed through this arduous process. I would like to thank my brother, Gareth, for being there for me and talking me out to get my mind off of things when I had one of those "productive" weeks that I might as well have just stayed at home. I of course have to thank my parents for always telling me how proud they are of me and giving me the support and confidence that I needed.

I would of course like to thank everyone from my lab over the years. I would first like to thank Xia Zhang for his many good ideas and helping me with many of the technical aspects of my work. I would like to that Sean Conrad, Bryan Flemming, and Ricardo Gonçalves for not only being good friends, but also providing that much needed comic relief that we all need. I would like to thank my advisor, David Mosser, for taking in a 20 year-old "punk" kid into his lab in 2003 and for pushing me along when I needed to be pushed. I would like to thank Anne Field for being good friends over the years and being there to vent to whenever necessary. I would of course like to thank Suzanne Miles for being a great friend to me this whole time. She has put up with me and my moodiness on a regular basis and for that she is a saint.

I of course have to give a special thanks to my roommate Kevin who was had to deal with me and my erratic moods every day for the past three years and has been a great friend to me throughout.

TABLE OF CONTENTS

LIST OF TABLES

LIST OF FIGURES

LIST OF ABBREVIATIONS

AA-MΦ	Alternatively Activated Macrophage
ADAM	A Disintegrin and Metalloproteinase Domain
ADCC	Antibody Dependant Cell-Mediated Cytotoxicity
APC	Antigen Presenting Cell
Arg-1	Arginase-1
aTregs	Adaptive Regulatory T-cells
BCR	B-cell Receptor
βIG-H3	TGF-β-inducible gene-h3
BMMΦ	Bone Marrow Derived Macrophages
C/EBP	CCAAAT/enhancer-binding protein
Ca-MΦ	Classically Activated Macrophage
cAMP	Cyclic Adenosine Monophosphate
CARD	Caspase Recruitment Domain
CCR	Chemokine C-C Motif Receptor
CD	Cluster of Differentiation
Cdx22	Caudal type homeobox transcription factor 2
CFU	Colony forming units
ChIP	Chromatin Immunoprecipitation
CLS	Coffin-Lowry syndrome
c-MAF	Musculoaponeurotic fibrosarcoma oncogene homolog
Cox-2	Cyclooxygenase-2
CREB	cAMP responsive element binding protein
CTKD	C-terminus kinase domain
CTL	Cytotoxic T-Lymphocytes

DAI	DNA-dependent activator of IFN-regulatory factors
dB-cAMP	Dibutyryl cAMP
DC	Dendritic Cells
dsRNA	double-stranded Ribonucleic Acid
ECM	Extracellular matrix
EGF	Epidermal growth factor
EGFR	Epidermal growth factor receptor
E-IgG	IgG-opsonized erythrocyte
ELISA	Enzyme-Linked Immunosorbent Assay
EMSA	Electrophoretic mobility shift assay
ErbB	Epidermal growth factor receptor family
ERK	Extracellular signal-regulated kinases
FcR	Fc (fragment crystallizable region) Receptor
FITC	Fluorescein isothiocyanate
FIZZ1	Found in inflammatory zone-1
Foxp3	Forkhead box P3
GAPDH	Glyceraldehyde-3-phosphate dehydrogenase
GATA-3	GATA binding protein 3
GEO	Gene-expression omnibus
HB-EGF	Heparin-binding EGF-like Growth Factor
HIV	Human immunodeficiency virus
HMG-14	High-mobility group protein 14
HRP	Horseradish peroxidase
HSP	Heat Shock Protein
HVEM	Herpes virus entry mediator

IC	Immune complex
IFN	Interferon
IgG	Immunoglobulin G
iκB	Inhibitor of kappa B
IKK	IκB kinase
IL	Interleukin
iNOS	Inducible nitric oxide synthase
IRAK	Interleukin-1 receptor-associated kinase
IRF	Interferon regulatory factor
ITAM	Immunoreceptor Tyrosine-based Activation Motif
ITIM	Immunoreceptor Tyrosine-based Inhibitory Motif
Jak	Janus kinase
JNK	c-Jun N-terminal kinase
LDL	Low-density lipoprotein
LIGHT	Homologous to Lymphotoxins, shows inducible expression and competes with herpes simplex virus glycoprotein D for herpes virus entry mediator (HVEM)/TNF-related 2
LMW-HA	Low-molecular weight hyaluronic acid
LOX-1	Lectin-type oxidized LDL receptor 1
LPS	Lipopolysaccharide
LTA	Lipoteichoic acid
Ly6C	Lymphocyte antigen 6 complex
MAPK	Mitogen activated protein kinase
MCP-1	Monocyte chemotactic protein-1
M-CSF	Macrophage colony stimulating factor
MDA-5	Melanoma differentiation associated protein-5

MEK	MAP/ERK kinase kinase
MΦ-II	Type-II Activated Macrophage
MHC	Major histocompatibility complex
MK	MAPK activated protein kinase
MMP	Matrix metalloproteinase
MMR	Macrophage mannose receptor
MPO	Myeloperoxidase
MSK	Mitogen and stress activated protein kinase
MTT	1-(4,5-Dimethylthiazol-2-yl)-3,5-diphenylformazan
MyD88	Myeloid differentiation primary response gene 88
Myo-D	Myogenic differentiation
NADPH	Nicotinamide adenine dinucleotide phosphate
NF-κB	Nuclear Factor-κ B
NK Cells	Natural Killer Cells
NO	Nitric Oxide
NOD-LRR	Nucleotide binding oligimerization domain-leucine rich repeat
NTKD	N-terminus kinase domain
nTregs	Naturally occurring regulatory T-cells
OVA	Ovalbumin
OxLDL	Oxidized Low-density lipoprotein
PAMP	Pathogen associated molecular patterns
PBMC	Peripheral blood mononuclear cells
PCR	Polymerase chain reaction
PD-1	Programmed cell death 1
PDL-1	Programmed cell death ligand 1

PE	Phycoerythrin
PGE2	Prostaglandin E(2)
PI3K	Phosphoinositide 3-kinases
PKA	Protein kinase A
PKC	Protein kinase C
PKR	Protein kinase R
PLZF	Promyelocytic leukemia zinc-finger
PRR	Pattern recognition receptors
QRT-PCR	Quantitative Real-Time PCR
RACE	Rapid Amplification of cDNA Ends
RIG-I	Retinoic Acid Inducible Gene-1
RIP	Receptor interacting protein
RNI	Reactive Nitrogen Intermediates
ROI	Reactive Oxygen Intermediates
RSK	Ribosomal S6 Kinase
S10	Serine 10
SHIP	SH2-containing inositol phosphatase
siRNA	Small Interfering RNA
SMC	Smooth Muscle Cell
SOD	Superoxide Dismutase
SOS	Son of Sevenless
Sp1	Specificity protein 1
SPHK-1	Sphingosine Kinase-1
STAT	Signal Transducers and Activators of Transcription
SYK	Spleen tyrosine kinase

TAB1/2/3	TAK binding protein
TAK1	Transforming growth factor beta-activated kinase 1
TAM	Tumor Associated Macrophage
Tat	Transactivator
TBK	Tank-binding protein
TCR	T-cell Receptor
TdT	Terminal Deoxynucleotidyl Transferase
TGF-β	Transforming growth factor
Th	T-helper lymphocyte
TIR	Toll/Interleukin-1 receptor
TIRAP	TIR domain-containing adaptor protein
TLR	Toll-like receptor
TNF-α	Tumor necrosis factor
TPA	Tetradecanoyl phorbol acetate
TRAF	TNF receptor-associated factor
TRAM	Trif-related adaptor molecule
Treg	Regulatory T-cell
TRIF	Tir domain-containing adaptor inducing interferon-beta
Tyk2	Tyrosine Kinase 2
UTR	Untranslated region
VEGF	Vascular endothelial growth factor

CHAPTER 1: INTRODUCTION

Innate Immunity

Overview

The innate immune response is the first line of defense against potential pathogens. Unlike the adaptive immune response, defensive mechanisms mediated by cells of the innate immune response are at full potential before an encounter with an invading microbe. These responses are mediated primarily by neutrophils, dendritic cells, macrophages and natural killer (NK) cells. Oftentimes the initial innate immune response is sufficient to prevent infection and eliminate the invading microbe. If this is not the case, innate immunity works to initiate the adaptive immunity. Adaptive immune cells can in turn contribute to the initiation of the full repertoire of mechanisms of innate immunity. The cytokine interferon-γ (IFN-γ), for example, can be produced by both innate and adaptive immune cells and contribute to the full activation of macrophages. This in turn initiates the full repertoire of their microbicidal abilities. Futhermore, opsonization of invading microorganisms or their toxins by antibody, a product of B-cells, can mediate their phagocytosis and destruction by cells of the innate immune system. Therefore, although innate and adaptive immunity are thought of as two separate "arms" of the immune system, there is a high degree of codependence by which one can not fully function without the presence of the other.

Cells of innate immunity express a variety of receptors which allow them to efficiently discriminate between self and non-self. These receptors recognize structurally conserved motifs of microbes which are essential and thus cannot readily be discarded by

microbes. These structurally conserved elements are known as PAMPs, or pathogen associated molecular patterns, and are recognized by pattern recognition receptors (PRRs). These receptors include the mannose receptors, scavenger receptors, receptors for opsonins, mannose-binding lectin, receptors for chemotactic factors, and the signaling pattern-recognition receptors (PRRs), which will be discussed in detail below. PAMPs share several common features including that they are usually produced by microbes, but not the host. Additionally, PAMPs are usually vital for the microbial pathogen's survival or pathogenicity. Furthermore, these structures are usually shared by large classes of microbes and not specific pathogens. These include structural components of bacteria, such as lipopolysaccharide (LPS), or nucleic acids, such as the double stranded RNA (dsRNA) of some viruses.

The mannose receptor is a lectin found on macrophages that binds to terminal mannose and fucose residues found on microbial cell walls. Scavenger receptors bind anionic polymers and acetylated low-density lipoprotein[1]. Receptors for opsonins include the receptors for IgG (Fcγ-receptors), discussed in detail below, and the complement receptors. The complement receptors bind to activated or degraded portions of complement associated with microbes, notably fragments of the C3 protein[2]. Bacterial proteins initiate with N-formylmethionyl residues. Short peptides containing these residues serve as chemotactic factors to innate immune cells, especially NK cells. Binding to these receptors initiates a number of different effector functions, including phagocytosis, production of reactive nitrogen and reactive oxygen intermediates (RNI and ROI, discussed below) to kill phagocytosed microbes, release of cytokines,

chemotaxis, etc. The signaling PRRs, the Toll-like receptors (TLRs) and the cytoplasmic PRRs, are discussed in detail below.

Signalling Pattern-Recognition Receptors

One important element of innate immunity is a limited number of germline-encoded signaling pattern-recognition receptors (PRRs). There appear to be two main groups of these receptors, the toll-like receptors (TLRs) and the cytoplasmic PRRs.

The first group of these receptors, the TLRs, is expressed by many cells of the immune system, including macrophages and dendritic cells, as well as non-immune cells such as epithelial cells. Thirteen potential TLRs are now recognized, although the functions of some are currently not understood. TLRs 1, 2, 4, 5, 6, 10, and 11 are expressed on the cell surface while TLRs 3, 7, 8, and 9 are found almost exclusively in intracellular compartments such as endosomes[3]. The TLRs recognize a variety of microbial components, such as lipopolysaccharide (LPS, TLR4)[4], peptidoglycan (TLR2)[5], dsRNA (TLR3)[6], CpG-DNA (TLR9)[7], etc. It is important to note, however, that although TLRs recognize specific PAMPs, there can be a great deal of diversity in the TLR ligands for a specific TLR. TLR4, for example, not only binds LPS, but structurally unrelated molecules such as fungal mannan, the fusion protein of respiratory syncytial virus, fibrinogen, etc.[3] Mutations in toll like receptors render the host more susceptible to infection with the pathogen meant to be recognized. For example, TLR2 deficient mice are highly susceptible to infection with the gram positive bacteria *Streptococcus pneumoniae*[8].

The TLRs are very successful at detecting most potential pathogens at the cell surface or within endosomes, but they are ineffective at detecting pathogens that have invaded the cytosol. The NOD-LRR (nucleotide binding oligimerization domain-leucine rich repeat) proteins, which include the NOD and NALP proteins, and the CARD (caspase recruitment domain)-helicase proteins recognize bacterial and viral components, respectively. For example, NOD1 and NOD2 recognize different portions of bacterial peptidoglycan[9,10], whereas RIG-1 (retinoic-acid-inducible protein-1) and MDA-5 (melanoma differentiation associated gene 5) have been recognized as detectors of cytoplasmic dsRNA (viral dsRNA)[11,12]. Recently, the factor DAI (DNA-dependent activator of IFN-regulatory factors), which belongs to neither the NOD-LRR nor the CARD-helicase protein families, has been recognized as the cytoplasmic detector of dsDNA[13]. A list of known PRRs and select list of their associated ligands is present in table 1.

It is important to note, however, that the TLRs also recognize some host-derived antigens in addition to microbial antigens. Most of these antigens are released a result of injury, cell death, or inflammation. This includes extracellular matrix (ECM) components, heat shock proteins (HSP), and host-derived nucleic acids[14].

Although differing in the specific signaling pathways derived from ligand binding, the pattern-recognition receptors, in general, converge to activate similar factors downstream. This includes activation of the mitogen activated protein kinases (MAPK), nuclear factor-κ B (NF-κB), and the interferon regulatory factors (IRF), which results in the production of inflammatory cytokines and type I interferons (IFN-α/IFN-β). TLR4 specifically activates two separate, yet intertwining pathways known as the MyD88-

Pattern-Recognition Receptor	Known Ligands
TLR1	Triacyl lipopeptides
TLR2	Lipoproteins, Lipoteichoic Acid, Porins, Zymosan, Lipoarabinomannan, Phospholipomannan, tGP1-mutin, Hemaglutinin protein
TLR3	dsRNA
TLR4	Lipopolysaccharide, Mannan, Glycoinositolphospholipids, Viral Envelope Proteins, Heat Shock Proteins, Fibrinogens, Hyaluronic Acid, Heparin Sulfate, β-defensin 2, HMGB-1, Surficant Protein-A, gp96
TLR5	Flagellin
TLR6	Lipoproteins, Lipoteichoic Acid, Zymosan
TLR7	ssRNA, Imidazoquinoline (synthetic compound), Loxoribine (synthetic compound), Bropirimine (synthetic compound)
TLR8	ssRNA
TLR9	CpG-DNA, Hemozoin
TLR11	profilin-like protein
NOD1	Cytoplasmic γ-D-glutamyl-meso-diaminopimelic acic (iE-DAP of peptidoglycan)
NOD2	Cytoplasmic Muramyl dipeptide (MDP of peptidoglycan)
MDA-5	Cytoplasmic dsRNA
NAIP5	Cytoplasmic *L. pneumophila* (specific ligand unknown)
NALP-3	Cytoplasmic Bacterial RNA, ATP, Uric Acid Crystals
RIG-1	Cytoplasmic dsRNA
DAI	Cytoplasmic dsDNA

Table 1: Pattern-Recognition Receptors (PRRs). PRRs and a selection of known endogenous and exogenous ligands.

dependant and MyD88-independent pathways (Figure 1). Activation of TLR4 leads to the activation of several adaptor proteins through the interaction with its intracellular TIR domain. Activation of TRAM leads to the activation of MyD88-independent pathways, while the activation of TIRAP and MyD88 leads to the activation of MyD88 dependant pathways. Activation of MyD88 subsequently leads to the activation of IRAK4, which dissociates and activates TRAF6. TRAF6 forms a complex to form an active polyubiquitin ligase, which through ubiquitination activates the MAP3K TAK1. TAK1 forms a complex with TAB1/2/3 to activate the MAPK (mitogen activated protein kinase) pathways. TRAF6 can additionally lead to the activation of NF-κB through the activation of the IKK complex[15].The MyD88-independent pathways, as mentioned above, are mediated through the adaptor TRAM, which in turn activates TRIF. TRIF activates RIP, which in turn activates the IKK complex, leading to the phosphorylation and subsequent degradation of IκB, the inhibitory subunit of NF-κB. NF-κB, free of its inhibitory subunit, is then able to translocate into the nucleus. TRIF also initiates the activation of the interferon regulatory factors, which is mediated by the TBK1/IKKi complex[15].

Fcγ-Receptors

One mechanism by which antibody is able to regulate immune responses is through the interaction with the Fc-receptors. Specifically, IgG antibodies interact with Fcγ-receptors (FcγRs) of which there are four classes, FcγRI, FcγRII, FcγRIII, and FcγRIV. In mice there are four known Fc-receptors, the high affinity FcγRI and the low affinity FcγRIIb, FcγRIII, and FcγRIV. All the FcγRs, except FcγRIIb, signal through an accessory immunoreceptor tyrosine based activating motif (ITAM)-containing γ-chain,

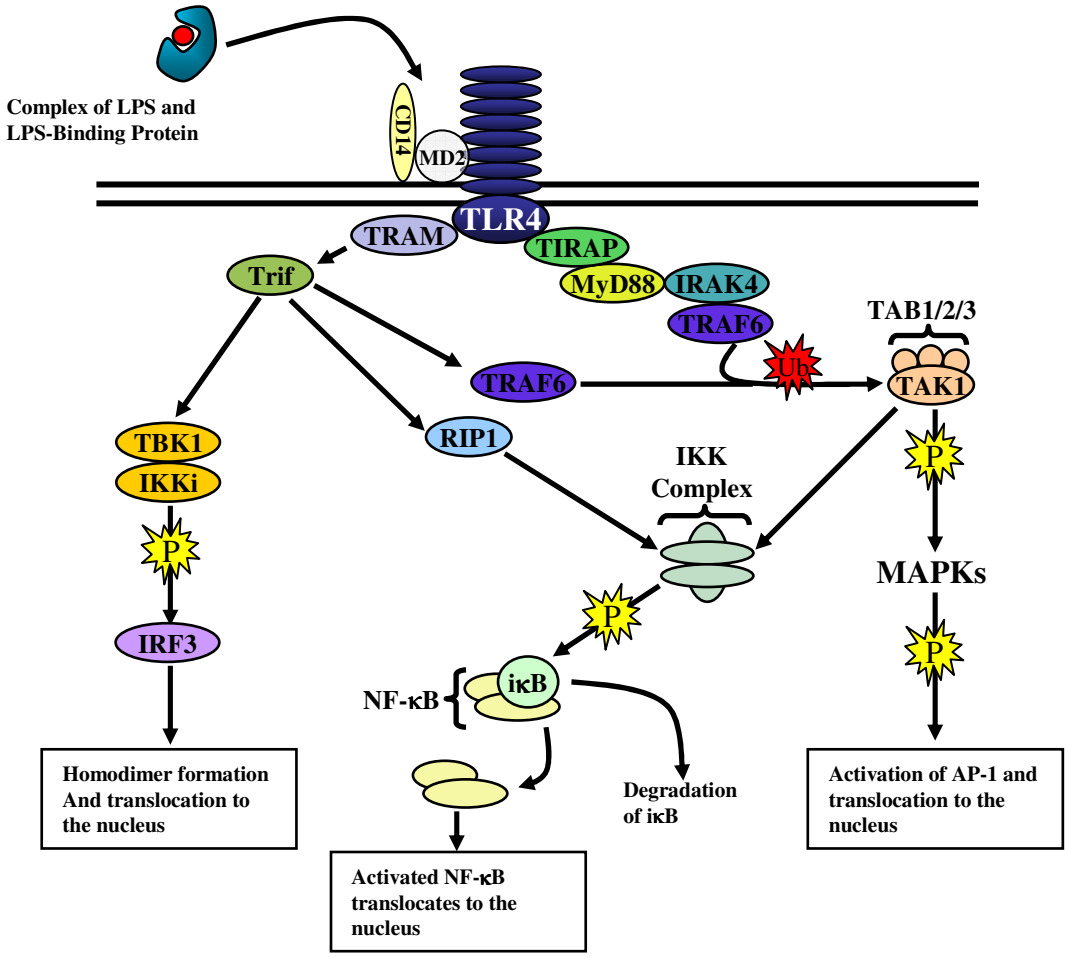

Figure 1: Toll-like receptor 4 (TLR4) mediated signaling pathways.
The LPS/LPS binding protein (LBP) complex interacts with the LPS coreceptors CD14 and MD2, leading to the activation of TLR4. Activation of TLR4 initiates a series of MyD88-dependant and MyD88-independent signaling pathways, ultimately leading to the activation of the interferon response factors (IRFs), nuclear factor-κ B (NF-κB), and the mitogen activated protein kinases (MAPK). This drives the production of inflammatory cytokines and type I interferons (IFN-α/IFN-β).

and thus are termed activating FcγRs. Signals arising from the cross-linking of the activating FcγRs are negatively regulated by the inhibitory FcγRIIb, whose cytoplasmic domain contains an immunoreceptor tyrosine based inhibitory motif (ITIM). Most innate immune effector cells express both activating and inhibitory FcγRs, whereas NK cells express only the activating FcγRIII and B cells express only the inhibitory FcγRIIb[16,17].

Crosslinking of the activating FcγRs by immune complexes induces the phosphorylation of the ITAMs of the γ-chain by Src family kinases, which recruits and activates SYK. This directly activates a number of signal transduction molecules including Phosphoinositide 3-kinase (PI3K) and the guanine nucleotide exchange factor SOS (son of sevenless homolog). This results in the activation of a number of downstream signaling pathways, including the MAPKs and calcium dependant signaling pathways (Figure 2). Activation mediates a number of critical immune functions, including ADCC (antibody dependant cell-mediated cytotoxicity), phagocytosis, cytokine release, and the oxidative burst. Crosslinking of the inhibitory FcγRIIb induces the phosphorylation of the ITIM on its cytoplasmic tail, which recruits the phosphatase SHIP. The activation of SHIP interferes with signals generated by the activating FcγRs though hydrolysis of phosphoinositide intermediates generated by PI3K. Taken together, expression of the inhibitory FcγRs with the activating FcγRs controls excessive activation of the aforementioned functions[16,17].

FcγRI, the high affinity Fcγ-receptor, binds monomeric IgG. In the human system, this receptor binds IgG1 and IgG3 tightly, while in the mouse, IgG2a and IgG2b are tightly bound. Unlike the other activating Fcγ-receptors, this receptor is constantly saturated with monomeric IgG and therefore the role of this receptor in binding immune

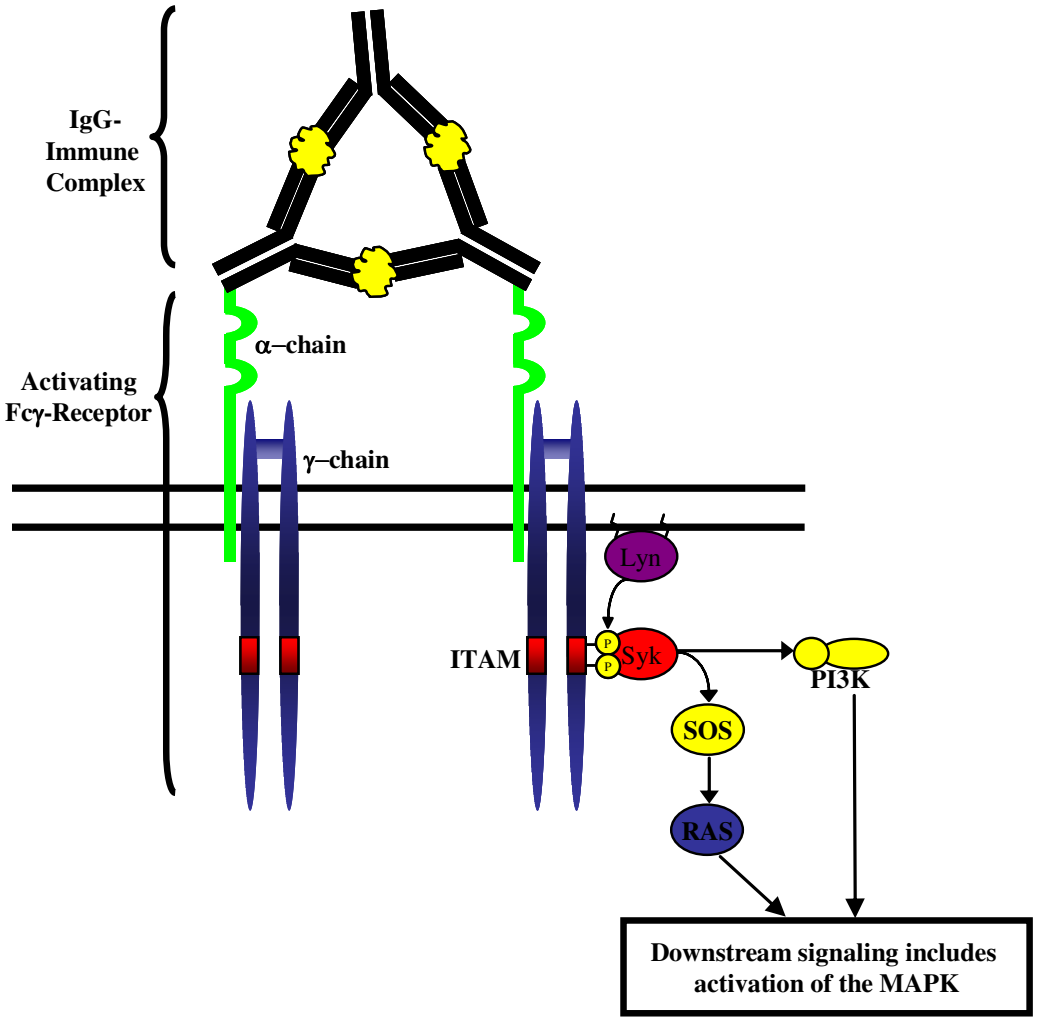

Figure 2: Activating Fc-γ Receptors.
Crosslinking of the activating Fc-γ receptors by the presence of IgG-immune complexes results in phosphorylation of the immunoreceptor tyrosine-based activation motif (ITAM) by a Src-family kinase (i.e. Lyn). Phosphorylated ITAMs recruit Syk through its SH2 domain, which is then activated and in turn activates a number of downstream signaling pathways through the activation of SOS (Son of Sevenless) and PI3K (phosphoinositide 3-kinase).

complexes is questioned. FcγRII and FcγRIII, also known as CD32 and CD16, respectively, are low affinity receptors which bind poorly, if at all, to monomeric IgG, but can bind to IgG immune complexes[17]. The recently discovered FcγRIV, whose expression is restricted to myeloid cells, binds exclusively to IgG2a and IgG2b[18].

Reactive Oxygen Intermediates and Reactive Nitrogen Intermediates

Activated macrophages have a number of mechanisms by which phagocytosed microbes are killed. Two important mechanisms are the generation of reactive oxygen intermediates (ROI) and reactive nitrogen intermediates (RNI). Generation of ROI is mediated by the multisubunit NADPH oxidase. Activation triggers translocation of cytosolic proteins to the membrane associated complex carrying cytochrome C. Activation is triggered by a number of stimuli, including microbial products, IFN-γ, IL-8, and FcγR crosslinking by IgG immune complexes. The reaction catalyzed by the NADPH oxidase generates superoxide (O_2^-). The primary ROI superoxide can be converted to a number of other reactive products, including H_2O_2 by SOD (superoxide dismutase), hydroxyl radicals, hydroxyl anions, and to hypochlorous acid and chloramines by MPO (myeloperoxidase)[19].

Reactive nitrogen intermediates are generated by nitric oxide synthases (NOSs). NOSs convert L-arginine to L-citrulline and nitric oxide (NO). The intermediate product in this reaction, L-hydroxy-arginine, inhibits the opposing enzyme Arginase, discussed below[20]. The macrophage NOS, also known as inducible NOS (iNOS), is absent in resting cells. Its expression is regulated by a number of cytokines and microbial products. ROI and NO can combine to form peroxynitrite and other RNI. Nitric oxide reacts with

SH-groups of free cysteine or cysteine associated with proteins or peptides, resulting in S-nitrosothiols[19]. This can have an adverse affect on microbial proteins. For example, NO inactivates the Coxsackievirus cysteine protease 3C by S-nitrosylation of the cysteine residue in the active site, resulting in the disruption of the viral life cycle [21].

Adaptive Immunity

Overview

Unlike the innate immune response, the adaptive immune response mediates recognition of specific antigens and not conserved motifs found on many potential pathogens. This is mediated by germline rearrangements of the antigen receptors for B and T lymphocytes, called the B-cell receptor and T-cell receptor (BCR and TCR), respectively. This allows for both antigen specificity as well as a great deal of diversity in the receptor repertoire. The power of adaptive immunity is immunological memory, which allows for changes in both the quality and quantity of the response upon reexposure to antigen. There are two types of adaptive immune responses, humoral and cell-mediated. These are mediated primarily by the B-cells and T-cells, respectively, and each eliminates different categories of organisms. Cell-mediated immunity is primarily generated against intracellular microbes, which survive and proliferate inside host cells. Cell mediated immunity leads to the destruction of the microbes or lysis of the infected cells. Humoral immunity is generated in response to extracellular microbes and their toxins. This is mediated by antibodies in the blood, the product of B lymphocytes. Antibodies specifically bind to antigens and neutralize their activity or target them for elimination by other effector mechanisms, such as complement and phagocytosis. The

focus below is antigen presentation to T-lymphocytes and sub-populations of T-lymphocytes.

T cells and Antigen Presentation to T-cells

Mature T cells are first divided into subsets based on their exclusive expression of either CD4 or CD8. The subsets are referred to as $CD4^+$ helper or regulatory T cells and $CD8^+$ cytotoxic T cells. CD4 or CD8 positivity defines which MHC complex can interact with the T cell. $CD4^+$ T cells are restricted to interaction with the MHC class II, while $CD8^+$ T cells are restricted to MHC class I. $CD8^+$ T cells mature into cytotoxic T lymphocytes (CTLs), which function in the lysis of pathogen infected cells. CTLs release lytic granules containing perforin, granzymes, and granulysin, all of which contribute to the destruction of targeted cells. $CD4^+$ T cells are further divided into distinct subsets based on their function and cytokine production, which is the focus below. These cells regulate the humoral and cell mediated immune responses. Naïve $CD4^+$ T cells are activated by antigen presenting cells though the primary signal of the antigen specific T cell receptor (TCR) and CD4 interacting with peptide bearing MHC class II on the APC. This must be combined with a costimulatory signal of B7.1/B7.2 (CD80/CD86) interacting with CD28 on the surface of the T cell. Without this secondary signal the T cell goes into a state on non-responsiveness called anergy.

There are a several distinct populations of $CD4^+$ T cells, which include both the "helper" T cell (Th) populations as well as the regulatory T cell populations (Tregs) (Figure 3). Currently there are three populations of Th cells recognized, and these are known as Th1, Th2, and Th17 cells. Th1 differentiation is the result of coordinate

signaling through the TCR and STAT1-associated cytokine receptors (i.e. IFN-γ), resulting in the upregulation of the master regulator of Th1 differentiation, the transcription factor T-bet[22]. T-bet drives expression of IFN-γ and the IL-12 receptor. Expression of the IL-12 receptor allows for IL-12 sensitivity, activating STAT4 which enhances IFN-γ expression and potentiates Th1 differentiation. Th2 differentiation is initiated by TCR signaling in combination with IL-4 receptor signaling through STAT6, resulting in the expression of the transcription factor GATA-3, the master regulator of Th2 differentiation[23]. GATA-3 enhances its own expression while driving epigenetic modifications to the Th2 gene cluster for the cytokines IL-4, IL-5, and IL-13[24,25]. Additionally, GATA-3 suppresses factors critical for Th1 differentiation, such as STAT4 and the IL-12Rβ2 chain[26].

Although the specific helper subsets are not exclusively present during an immune response, Th1 versus Th2 cells do generally play specific roles during an effective immune response. Th1 responses are generally thought to help in the clearance of intracellular pathogens. For example, their production of IFN-γ aids in the activation process of macrophages and strongly enhances their microbicidal effector functions. Conversely, Th2 can function in the control and clearance of extracellular pathogens.

Unchecked Th1 differentiation was until recently believed to be the cause of chronic inflammation, such as what is seen in the experimental models of autoimmunity, experimental autoimmune encephalitis or collagen induced arthritis. This was based on the fact that IL-12p40$^{-/-}$ mice proved to be resistant to these pathologies[27]. Once it was discovered that the cytokine IL-23 uses the p40 subunit as well as the IL-23 specific subunit p19 that these studies needed to be reassessed[28]. Using IL-23p19 and IL-12p35

specific knockouts it was found that these pathologies were dependant on IL-23 and the IL-17 secreting T-cells, known as Th17 cells. The development of Th17 cells, however, is not dependant upon IL-23. IL-23 is able to drive IL-17 expression from memory populations, but not from naïve T-cells. Instead, the Th17 lineage is critically dependant upon TGF-β, proposed to be from a population of regulatory T-cells, as well as IL-6 from activated antigen presenting cells. Activation in the presence of these factors upregulates the IL-23 receptor, allowing for IL-23 responsiveness and thus potentiation of the Th17 phenotype[29].

The regulatory population of $CD4^+$ cells also has several functionally distinct populations. There appears to be at least three different Treg populations, including the naturally occurring Tregs (nTregs) and two populations of adaptive or induced Tregs (aTregs). The nTregs develop intrathymically and are characterized by expression of the transcription factor Foxp3 (forkhead box P3) and contact dependant suppression of effecter T-cell development. They appear to suppress effector $CD4^+$ T cell development before it begins and are important for controlling autoimmunity. In contrast, aTregs are distinguished from nTregs by their differentiation from naive $CD4^+$ T cells in the periphery. They appear to develop in parallel to effector T cells to control effector T cell-driven inflammation. There appears to be at least two populations of aTregs. The first, the Tr1 cells arise in response to IL-10 exposure and suppress through high expression of IL-10. The second type, like the nTregs, expresses the transcription factor Foxp3. These are driven by exposure to TGF-β and are characterized by their expression of TGF-β[29]. An overview of the populations of $CD4^+$ T-lymphocytes is present in Figure 3.

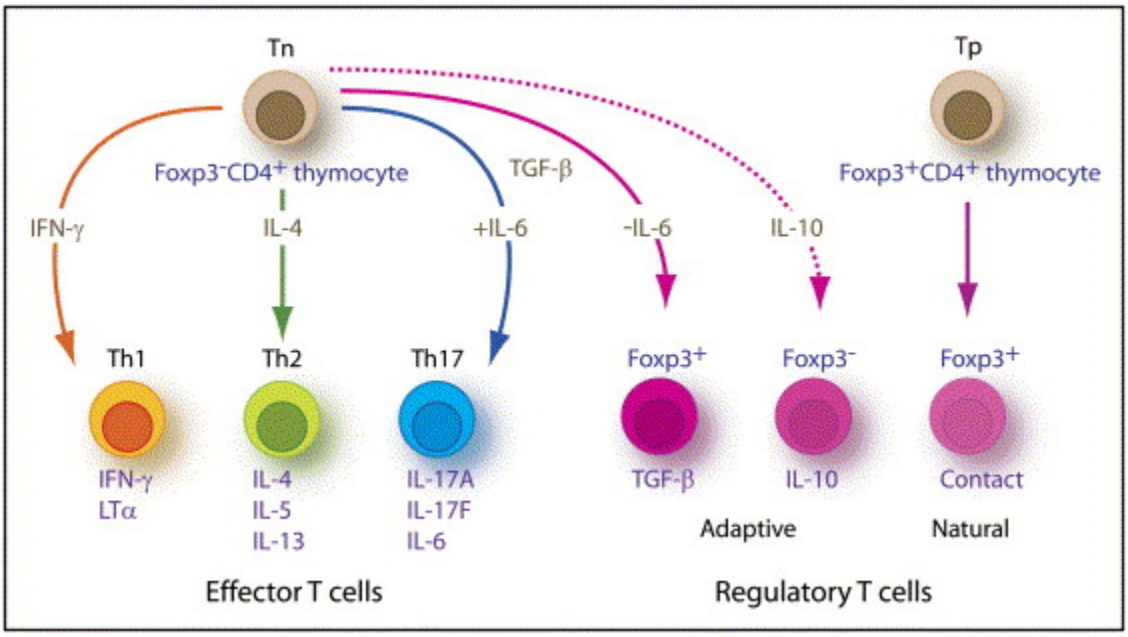

Figure 3: Populations of CD4+ T-lymphocytes.
It was originally believed that $CD4^+$ T-cells could either differentiate into IFN-γ secreting Th1 cells or IL-4 secreting Th2 cells, it is now widely believed that they can differentiate into IL-17 secreting Th17 cells as well as regulatory T-cell populations depending on specific cytokine signals. Figure reproduced with permission from Elsevier. Copyright 2006. [29]

Cytokines

Overview

Cytokines are proteins secreted by the cells of the innate and adaptive immune response that mediate many of the effects of these cells. Most cytokines have both local and systemic effects, having autocrine, paracrine, and endocrine activity. Despite the fact that cytokines have diverse biological activities, they share several general properties in their influence on the immune system, in that they have pleiotropic, redundant, antagonistic, and synergistic properties. The pleiotropic property imparts their ability to have diverse biological functions. For example, tumor necrosis factor (TNF)-α's autocrine activity helps to activate macrophages whereas its endocrine activity can influence cells of the hypothalamus to induce fever. The redundant property allows several cytokines to have the same or similar biological effects, for instance both interleukin (IL)-4 and IL-13 drive alternative activation of macrophages (see below). Cytokines can have both synergistic properties, in the case of TNF-α and IFN-γ which when combined can activate macrophages, and antagonistic properties, in the case of IFN-γ and IL-10 which activate and inhibit activation of macrophages, respectively. These properties allow the effects of cytokines to be amplified, but also tightly controlled.

During classical macrophage activation, as will be discussed, a number of important inflammatory cytokines are produced, including IL-1, IL-6, IL-12, IL-23, and TNF-α as well as low levels of the anti-inflammatory cytokine IL-10. Of these, IL-12, IL-23, and IL-10, are discussed in detail below.

IL-12

IL-12 is an important inflammatory cytokine produced primarily by dendritic cells and macrophages in response to stimulation with microbes or their products. It was originally identified in the supernatants of a human B-cell line infected with Epstein-Barr virus which had profound effects on natural killer (NK) and T-cells[30]. IL-12 is a heterodimeric cytokine consisting of a p40 subunit (IL-12α, 40kd) and p35 (IL-12β, 35kd). IL-23 is an IL-12 family member which shares the p40 subunit. The heterodimer, known as IL-12p70, binds to the IL-12 receptor which consists of IL-12Rβ1 and IL-12β2, expressed mainly by activated T-cells and NK cells. Once activated by the binding of IL-12p70, the IL-12R activates the JAKs TYK2 and JAK2, which are constitutively associated with IL-12Rβ1 and IL-12Rβ2, respectively. Activated Tyk2/Jak2 activate a number of the STATs, primarily STAT4, which drives most of the effects of IL-12. The p40 subunit is generally made in much higher concentrations than the p35 subunit or p19, the IL-23 equivalent. As a result, p40 is often secreted as a monomer or homodimer. In mice, but not humans, this homodimer has been shown to have an affinity for the IL-12 receptor comparable to that of the heterodimer, despite the lack of biological activity[31]. Therefore, in some setting p40 homodimers can inhibit the activity of p70.

In general, activation of the TLR pathway is not sufficient to drive high levels of IL-12 production from macrophages. The presence of IFN-γ, coming primarily from Th1 cells or NK cells, enhances the production of both subunits, thus increasing overall biologically active p70[32]. T-cells also enhance IL-12 production though interaction of surface associated CD40L with CD40 of macrophages or dendritic cells[33].

IL-12 production is negatively regulated by a number of conditions. This includes stimulation with the potent anti-inflammatory cytokine IL-10 and transforming growth factor (TGF)-β. Additionally, activation of a number of G-protein coupled receptors, such as EP2/EP4 (via treatment with prostaglandin E-2), α2-adrenergic, adenosine A2a, etc., can suppress IL-12. This has been found to be primarily due to increased levels of cyclic AMP[31].

The primary function of IL-12 is to drive Th1 responses during T-cell activation. Activation of naïve $CD4^+$ T-cells drives the upregulation of IL-12R. Stimulation with IL-12 at this time drives the production of several cytokines, especially IFN-γ. This IFN-γ can then in turn help to further enhance the secretion of biologically active IL-12, thus driving a powerful positive feedback mechanism and commitment of $CD4^+$ T-cells to the Th1 cell lineage[31].

IL-23

IL-23, as mentioned above, is a structurally related cytokine to IL-12. It shares the p40 subunit with IL-12, which combines with the p19 subunit to form the physiologically active IL-23. In addition to sharing a subunit, the receptor consists of IL-12βR1 and IL-23 specific IL-23R. IL-23 has been shown to be essential for expansion of a population of $CD4^+$ cells, the Th17 cells, discussed above[34].

IFN-γ

IFN-γ was originally identified in 1965 in the culture supernatants of phytohemagglutinin activated human leukocytes and was found to have antiviral

activity[35]. IFN-γ is produced primarily by NK cells, $CD8^+$ T-cells, and $CD4^+$ Th1 cells. Biologically active IFN-γ is a noncovalent homodimer which binds to the IFN-γ receptor (IFNGR), which consists of a high affinity ligand-binding α-chain (IFNGR1) and a signaling β-chain (IFNGR2). Binding to the receptor activates the Jak/Stat pathway, activating Jak1 and Jak2, which are constitutively associated with the α-chain and β-chain, respectively, and Stat1[36].

The main function of IFN-γ is to promote cell-mediated immunity against intracellular pathogens. IFN-γ aids in the activation process of macrophages and strongly enhances their microbicidal effector functions. One mechanism is by inducing the production of reactive oxygen species (ROS) and reactive nitrogen intermediates (RNI) by macrophages. IFN-γ induces the production of RNI primarily by upregulating the inducible nitric oxide synthase (iNOS) as well upregulating the synthesis of the L-arginine substrate and tetrahydrobiopterin cofactor. IFN-γ drives ROS production by up-regulation of $gp91^{phox}$ and $p67^{phox}$, two components of the NADPH oxidase complex. IFN-γ also drives tryptophan depletion, primarily an antiparasitic mechanism, by generating N-formylkynurenine from free tryptophan via IDO. Another mechanism is the induction of the antiviral enzyme protein kinase R (PKR), which when activated by dsRNA inhibits the activity of eIF-2α, a factor involved in translation of cellular and viral RNAs. Another important function of IFN-γ is improvement of the antigen presenting function by enhancing antigen processing as well as presentation to T-cells by upregulation of MHC class I and class II[37]. Overall, the net effect of IFN-γ is to make macrophages much more efficient in their innate microbicidal functions and their contribution to the adaptive immune response. As a result, deficiencies in IFN-γ or IFN-γ

signaling render the host particularly susceptible to intracellular bacterial, parasitic, and viral infections, such *Mycobacteria*[38], *Leishmania*[39], and vaccinia virus[40].

IL-10

IL-10 is a potent anti-inflammatory cytokine produced by many cells of the immune system, including macrophages, helper T cells, regulatory T cells, mast cells, and eosinophils. It was originally known as "cytokine synthesis inhibitory factor" due to its ability to suppress Th1 cell function by Th2 cells[41]. Functional IL-10 forms a non-covalent homodimer that binds to the ligand binding subunit of the IL-10 receptor (IL-10Rα). IL-10Rα associates with IL-10Rβ, the signaling subunit. Lacking either subunit renders cells refractory to the effects of IL-10. Binding triggers activation of the Jak/STAT pathway, utilizing Jak1/Tyk2 and primarily Stat3. Stat1 and Stat5 (in non-macrophage cells) have also been implicated[42].

Although IL-10 was originally identified as a cytokine produced by Th2 helper T cells, it is known to be produced by a number of T cell subsets. IL-10 has been found to be produced by IFN-γ producing Th1 cells in response to *Toxoplasma gondii* [43] and infection with NIH/Sd strain *Leishmania major*[44]. It is believed that the production of IL-10 in these systems is to moderate what could potentially be an excessive inflammatory response and thus limit damage to the host. IL-10 is also produced by a population of regulatory T-cells. This population of cells seems to arise in response to repeated administration of antigen in conditions promoting T-cell anergy. These Treg cells are able to block proliferation of naïve cells in an IL-10 dependant manner[45].

IL-10 essentially "deactivates" macrophages and makes them refractory to activating stimuli. IL-10 inhibits most cytokine and chemokine secretion by activated macrophages. These include the inflammatory cytokines IL-1, IL-6, IL-12, and TNF, as well as anti-inflammatory IL-10 itself. IL-10 also down-regulates Cox-2, the enzyme responsible for prostaglandin E(2) synthesis. Additionally, IL-10 up-regulates antagonists of inflammatory cytokine function, such as IL-1 receptor antagonist and soluble TNF receptor[42]. It is important to note, however, that IL-10 is typically made by macrophages late after activation and in relatively low quantities and therefore is thought to control excessive inflammation.

In addition to blocking the production of secreted factors, IL-10 affects surface associated proteins of macrophages. Importantly, IL-10 blocks the antigen-presenting cell (APC) function of macrophages by driving the downregulation of major histocompatibility complex class-II (MHC class II) and the costimulatory molecules B7.1 and B7.2, which are both required for the activation of naïve T-cells. However, IL-10 drives the upregulation of macrophage Fcγ receptors CD16 and CD64, the low and high affinity FcγRIII and FcγRI, respectively. This allows for enhanced uptake of opsonized particles or potential pathogens. This is contrast to the decreased ability to dispose of potential pathogens due to suppressed respiratory burst associated with macrophage activation[42].

The Role of IL-10 in the maintenance of homeostasis and disease

The importance of IL-10 in the maintenance of homeostasis is best observed in the model of the IL-10 knockout (IL-$10^{-/-}$) mouse. In a model of endotoxic shock, IL-$10^{-/-}$

mice succumbed to lethal endotoxemia at a far lower concentration of LPS, which was associated with uncontrolled production of TNF[46]. Additionally, IL-10$^{-/-}$ mice spontaneously develop mucosal inflammation in response to enteric flora. Conventionally housed mice develop severe disease with lesions affecting both the upper and lower gastrointestinal (GI) tract, while mice housed in specific pathogen free conditions develop more mild disease restricted to the colon. Lesions within the GI tract contain large numbers of inflammatory cells, including macrophages, B-cells, and CD4$^+$ T-cells with abnormally high levels of the inflammatory cytokines IL-1, IL-6, IL-12 and TNF. T-cells within lesions were dominantly Th1 cells producing high levels of IFN-γ, which when transferred to T-cell deficient mice were capable of driving the development of colitis[47].

There is clear evidence that manipulation of IL-10 cytokine levels has a profound effect of the outcome of infectious diseases. In many instances, in susceptible models of infection, production of IL-10 allows for persistence of infection. In models where IL-10 has been manipulated though use of an IL-10 knockout or a neutralizing antibody to IL-10, oftentimes there is enhanced disease resistance. Conversely, when IL-10 levels are increased by use of recombinant IL-10 or a transgenic pathogen, there is enhanced disease susceptibility[42]. Manipulation of IL-10 by these methods showing these effects has been shown for a number of diseases, including infection with the bacteria *Listeria monocytogenes*[48,49], *Streptococcus pneumonia*[50], *Mycobacterium bovis* (BCG)[51,52], the fungus *Candida albicans*[53,54], and the protozoa *Leishmania major*[55,56].

In the case of leishmaniasis, however, it appears that the manipulation of IL-10 levels is more complicated. In susceptible mouse models of cutaneous leishmaniasis, the

production of IL-10 plays a detrimental role by promoting disease progression. Infection of IL-$10^{-/-}$ mice on a normally susceptible background results in relative resistance to disease progression[55]. IL-10 produced from macrophages due to the presence of opsonized parasites allows for dramatic enhancement of parasite intracellular survival[55,56]. However, in healing models of infection, the presence of IL-10 secreting regulatory T-cells is thought to sustain immunity to reinfection by allowing for antigen persistance. IL-10, in this case, controls complete eradication of parasites driven by effector T-cells. Infection of IL-10 knockout mice that are on normally resistant background results in sterile clearance of the parasite[57]. Complete clearance, however, results in loss of immunity to reinfection, indicating that the equilibrium established between effector and regulatory T cells allows for control of initial infection while promoting resistance to reinfection[57]. This observation, however, is considered controversial.

In general, IL-10 is important for establishing equilibrium between protective and detrimental inflammatory responses. IL-10 may control the absolute effectiveness of anti-pathogen responses, but at the same time it is limiting potentially significant and irreparable damage to the host.

Monocyte and Macrophage Heterogeneity and Macrophage Development

Overview

Macrophages are specialized immune cells, which contribute primarily to innate immunity and serve as a bridge to adaptive immunity. Macrophages develop from circulating peripheral blood mononuclear cells (PBMCs) after migration into tissues

during homeostasis or in response to inflammatory stimuli. Monocytes develop in the bone marrow from a common myeloid progenitor, a precursor for a number of cell types including neutrophils, eosinophils, basophils, macrophages, dendritic cells (DCs), and mast cells. Specifically, during monocyte development common myeloid progenitors develop into granulocyte/macrophage colony forming units (CFUs), which sequentially develop from monocyte CFUs, to monoblasts, to pro-monocytes, and then finally circulate in the blood stream as monocytes. In response to infections or in order to replenish long-lived tissue-specific macrophages of the bone, alveoli, central nervous systems, connective tissue, gastrointestinal tract, liver, spleen, peritoneum, etc., monocytes migrate from the blood into the tissue. Macrophages can then perform a variety of functions, including clearance and killing of pathogens, clearance of apoptotic cells, contributing to tissue remodeling and wound healing, and maintenance of homeostasis (especially for long-lived resident macrophages).

Monocyte Heterogeneity and Development of Macrophages

Monocytes are a relatively heterogeneous population of cells, the functions of which are only recently being realized. It now appears that monocytes develop along a continuum and at what point along the maturation process that monocytes are recruited out of the blood may define their function. These monocyte subpopulations are defined by the expression (or lack thereof) of a set of surface markers, which in mice are defined by CCR2 (the receptor for the chemokine MCP-1), Ly6C, CCR7, CCR8, and CX_3CR1. Initially monocytes appear in the blood as $Ly6C^+$ and $CCR2^+$ cells and are known as 'inflammatory monocytes'. This population of cells is generally recruited from the blood

into inflamed tissue, where most develop into macrophages and contribute to clearance of pathogens and healing after trauma[58]. These macrophages appear to be relatively plastic and will respond to specific signals in the microenvironment in which they find themselves (discussed below). The appearance of these cells in an inflammatory focus generally correlates with control of an infection. For example, enhanced recruitment of 'inflammatory monocytes' through the expression of MCP-1 by transgenic *Leishmania* during an infection resulted in greater parasite killing as compared mice infected with wild-type *Leishmania*[59]. Most of these 'inflammatory monocytes' that are recruited during inflammation become macrophages, but it appears that a fraction of these cells are able to migrate into the tissue then into the lymph nodes as DCs[60].

'Inflammatory monocytes' that are not initially recruited further mature along the continuum and begin to lose expression of Ly6C (Ly6C Intermediate) while increasing their expression of the chemokine receptors CCR8 and CCR7. These cells appear to be more prone to developing into dendritic cells, and their recruitment into tissue then migration back into the lymph nodes appears to be dependant upon then expression of CCR7 and CCR8 and their associated chemokine ligands[58]. These monocytes appear to be an intermediate between inflammatory monocytes and a third population of monocytes called 'resident monocytes' which have lost their expression of CCR2 and Ly6C and gained the expression of CX_3CR1. This population has been hypothesized to contribute to the regeneration of tissue-resident macrophage populations[58]. It appears that this hypothesis is probably an over-simplification of what actually occurs. Specialized dendritic cells of the skin called Langerhans cells are self-renewing throughout life in steady state conditions, meaning that under normal conditions they are not repopulated by

'resident monocytes'[61]. However, if Langerhans cells are depleted by UV irradiation, they are replenished by precursors from the bone marrow. Conversely, tissue-specific macrophages of the liver called Kuppfer cell are directly replaced by bone marrow progenitors[62]. Therefore, this 'resident monocyte' population may be the precursor cell responsible for replenishing these cells. It appears that this 'resident monocyte' population may contribute to the generation of certain tissue resident macrophages and DCs, but most likely not all of these cells.

Heterogeneity of Activated Macrophages

Macrophages express a variety of receptors which allow them to respond to the microenvironment into which they are recruited. This includes responding to a variety of cytokines, chemokines, products derived from pathogens, etc. The combination of these stimuli drives the development of specific subpopulations of macrophages, including the classically activated macrophage (Ca-MΦ), the alternatively activated macrophage (AA-MΦ), and the type II activated macrophage (MΦ-II). These phenotypes are highly reproducible in vitro and appear to reflect populations that appear in vivo (Figure 4).

The Classically Activated Macrophage

Classically activated macrophages (Ca-MΦ) have been thoroughly characterized. They were initially characterized in 1964, where it was shown that infection of mice with *Listeria monocytogenes, Brucella abortus,* or *Mycobacterium tuberculosis* increased the bactericidal activity of macrophages[63]. As the name implies, they were once considered to be the only type of activated macrophage. These cells arise by exposure to two signals.

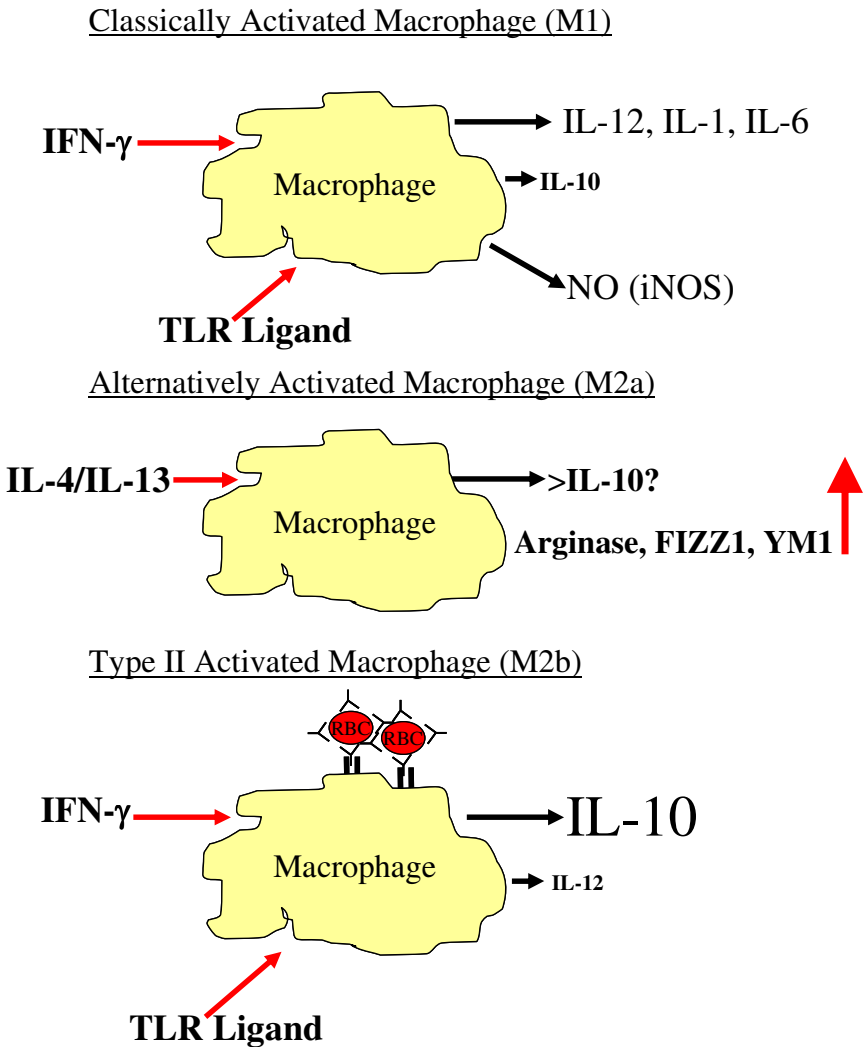

Figure 4: Activated macrophage populations.
Classically activated macrophages (Ca-MΦ) or M1 cells arise in response to IFN-γ as well as an activating stimulus, such as a Toll-like receptor ligand. Ca-MΦ cells produce a battery of inflammatory cytokines, as well nitrogen and oxygen radicals. These macrophages produce low levels of the anti-inflammatory cytokine IL-10. Alternatively activated macrophages (AA-MΦ) arise in response to the Th2 associated cytokines IL-4 and IL-13. These cells have been associated with a number of markers including FIZZ1, YM1, and the arginine consuming enzyme arginase-1. Additionally, the cells have been reported to express elevated levels of IL-10. The Type II activated macrophage arises in response to classical activating stimuli in the presence of Fcγ-Receptor signaling through the presence of IgG-immune complexes (i.e. an opsonized erythrocyte). This results in the suppression of IL-12 production and high levels of anti-inflammatory IL-10. The aims of this work are to characterize the MΦ-II in the context of the Ca-MΦ and the AA-MΦ, determine the functionality of these cells, and to identify novel markers for these cells.

The first is IFN-γ, which is necessary for priming but not sufficient for activation[64]. This first signal must be combined with an activating stimulus. This can be TNF-α or an inducer of TNF-α such as a toll like receptor (TLR) ligand. Once activated, these macrophages up-regulate the TNF receptor, which enhances the autocrine activity of TNF-α. CD40 also aids in activation by binding CD40L on IFN-γ secreting Th1 cells[65].Once activated, these macrophages serve a variety of functions. They up-regulate MHC class II and costimulatory B7, which enhances their ability to present antigens. They secrete a full battery of inflammatory cytokines including IL-12, IL-1, IL-6 and TNF-α, as well as modest amounts of anti-inflammatory IL-10. These cells are very effective in killing intracellular pathogens. Killing can be mediated by the production of reactive oxygen intermediates (ROI) and the activation of iNOS (inducible NO synthase), as well as by restriction of nutrients such as iron and tryptophan[65].

It is important to note, however, that many inflammatory autoimmune pathologies such as arthritis[66], multiple sclerosis[67], and inflammatory bowel disease[68], are associated with uncontrolled macrophage activation. This can also be applied to uncontrolled activation during chronic infections, such as mycobacterial infections. Some microbes can resist the microbicidal effects of activated macrophages, resulting in chronic infection. What often results is a granuloma, consisting of a central area of activated and often fused multi-nucleated macrophages surrounded by activated lymphocytes[65]. These collections of activated macrophages can induce tissue pathology, DNA damage, and occasionally give rise to cancer.

The Alternatively Activated Macrophage

The alternatively activated macrophage (AA-MΦ) was originally characterized in conditions that allowed for overexpression of the macrophage mannose receptor (MMR)[69]. The macrophage mannose receptor is important in the binding and phagocytosis of microorganisms with surface mannose residues. The MMR is expressed on tissue macrophages, but its expression decreases in response to IFN-γ activation. However, it was found that the Th2 associated cytokine IL-4 could enhance both MMR surface expression 10-fold and activity 15-fold[69]. It was later shown that both IL-4 and another type 2 cytokine, IL-13, were similar in their ability to induce the alternative activation phenotype[70]. The more recently described cytokine IL-21 also seems to play an indirect role by increasing responsiveness to IL-4 and IL-13[71]. AA-MΦ have been described in a variety of helminth infections, including *Schistosoma mansoni*[72], *Heligmosomoides polygyrus*[73], *Nippostrongylus brasiliensis*[74], *Taenia crassiceps*[75], *Trichinella spiralis*[76], *Faciola hepatica*[77], *Ascaris suum*[78], and parasitic infections, including *Trypanosoma*[79].

Perhaps the most important element of the AA-MΦ phenotype is differential L-arginine metabolism relative to the classically activated macrophages. This was originally observed in the regulation of fibrotic liver pathology in response to type 1 versus type 2 cytokines in mice infected with *Schistosoma mansoni*[20]. It had previously been shown that skewing the immune response towards Th1 could alleviate the pathogenic response due to the activation of iNOS, as mice deficient in this gene failed to control infection with *S. mansoni*. The induction of Arg-1 (Arginase-1) by macrophages was found to be type-2 cytokine dependant. Arg-1 hydrolyses L-arginine to urea and ornithine (Figure 5). Ornithine is required in the synthesis of proline and polyamines, which are required for

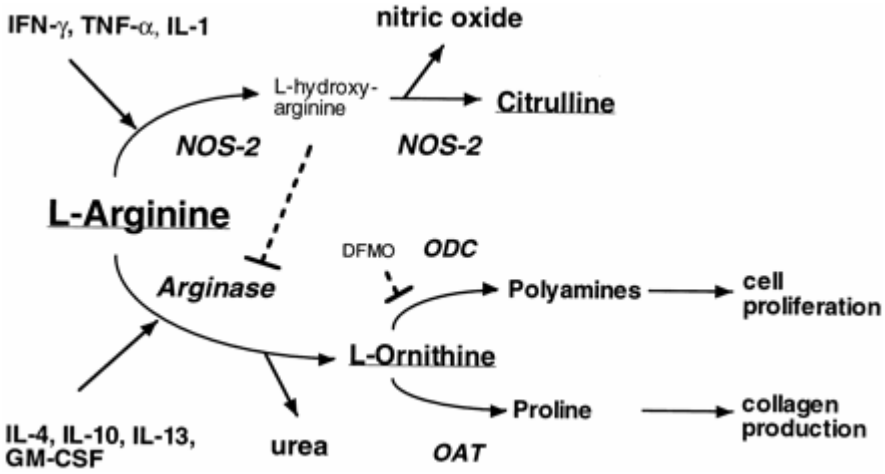

Figure 5: L-arginine metabolism is differentially controlled by Th1 versus Th2 associated cytokines by macrophages.
NOS-2 (iNOS) is induced by the presence of Th1 cytokines, resulting in the production of nitric oxide (NO) and citrulline. Arginase is induced by Th2 cytokines, resulting in the production of urea and L-ornithine. L-ornithine is further metabolized by ornithine aminotransferase (OAT) or ornithine decarboxylase (ODC) to produce proline or polyamines, respectively. Figure reproduced with permission from the *Journal of Immunology*. Copyright 2001The American Association of Immunologists, Inc.[20]

cell proliferation and collagen production. As both iNOS and Arg-1 use arginine as a common substrate, cytokine mediated activation of one enzyme corresponds with the suppression of the other. The shift in a Th1 towards a Th2 reseponse correlating with a shift in arginine metabolism from iNOS activity towards Arg-1 is associated with the magnitude of pathology in this model[20].

Subsequently many markers have been shown to be reliably associated withalternatively activated macrophages. In the murine disease model of *Trypanosoma brucei brucei* infection, early infection is characterized by the development of Ca-MΦ, whereas the chronic stages are characterized by AA-MΦ. It was shown that both FIZZ1 (found in the inflammatory zone 1) and Ym1 are strongly induced in the late stages of infection. FIZZ1 is a secreted protein that has been associated with allergic and pulmonary inflammation. Ym1 is a secretory lectin that has been associated with lung inflammation due to its ability to form crystals in alveolar spaces, but also has been shown to have anti-inflammatory properties due to its ability to bind to local ECM and compete with leukocytes for binding sites. FIZZ1 and Ym1 were both shown to be strongly induced in the in vivo disease model and in vitro with IL-4 treatment. This was antagonized by the presence of IFN-γ. Insulin-like growth factor-I (IGF-I), a protein implicated in interstitial lung disease and pulmonary fibrosis, has also been associated with macrophages exposed to Th2 cytokines. IGF-I promotes the proliferation and survival of fibroblasts and stimulates collagen synthesis by them. AMAC1 (alternative macrophage activation-associated chemokine), IL-1 decoy receptor (an anti-inflammatory inhibitor of the effects of IL-1), TGF-β, and MMP-1 (matrix-metalloproteinase-1) have also been associated with AA-MΦ[80]. It is unclear, however, if the presence of these

markers is as a direct result of Th2 cytokines, as they are associated with complex diseases.

The kinetics of the induction of AA-MΦ seem to depend on the specific infection model being studied. Infection with the helminth *H. polygurus* only results in the accumulation of AA-MΦ during a memory response[73]. In contrast, during the *N. brasiliensis* infection model in SCID, mice which lack T-cells, AA-MΦ appear soon after infection, indicating that Th2 cytokines produced by innate immune cells are sufficient. Of note, however, is that AA-MΦ rapidly disappear in SCID mice while they are retained in wild type mice, indicating that Th2 cytokines from adaptive immune cells are required to sustain AA-MΦ[74].

Although it appears that the generation of AA-MΦ plays a detrimental role in the immune system, especially in the model *Schistosoma mansoni,* this is certainly an oversimplification. The generation of AA-MΦ may control excessive inflammatory responses. Alternatively activated macrophages have been shown to suppress T-cell activation in vivo and in vitro, possibly through TGF-β or interactions with programmed death-1 (PD-1) on T-cells with programmed death ligand-1 or -2 (PDL-1 and PDL-2)[81,82] on macrophages. During the murine model of inflammatory renal disease, infusion of ex vivo generated AA-MΦ ameliorates disease while Ca-MΦ exacerbate disease[83]. Additionally, it has been shown that microglial cells have an alternatively-activated phenotype (Ym-1 positive), and in the murine model of multiple sclerosis, IL-4 is critical for controlling the phenotype of infiltrating macrophages[84]. Additionally, the phenotype of adipose tissue macrophages is critical for protection against insulin resistance. Lean mice have macrophages with an alternatively activated phenotype, which are decreased in

response to diet induced obesity. However, this is not the case in mice predisposed to obesity and insulin resistance, which retain their AA-MΦ pehonotype. AA-MΦ in this model protect from TNF-α induced insulin resistance[85]. Another potential function of these cells is their contribution to wound healing. IL-4 activation of macrophages induces extracellular matrix (ECM) proteins fibronectin, tenascin-C, and βIG-H3 and ECM modifying enzymes matrix crosslinking-enzyme tissue transglutamase (tTG), matrix-metalloproteinase (MMP)-1, and MMP-12[86].

In addition to the liver fibrosis associated with a Th2 dominant response to Schistosomiasis, AA-MΦ can play a detrimental role in other pathological conditions. In the murine model of *Cryptococcus neoformans*, a fungal disease typically associated with AIDS patients, the expression of IL-13 is responsible for disease susceptibility and drives the production of AA-MΦ[87]. In co-infection models, such as *T. crassiceps* with *Leishmania* or *H. polygyrus* with *Citrobacter rodentium*, generally effective inflammatory responses are overridden by helminth infection[88].

The Type II Activated Macrophage

The Type II activated macrophage (MΦ-II) was originally characterized in this lab while investigating scenarios that led to the abrogation of IL-12 transcription. Macrophages were stimulated with IFN-γ and LPS, conditions that normally promoted the production of IL-12 and classical activation, along with the presence of IgG opsonized-erythrocytes (E-IgG). These E-IgG ligated the Fcγ receptors, resulting in the production of large amounts of IL-10, coincident with the inhibition of IL-12 production[89]. However, this was not the only scenario under which this cytokine skewing

could be reproduced. A variety of activating signals when combined with Fcγ receptor ligation with immune complexes, including the TLR4 ligand LPS and TLR2 ligand lipoteichoic acid (LTA), as well as mimicking T-cell CD40 ligand with an antibody against CD40 and with the endogenous TLR ligand low molecular weight hyaluronic acid (LMW-HA) all showed similar alterations in cytokine production. Importantly, cytokine modulation in response to immunce complexes was specifically limited to IL-10, IL-12p40 and IL-12p35. A number of other cytokines, including TNF-α, IL-1, and IL-6, remained largely unchanged[90].

This phenomenon of enhanced IL-10 production was shown to have in vivo significance by reversing LPS associated toxicity. Mice were passively immunized with anti-LPS IgG and later injected with LPS. It was found that in mice given IgG against LPS had modest levels of IL-12 and high levels of IL-10 in the serum. Additionally, mice that were given macrophages activated in vitro with LPS in the presence of E-IgG then challenged with a lethal dose of LPS, survived. However, mice that were given macrophages stimulated with LPS or macrophages from IL-10 deficient mice stimulated with both LPS and E-IgG quickly succumbed to the effects of endotoxic shock[90].

The name type II activated macrophage (MΦ-II) was later coined based on the ability of these macrophages to bias T-cells towards a Th2 phenotype. MΦ-II could bias T-cells differently than classically activated macrophages (Ca-MΦ). DO11.10 T-cells (transgenic OVA-specific) were activated with macrophages stimulated with either LPS plus ovalbumin (OVA) or macrophages stimulated with LPS and OVA in immune complexes (IgG-OVA). It was found that upon stimulation, T cells exposed to MΦ-II produced relatively low levels of IFN-γ and high levels of IL-4, whereas those stimulated

with Ca-MΦ produced low levels of IL-4 and high levels of IFN-γ. It was shown with IL-10 and IL-12 deficient mice that the ability of Ca-MΦ and MΦ-II to bias T-cells towards Th1 and Th2, respectively, was contingent upon the reciprocal modulation of these two cytokines. Furthermore, this biasing was irreversible, as cytokine production remained the same even if T cells were reactivated in the presence of macrophages activated in the opposite manner[91,92].

Type II activated macrophages have also been shown to influence the antibody response in mice. In these studies, DO11.10 mice were injected with a combination of OVA and in vitro activated macrophages (Ca-MΦ or MΦ-II). Mice receiving Ca-MΦ generated significant titers of OVA-specific antibody, comprised of both IgG1 and IgG2a. Mice receiving MΦ-II generated antibodies of the same isotypes. Injection of MΦ-II, however, did result in the production of higher total antibody levels, and this increase was largely due to an increase in IgG1 production[92].

It appears that in certain infections, MΦ-II could contribute to persistence due to the formation of immune complexes. Increases in pathogen numbers can overlap with high antibody titers, thus creating a scenario where immune complexes could easily form. The production of IL-10 in this case could potentially create a more favorable environment for intracellular pathogens and exacerbate disease. In the susceptible model of murine cutaneous leishmaniasis as well as human visceral leishmaniasis this seems to be the case. IgG-opsonized parasites drive the production of IL-10 from macrophages and disease severity directly correlates with antibody titers[56].

Deactivated Macrophage Phenotypes

In addition to classically activated, type II activated, and alternatively activated macrophages, deactivated macrophages also seem to be a relevant population of macrophages. These are generated by a number of stimuli, including exposure to the cytokines IL-10 and TGF-β, treatment with glucocorticosteroids, or ligation of the inhibitory receptors SIRPα or CD200R by CD47 and CD200, respectively (generally by apoptotic cells). These cells downregulate MHC class II and produce higher levels of anti-inflammatory IL-10 and TGF-β[80].

Molecular Regulation of IL-10 in Macrophages

mRNA Stability and Transcription Factors

There is general agreement that the most important aspect of the regulation of il-10 gene expression occurs at the level of transcription. However, similar to many other cytokines, IL-10 mRNA contains several potential mRNA-destabilizing sequences (AU-rich elements) in the 3'-UTR of mouse and human IL-10 mRNA that make this mRNA relatively short-lived. Many cell types appear to express low levels of IL-10 mRNA, yet do not make detectable levels of IL-10 protein. Powell MJ, et al. systematically addressed the 3'-UTR of IL-10 mRNA and postulated that some cell types might constitutively transcribe low levels of IL-10 mRNA, but due to mRNA-destabilizing signals insufficient message persisted to allow detectable protein production. Therefore, it is certainly plausible that the increased IL-10 production associated with the activation of cells may not only be due to an induction of IL-10 transcription, but it may also involve some measure of increased mRNA stability[93].

A number of different transcription factors have been associated with the regulation of IL-10 in macrophages. These include Sp1 (specificity protein 1)[94], C/EBP (CCAAT/enhancer binding protein)[95], CREB (cAMP-response element-binding protein)[96], STAT3 (signal transducer and activator of transcription-3)[97], c-MAF (musculoaponeurotic fibrosarcoma)[98,99], IRF-1 (interferon regulatory factor-1)[100], and NF-κB (nuclear factor-κ B)[101]. The roles of Sp1, STAT3, and NF-κB will be discussed in detail.

The Sp1 binding site located at -89/-78 is a central mediator for murine IL-10 production. LPS induced IL-10 promoter activity was shown to be dependant upon this element, despite the fact that activation of murine macrophages was not required for Sp1 binding to labeled DNA oligonucleotides[94]. When it was originally described, Sp1 was shown to be phosphorylated by a DNA-dependent protein kinase, Sp1 kinase, to activate transcription[102]. However, work with the human IL-10 promoter indicates that Sp1 phosphorylation depends on p38 MAPK. Stimulation of human macrophages in the presence of p38 inhibitors results in a dramatic curtailment of IL-10 production, but it is not clear whether this inhibition directly affects Sp1 phosphorylation or not[103].

STAT3 binds to the human IL-10 promoter at -120 and mediates the upregulation of IL-10 production in multiple myeloma cell lines[97]. IL-10 itself can induce IL-10 production in an autocrine fashion in human monocyte-derived macrophages via the activation of STAT3[104]. In murine cells it was demonstrated by ChIP (Chromatin Immunoprecipitation) that STAT3 potentially binds two sites (-629/-621 or -479/-471) of the IL-10 promoter following LPS stimulation[105,106]. This analysis, however, did not distinguish between binding to either site. STAT3 does not appear to be required for IL-

10 transcription. Macrophages and neutrophils from conditional knockout mice actually exhibit higher IL-10 expression both in the serum and peritoneal fluid after endotoxin stimulation. Additionally, thioglycolate-elicited peritoneal macrophages from these mice had higher IL-10 production upon LPS stimulation[107]. Thus, while STAT3 clearly binds to the IL-10 promoter and participates in IL-10 transcription, this transcription factor does not appear to be required for IL-10 gene expression.

It was previously believed that NF-κB does not participate in any significant way in the regulation of IL-10 gene expression. The IL-10 promoter lacks the typical consensus NF-κB cis-elements. However, Mori and Prager reported that high IL-10 expression correlated with high NF-κBp50 expression in a T cell line, suggesting that some NF-κB members may be involved in IL-10 transcription[108]. Cao et al. employed an overexpression approach to examine the role of individual NF-κB family members in IL-10 gene expression. Overexpression of four of the five NF-κB family members, including p65, c-Rel, RelB, and p52 had no effect on IL-10 transcription. However, the overexpression of NF-κB1 (p50) caused a dramatic increase in IL-10 promoter-driven luciferase activity, whereas several different heterodimers actually inhibited activity. The conclusion was that p50 homodimers can promote IL-10 synthesis. Most importantly, p50 knockout mice are more susceptible to lethal endotoxemia as macrophages from these mice exhibit skewed cytokine responses to lipopolysaccharide, characterized by decreased IL-10 and increased TNF-α and IL-12[101].

Epigenic Modifications and Regulation of IL-10 by the MΦ-II

An important element of the regulation of IL-10 is epigenic modifications of the IL-10 promoter. This is evident in both macrophages and T-cells, albeit by different mechanisms. It has previously been shown that in T cells GATA3 induces remodeling of the chromatin structure at the IL-4 locus by binding to sites localized upstream of the IL-4 gene and in the IL-4/IL-13 intergenic region. GATA3, however, only weakly transactivates the IL-4 promoter. On the same note, forced expression of GATA-3 in naïve T-cells resulted in enhanced expression of IL-10 driven by changes in the chromatin structure at the IL-10 locus. GATA3, in this case, does not transactivate the IL-10 promoter. Rather the role appears to be primarily in driving remodeling of the IL-10 locus to be more transcriptionally competent[109]. A series of chromatin modifications at the IL-10 locus in differentiated Th1 and Th2 cells modulates repression and function of the IL-10 promoter, respectively. It is noteworthy that these chromatin modifications are long-term and heritable in daughter cells[110].

Similar to T cells, macrophage IL-10 gene transcription is regulated both by modifying chromatin and by activation of necessary transcription factors. However, this mechanism appears to be quite distinct from that which occurs in T cells. In macrophages, transcription factor binding to the IL-10 promoter appears to be preceded by the transient phosphorylation of chromatin associated with the IL-10 promoter. The phosphorylation of histones associated with the IL-10 promoter is dependent on the activation of the mitogen-activated protein kinase (MAPK), ERK. The resultant histone phosphorylation makes the DNA accessible to transcription factors, allowing them to bind to the il-10 promoter[105,106].

Thus, optimal IL-10 production by the type II activated macrophage is the result

LPS Stimulation

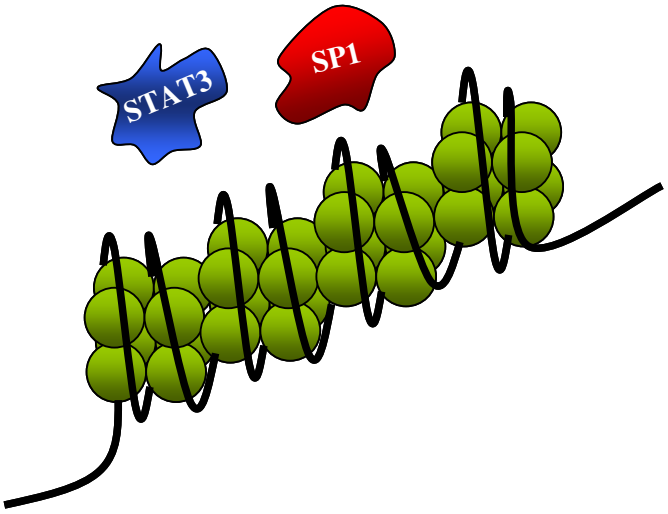

LPS+IC Stimulation

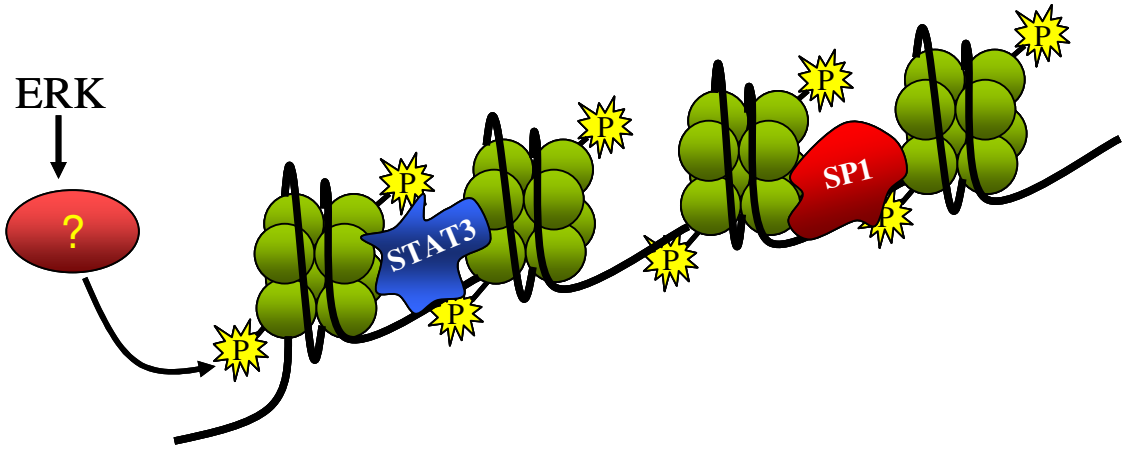

Figure 6: Model for the regulation of IL-10 by Type II activated macrophages. Stimulation of macrophages with LPS alone activates the necessary transcription factors for IL-10, yet the "closed" confirmation of the IL-10 locus results in relatively inefficient transcription factor binding and thus inefficient transcription. However, stimulation with LPS in the presence of immune complex leads to rapid and prolonged ERK activation, leading to the activation of an undetermined ERK-dependant kinase. This ERK-dependant kinase phosphorylates histone H3 (at S10), which results in a looser chromatin conformation and allows for efficient transcription factor binding and thus high IL-10 transcription.

of a confluence of two cellular signaling pathways. The first pathway activates the transcription factors that drive cytokine gene expression. This is usually initiated by the ligation of any of the Toll-like Receptors (TLRs). This first pathway is common to the inflammatory cytokines as well as IL-10, and TLR activation is the prototypical way that inflammatory cytokine genes are induced. The ligation of TLRs, however, is generallynot sufficient to induce high levels of IL-10 in macrophages because the necessary transcription factors do not gain access to the IL-10 promoter[105].

There is, however, a second level of regulation that appears to be fairly unique to IL-10. This second signal required is the rapid and prolonged activation of ERK. This pathway is not activated by the typical Ras/Raf pathway that is associated with growth factor receptor signaling, but through activation of the protein tyrosine kinase Syk. This is achieved efficiently though the cross-linking of Fcγ receptors by immune complexes. The result of ERK activation is the phosphorylation of histone H3 associated with the IL-10 promoter. This results in a more accessibility promoter, allowing for efficient transcription factor and thus a high level gene expression[105,106]. So, without the activationof ERK, these modifications do not occur and associated transcription factors are not efficiently able to gain access (Figure 6).

The kinetics of the chromatin modifications occurring to the promoter of IL-10 appear to be quite unique. ERK activation results in the rapid phosphorylation of histones. Phosphorylation peaks within 30 minutes of activation, with transcription factor binding following closely thereafter. Second, the phosphorylation is remarkably transient. By one hour post-stimulation there is no longer detectible phosphorylation of histones associated with the IL-10 promoter, and transcription rapidly subsides. The

kinetics of chromatin modifications of the IL-10 gene in macrophages are quite distinct from the well-described epigenetic modifications associated with the stable "marking" of genes for expression, i.e. IL-10 expression in Th2 T-cells. These studies concluded that macrophages undergo ERK-dependant transient modifications to the chromatin associated with the IL-10 promoter that temporarily make the promoter accessible to transcription factors. Additionally, the activation of the MAPK p38 is required for proper activation of transcription factors required for IL-10 transcription[105,106].

MAPK Mediated Chromatin Modifications

Overview

The induction of IL-10 induction seems to follow the module of an immediate early (IE) gene, in that its induction is directly connected to signaling systems[111]. The IE module of gene regulation takes advantage of chromatin structure. Post-translational modification of histones, such as phosphorylation or acetylation, may alter DNA-histone contacts. Additionally, they may act as binding platforms for other proteins. For instance, bromodomains are proposed to interact with acetyl-lysine and chromodomains are proposed to interact with methyl-lysine of histones[111].

IE genes can be regulated by several different signaling pathways, including the JAK/STAT, NF-κB, and MAPK pathways. However, the MAPK pathways, in particular p38 and ERK1/2, are associated with histone H3 modifications. The MAPK cascades can elicit a rapid and transient phosphorylation of H3 at serine 10 and/or 28 and the protein HMG-14 (High Mobility Group protein 14). This is known as the nucleosomal response. There are three candidate MAP kinase activated protein kinases (MKs) known to date

that may play are role in the nucleosomal response, all of which have been implicated in some system. These are MSK1 (mitogen and stress activated protein kinase), MSK2, and RSK2 (ribosomal S6 kinase). These three proteins belong to the larger MK family which is comprised of 11 members to date. They can be activated by p38 (MK2, MK3, and MK5), by ERK1/2 (RSK1-4 and MNK5), or by both p38 and ERK1/2 (MSK1, MSK2, and MNK1). Those involved in the nucleosomal response, the RSKs (p90 ribosomal S6 kinases) and MSKs (mitogen and stress activated protein kinases), have two kinase domains. The N-terminal kinase domain (NTKD) seems to be important for substrate phosphorylation and autophosphorylation of several residues important for activation. The C-terminal kinase domain (CTKD) seems to play a role only in activation through autophosphorylation[112].

The RSKs contain a D-domain near the C-terminus necessary for ERK1/2 docking. Docking is a rather transient event as a serine residue near the D domain is rapidly phosphorylated which drives dissociation. These proteins are normally associated with the cytoplasm of quiescent cells, but upon stimulation a significant portion translocates to the nucleus. The MSKs are structurally very similar to the RSKs. They also contain a D-domain near the C-terminus necessary for the docking to ERK1/2 and p38. However, unlike the RSKs, the MSKs are predominantly nuclear in localization of both activated and quiescent cells[112].

Ribosomal S6 Kinase-2 (RSK2) and the Mitogen and Stress Activated Protein Kinases (MSK)1 and 2

Sassone-Corsi et al. initially investigated the ability of fibroblasts derived from patients with Coffin-Lowry syndrome (CLS), an X-linked mental retardation disorder caused by mutation of RSK2, to phosphorylate histone H3 in response to epidermal growth factor. Wild-type serum starved fibroblasts underwent rapid phosphorylation of histone H3 in response to epidermal growth factor. CLS derived RSK2 deficient fibroblasts, however, were unable to undergo phosphorylation of histone H3 in response to EGF. In addition, transfection of RSK2 expression vector restored the ability to phosphorylate H3 in response to EGF[113].

Others have shown that MSK1 and/or MSK2 are more likely to be candidates for the H3 kinase involved in the nucleosomal response. Thomson et al. showed that the phosphorylation of H3 and HMG-14 in response to TPA (ERK dependant) or anisomycin (p38 dependant) could be inhibited by the protein kinase inhibitor H89. They demonstrated that that of these candidate H3 kinases, only the activity MSK1 was inhibited by H89. Additionally, MSK1 was found to have higher H3 and HMG-14 kinase activity relative to either RSK1 or RSK2[114].

Soloaga et al. reported that MSK1 or MSK2 are the major kinases involved in the nucleosomal response to mitogenic or stress stimuli. Mouse fibroblasts from MSK double knockout cells were unable to phosphorylate histone H3 or HMG-14, and this activity could be restored with transfection with a construct encoding MSK2. Treatment of wild-type fibroblasts with anisomycin resulted in transient induction of c-jun and c-fos. MSK1/2 knockouts, however, had significant reduction of c-fos induction and delayed induction of c-jun. Importantly, this group demonstrated that H3 phosphorylation was not affected in CLS derived cells despite the RSK2 deficiency. This group concluded that the

MSKs, most likely MSK2, and not RSK2 are the kinases responsible for the nucleosomal response[115].

Heparin-Binding Epidermal Growth Factor-Like Growth Factor (HB-EGF)

The focus of chapter 4 is the regulation of heparin-binding epidermal growth factor-like growth factor (HB-EGF) by the type II activated macrophage. HB-EGF was originally identified in the culture supernatants of the U-937 macrophage like cell line[116]. It was found to be mitogenic for a number of cell types, including fibroblasts, smooth muscle cells, and a number of other cell types. HB-EGF is synthesized as a transmembrane precursor (proHBEGF) that can serve as a juxtacrine growth factor[117], and in some species as the receptor for diphtheria toxin[118]. A number of proteases have been implicated as being responsible for ectodomain shedding, resulting in the formation of soluble HB-EGF (sHB-EGF). These include MMP3, MMP9, ADAM9, ADAM10, ADAM12, and ADAM17[119]. Recently, the metalloendopeptidase nardilysin (NRDc) was demonstrated to enhance ectodomain shedding by activation of ADAM17[120]. The resulting carboxy-terminal (membrane associated) fragment of proHB-EGF can contribute to cell cycle progression by translocating to the nucleus and interacting with promyelocytic leukemia zinc finger (PLZF), the transcriptional repressor of cyclin A[121], or with Bcl6, the transcriptional repressor of cyclin D2[122]. sHB-EGF was shown originally to signal through the EGFR(ErbB1)[116], but was later demonstrated to also bind ErbB2 and ErbB4[123,124].

HB-EGF has been found to play a role in several normal physiological processes, including proper heart [124] and eyelid [125] formation and skin would healing by inducing

keratinocyte migration[126]. It has also been found to be associated with a number of pathological conditions. Macrophages, T-cells, and vascular smooth muscles cells (SMCs) of atherosclerotic plaques have been found to express HB-EGF[127,128]. Furthermore, not only is HB-EGF a potent mitogen for SMCs, but it also induces the expression of LOX-1, the receptor for oxidized LDL, by smooth muscle cells, potentially aiding foam cell formation. Additionally, OxLDL can induce the expression of HB-EGF by macrophages[129].

HB-EGF has also been shown to be an important regulator of tumor growth and angiogenesis. In vitro, HB-EGF has been shown to increase the growth rate of tumor cells and to induce the expression of VEGF, and in vivo to strikingly increase angiogenic potential and tumorigenicity[130]. Recently, it was shown that HB-EGF may contribute to angiogenesis primarily by driving remodeling of vascular endothelial cells[131]. HB-EGF expression has been found to be enhanced in many tumors[119,132-134]. HB-EGF can also contribute to chemotherapy resistance. A number of chemotherapeutic agents, including SN38, doxorubicin, and cisplatin, rapidly induce the expression of HB-EGF in several tumor cell lines, as well as increase enzymatic shedding, resulting in strong EGFR activation and thus resistance to apoptosis [135]. Bile acids, which have been implicated as cofactors of colon carcinogenesis, may mediate their activity through the upregulation and activation of MMP-7, resulting in increased shedding of HB-EGF and thus proliferation of a human colon cancer cell line[136].

Very little is known about the molecular regulation of HB-EGF. This is especially true for macrophages of which there are essentially no reports, despite the fact that HB-EGF was originally characterized as a product of macrophages. There is some evidence

that the 3'-UTR may play a role in the accumulation of message. Sorensen et al. reported that use of the chemotherapeutic agent VP16 on the HeLa human cervical cancer cell line resulted in an increase in HB-EGF mRNA that could only be partially accounted for an increase in transcription. Instead, the increase in HB-EGF was found to be due to increased HB-EGF mRNA stability, which was contingent upon an 186bp region of the 3'-UTR containing five AU-rich elements (ARE)[137]. In other systems, this has not been found to be a primary mechanism of increased HB-EGF mRNA induction. Ornskov et al. reported the induction of HB-EGF in RT4 bladder cancer cells was not due to increased stability, but due to a PI3K dependant increase in transcription[138]. In contrast, Ellis et al. reported that ERK and not PI3K or protein kinase C activity was required for HB-EGF induction in rat intestinal epithelial cells after scrape-wounding[139]. Similarly, HB-EGF induction was found to be due to ERK and the transcription factor Ets-2 in Ras/Raf transformed NIH 3T3 cells. Ets-2 was found to bind to a promoter element located at -974/-988[140]. Additionally, the function of a number of tissue-specific transcription factors have been reported, including the intestinal-specific Cdx-2[141] and MyoD, the family of transcription factors which regulate myogenesis[142]. Taken together, HB-EGF is a biologically significant growth factor whose regulation is only partially understood.

Tumor Associated Macrophages

It is now a well accepted concept that tumor-associated macrophages (TAMs) can contribute to the progression of cancer instead of controlling it, apparently by a number of mechanisms. A number of studies have established a correlation between high TAM numbers and decreased patient survival. TAMs appear to contribute to tumor cell

proliferation and survival, invasion into surrounding healthy tissue, and metastasis to distal locations. Biswas et al. showed that resting TAMs constitutively expressed, among other things, high levels of immunosuppressive IL-10. Additionally, in vivo TAMs were found to produce IL-10 and were devoid of iNOS. Upon stimulation of TAMs in vitro, they expressed high levels of the immunosuppressive cytokines IL-10 and TGF-β while being defective in their expressive of inflammatory IL-1β, IL-6, and TNF-α[143]. In agreement with Cao et al., who showed that the NF-κBp50 homodimers suppressed inflammatory cytokine production while enhancing IL-10 production[101], Saccani et al. recently showed that tumor-associated macrophages over-expressed p50 and this was responsible for the suppression of cytokines characteristic of classical activation of macrophages (IL-12, IL-6, TNF-α) and enhancement of IL-10 production. Importantly, tumor-associated macrophages from NF-κBp50$^{-/-}$ mice had normal expression of inflammatory cytokines which correlated with reduced tumor growth[144]. Thus, it appears that overexpression of NF-κBp50 is one mechanism by which macrophages are driven to promote tumor growth.

Functionally, tumor-associated macrophages have a reduced ability to lyse tumor cells, present tumor antigens to T-cells, and as mentioned above, produce inflammatory cytokines. This has been attributed to a number of factors produced by tumors, including prostaglandin E2 (PGE2), IL-4, IL-10, and transforming growth factor-β (TGF-β). TAMs appear to play a number of functions to promote tumor progression. During early tumor development, macrophages aid in the invasion into healthy tissue due to their expression of a number of extracellular matrix modifying enzymes (e.g. matrix metalloproteinases, MMPs). Additionally, TAM infiltration has been shown to correlate with tumor cell

proliferation, which has been attributed to their production of epidermal growth factor (EGF), platelet-derived growth factor, TGF-β, hepatocyte growth factor, and basic fibroblast growth factor (bFGF). TAMs also migrate into hypoxic areas within tumors, where they induce new vasculature by producing a number a proangiogenic factors, most importantly vascular endothelial growth factor (VEGF). Lastly, TAMs appear to contribute to tumor metastasis. Movement of tumor cells away from the main tumor mass appears to be in juxtaposition with macrophages. Furthermore, migration of tumor cells into blood vessels generally occurs at clusters of macrophages. Thus, tumor metastasis appears to be coordinated by macrophages[145].

Summary of Studies and Rationale

Previous studies in our lab made the observation that classical activating stimuli of macrophages combined with Fcγ-receptor ligation through IgG immune complexes results in a dramatic alteration in cytokine production. Macrophages now made high levels of anti-inflammatory IL-10 and low levels of inflammatory IL-12. The first part of these studies examines the functionality and biochemistry of these anti-inflammatory macrophages, herein known as Type II activated macrophages (MΦ-II). In the literature, these macrophages and macrophages populations that are not classically activated macrophages are known collectively as M2 cells. This work shows that type II activated macrophages are functionally distinct from other macrophage populations and therefore this terminology which combines all of these populations together may be inappropriate. We have begun to identify new markers for the MΦ-II that are not expressed on other populations.

The second part of these studies focuses on the molecular regulation of heparin-binding EGF-like growth factor (HB-EGF), a new marker for the MΦ-II with significant biological potential. Like IL-10, this factor is made in only modest quantities upon stimulation with LPS alone, whereas there is robust induction when this stimulation is combined with immune complexes. Additionally like IL-10, the MAP kinases are required for the production of HB-EGF, specifically the ERK1/2 and p38 pathways. ERK drives increased accessibility to the HB-EGF promoter, allowing for transcription factor binding. Additionally, 3 binding sites for the transcription factor Sp1 were identified within the HB-EGF promoter, with the site located at -83/-54 being required for the promoter's activity. Finally, as there was a great deal of similarity in the regulation of HB-EGF and IL-10, we decided to investigate if other conditions which promote the production of IL-10 also promote the production of HB-EGF. Macrophages were stimulated with LPS in the presence of immune complexes, prostaglandin E2, 4T1 culture supernantants, and dB-cAMP. All of these conditions enhance endotoxin driven IL-10 and also enhance HB-EGF production. Therefore, there appears to be a mechanism of coregulation. Lastly, as HB-EGF is an important growth factor in the contribution to both physiological and pathological conditions, such as cancer, and since IL-10 is produced in high quantities by tumor associated macrophages (TAMs), we investigated whether TAMs also produced high levels of HB-EGF.

The third part of these studies focuses on the molecular regulation of IL-10, specifically the potential histone kinases involved in its regulation and the role of PI3K. Histone phosphorylation at the IL-10 locus appear to drive increased accessibility to the promoter, allowing for transcription factor binding. We focused on the kinases MSK1

and MSK2, which the literature proposed to be kinases with the potential to phosphorylate histone H3 at serine 10 and serine 28. Preliminary data using siRNA supported the hypothesis that these kinases were required for the induction of IL-10. However, data using MSK1/2 double knockouts negated these findings. Additionally, PI3K appears to play a role in the regulation of IL-10. These preliminary studies were not completed, and form the basis for new projects in the lab.

CHAPTER 2: MATERIALS AND METHODS

Mice

Six- to 8-wk-old BALB/c mice were purchased from Taconic Farms (Germantown, NY). IL-$10^{-/-}$ and $OVA_{323-339}/A^d$-specific, DO11.10 TCR$\alpha\beta$ mice were purchased from the Jackson Laboratory (Bar Harbor, Maine). Mice were used at 6-10 weeks old as a source of bone marrow-derived macrophages (BMMΦ). All mice were maintained in HEPA-filtered Thoren units (Thoren Caging Systems) at the University of Maryland (College Park, MD). All procedures were reviewed and approved by the University of Maryland Institutional Animal Care and Use Committee.

Reagents

The MEK/ERK inhibitor, U0126, p38 inhibitor, SB203580, JNK Inhibitor II, the PI3K inhibitor, LY294002, the MSK/PKA inhibitor, H89, and the Syk Inhibitor, 3-(1-Methyl-1H-indol-3-yl-methylene)-2-oxo-2,3-dihydro-1H-indole-5-sulfonamide, were obtained from Calbiochem (EMD Biosciences, San Diego, CA). Actinomycin D, cycloheximide, and dibutyryl cAMP were purchased from Sigma-Aldrich (St. Louis, MO). Macrophages were pre-treated with inhibitors 1 hour before stimulation at concentrations given within the figures or figure legends. ChIP-grade Anti-Sp1 and histone H3 antibodies were purchased from Upstate (Lake Placid, NY). TRIzol reagent and DNase I were purchased from Invitrogen Life Technologies (Calsbad, CA). Klenow enzyme and restriction enzymes were purchased from New England Biolabs (Ipswich,

MA). Prostaglandin E(2) was purchased from Caymen Chemical Company (Ann Arbor, Michigan).

Cells

BMMΦ were prepared as previously described[106]. Briefly, bone marrow was flushed from the femurs and tibias of mice with PBS+penicillin/streptomycin and cells were plated in petri dishes in DMEM/F12 supplemented with 10% FBS, penicillin/streptomycin, glutamine, and 20% conditioned medium from the supernatants of M-CSF secreting L929 (LC14) fibroblasts (LCCM). Cells were fed on day 2, and complete medium was replaced on day 6. Cells were used at 7-10 days for experiments. Macrophages were removed from Petri dishes using Cellstripper (Mediatech, Manassas, VA) and plated out into 48-well plates (2×10^5 MΦ) for cytokine measurement and 6-well plates (2×10^6 MΦ) for RNA isolation. Cells were cutured overnight in complete media without LCCM.

The RAW264.7 macrophage and 4T1 mammary tumor cell lines were obtained from the American Type Culture Collection (Manassas, VA). RAW264.7 cells were maintained in RPMI supplemented with 10% FBS, penicillin/streptomycin, and glutamine.

Macrophage Activation

For studies involving the characterization of macrophage populations, Ca-MΦ and MΦ-II were prepared by priming BMMΦ overnight with 100 U/ml recombinant IFN-γ (R&D Systems, Minneapolis, MN). Ca-MΦ were washed and stimulated with 10ng/ml

Ultra-Pure LPS (*Escherichia coli* K12, Invivogen, San Diego, CA). MΦ-II received LPS along with immune complexes consisting of IgG-OVA. Immune complexes were made by mixing a tenfold molar excess of rabbit anti-OVA IgG (Cappel, Durham, NC) to OVA (Worthington, Lakewood, NJ) for 30 min at room temperature, as described[91]. AA-MΦ were prepared by stimulating BMMΦ with 10 U/ml recombinant IL-4 (R&D Systems) as previously described[20].

For studies directed at the regulation of Heparin-Binding EGF-like Growth Factor (HB-EGF), unless otherwise noted, macrophages were not primed with IL-4 or IFN-γ Macrophages were simply activated with LPS or LPS + Immune complexes (IC), as described above. Any contaminating endotoxin was removed from the anti-OVA IgG prior to immune complex preparation using EndoClean from BioVitage, as previously described[105]. In some experiments, macrophages were stimulated with PGE-2 (10^{-8}M), 4T1 culture supernatants (27%), and 100μM dibutyryl cAMP in the presence or absence of LPS (10ng/ml).

RT-PCR and Real-Time PCR

BMMΦ were subject to RNA extraction using TRIzol reagent. The contaminating DNA was removed by DNase I treatment. ThermoScript RT-PCR system (Invitrogen Life Technologies) was used to generate cDNA from total RNA using oligo$(dT)_{20}$ primers. Real-time PCR was conducted with the ABI Prism 7700 or Roche LightCycler 480 sequence detection system using iQ SYBR Green Supermix (Bio-Rad Laboratories, Hurcules, CA) following the manufacturer's instructions. Standard PCR analysis was performed using Platinum PCR Supermix (Invitrogen Life Technologies). PCR was

performed using primer pairs specific for iNOS, Arginase-1 (Arg-1), Sphingosine Kinase-1 (SPHK1), FIZZ1, IL-10, IL12/23p40, HB-EGF, TNF-α, and GAPDH. These primer pairs are presented in Table 2. For data analysis, the C_T value for GAPDH was used to normalize loading variations in the real-time PCRs. A $\Delta\Delta C_T$ value was then obtained by subtracting control ΔC_T values from the corresponding experimental ΔC_T. The $\Delta\Delta C_T$ values were converted to fold difference compared with the control by raising 2 to the $\Delta\Delta C_T$ power.

Microarray analysis

RNA was prepared from 5×10^6 classically activated or type II activated macrophages two hours after activation with LPS or LPS+Immune complexes (IC), respectively. High quality RNA was first purified using the TRIzol reagent (Invitrogen, Carlsbad, CA) according to the manufacturer's instructions. RNA was then DNase (Roche, Indianapolis, IN) treated and purified using the RNeasy Mini kit (Qiagen, Valencia, CA), following the RNA cleanup protocol. RNA quality assessment and microarray analysis was performed at the University of Maryland Biotechnology Institute's Microarray Core Facility. Microarray analysis was performed using the Affymetrix GeneChip Mouse Genome 430 2.0 (Santa Clara, CA) according to the manufacturers instructions. This array allowed for the assessment for changes in expression of approximately 39,000 transcripts. Robust changes in expression were determined according to the GeneChip Expression Analysis Data Analysis manual (Affymetrix), selecting for statistically significant changes in expression from Ca-MΦ (control) to MΦ-II (experimental). Briefly, robust changes from Ca-MΦ to MΦ-II had

Gene	Accession Number	Primers
iNOS	NM_010927	5’-CCCTTCCGAAGTTTCTGGCAGCAGC-3’ 5’-GGCTGTCAGAGCCTCGTGGCTTTGG-3’
Arg-1	NM_007482	5’-CAGAAGAATGGAAGAGTCAG-3’ 5’-CAGATATGCAGGGAGTCACC-3’
SPHK1	NM_011451	5’-ACAGCAGTGTGCAGTTGATGA-3’ 5’-GGCAGTCATGTCCGGTGATG-3’
SPHK1a	NM_011451	5’-CCATGTGGTGGTGTTGTGTT-3’ 5’-CTTCCGTTCGGTGAGTATCAG-3’
SPHK1b	NM_025367	5’-CCGCCGTTACCTCTAGCA-3’ 5’-GGTTATCTCTGCCTCCTCCA-3’
FIZZ1	NM_020509	5’-GGTCCCAGTGCATATGGATGAGACCATAGA-3’ 5’-CACCTCTTCACTGCAGGGACAGTTGGCAGA-3’
IL-l0	NM_010548	5’-CCAGTTTTACCTGGTAGAAGTGATG-3’ 5’-TGTCTAGGTCCTGGAGTCCAGCAGACTCAA-3’
IL-l0	NM_010548	5'-AAGGACCAGCTGGACAACAT-3' 5'-TCTCACCCAGGGAATTCAAA-3' (Real-Time PCR)
IL-12/23p40	NM_008352	5’-ATGGCCATGTGGGAGCTGGAGAAAG-3’ 5’-GTGGAGCAGCAGATGTGAGTGGCT-3’
GAPDH	NM_001001303	5’-GCACTTGGCAAAATGGAGAT-3’ 5’-CCAGCATCACCCCATTAGAT-3’
LIGHT/ TNFSF14	NM_019418	5’-CTGCATCAACGTCTTGGAGA-3’ 5’-GATACGTCAAGCCCCTCAAG-3’
HB-EGF	NM_010415	5’-CAGGACTTGGAAGGGACAGA-3’ 5’-GGCATTTGCAAGAGGGAGTA-3’
TNF-α	NM_013693	5'-CATCAGTTCTATGGCCCAGAC-3' 5’-TGGGCTACAGGCTTGTCACA-3'

Table 2: Polymerase chain reaction primers pairs used in both standard PCR and QRT-PCR analysis.

a signal call of “P” or present and had statistically significant increases or decreases based on the detection and change algorithm, respectively, as determined by the Affymetrix Microarray Suite software. Robust changes also had a signal log ratio greater than 1 for increases. Two sets of biological replicates were compared for consistent robust changes. Details of these arrays as well as raw data have been deposited in NCBI's Gene Expression Omnibus (GEO, http://www. ncbi.nlm.nih.gov/geo) and are accessible through GEO dataset GDS2041.

Immunoprecipitation and Western Blot Analysis

LIGHT/TNFSF14 was immunoprecipitated using 5μg of α-mouse LIGHT monoclonal antibody (R&D Systems, clone 261639) per ml of cell culture supernatant. Soluble heparin binding epidermal growth factor (HB-EGF) was immunoprecipitated using 5μg of polyclonal goat anti-mouse HB-EGF (M-18, Santa Cruz Biotechnology, CA) per ml of cell culture supernatant. Samples were subject to SDS-PAGE on 15% resolving gels and transferred to polyvinylidene difluoride membranes (Bio-Rad). Membranes were blotted with goat anti-mouse HB-EGF (1:200 dilution) or anti-mouse LIGHT monoclonal antibody and HRP-conjugated mouse anti-goat IgG secondary antibody or goat-α-Rat IgG secondary antibody (Santa Cruz), respectively. Membranes probing for HB-EGF were developed using ECL Western Blotting Detection Reagents (Amersham Biosciences, Buckinghamshire, England) according to the manufacturer’s instructions. Membranes probing for LIGHT were developed using Lumi-LightPLUS Western Blotting Substrate (Roche Diagnostics, Indianapolis, IN) according to the manufacturer’s instructions.

NO Production and Arginase Activity

NO production was estimated from the accumulation of NO_2- in the medium after 24 hours of macrophage activation using the Greiss reagent, as previously described[146]. Briefly, equal volumes of culture supernatant and Greiss reagent (100 μl) were mixed for 10 minutes at room temperature. Absorbance at 540λ was measured with a Labsystems Multiscan Ascent assay plate reader. A solution of NO_2 was used to construct a standard curve.

Arginase activity was measured in cell lysates as previously described[147]. Briefly, 5×10^5 cells were washed and lysed with 100 μl of 0.1% TritonX-100, 16 hours after activation. Lysates were combined with 25mM Tris-HC1 and 1 mM $MnCl_2$ and enzyme activated by heating for 10 mm at 55°C. The hydrolysis of arginine to ornithine and urea was conducted by incubating the lysates with 100 μl of 0.5M L-arginine (pH 9.7) at 37°C for 60 min. The reaction was stopped with 800 μl of H_2SO_4 (96%)/H_3PO_4 (85%)/H_20 (1/3/7, v/v/v). The urea concentration was measured at 550 nm after addition of 40 μl of α-isonitrosopropiophenone (9% solution in abs. ethanol) followed by heating at 100°C for 30 min.

T-Cell Stimulation Assays

$CD3^+$ T cells were prepared from the spleens of DO11.10 mice by negative selection using the SpinSep Mouse T Cell Enrichment Kit (StemCell Technologies Inc., Vancouver, BC.) according to the manufacturer's instructions. For primary stimulation assays, 2×10^5 macrophages were plated per well in 48-well plates and activated as

described above. Two hours following stimulation of macrophages, 5×10^5 T cells were added to each well in a total volume of 0.550 ml RPMI 1640 (Cellgro, Herndon, VA) supplemented with 10% FCS, HEPES, Glutamine, Pen/Strep, and 50 μM 2-mercaptoethanol. For proliferation assays, cells were stained with CFSE (Invitrogen/Molecular Probes, Eugene, OR). Briefly, T cells were washed with PBS and resuspended at $l\times10^7$ cells/ml in 5 μM CFSE in PBS. Cells were stained while rocking for 7 minutes, then quenched by adding an equal volume of FBS. Cells were washed an additional two times in complete media. For secondary stimulation assays, four days following the primary stimulation, fresh RPMI was added with 10 U/ml IL-2 (R&D Systems) to maintain cell viability. Seven days following the primary stimulation, cells were removed from culture, washed, counted, and added to immobilized anti-CD3 (eBioscience, San Diego, CA), which was prepared by adding 5 μg/ml anti-CD3 to tissue culture dishes in PBS overnight. Cytokines were measured 24h later by either ELISA or Real-Time PCR or after 6 hours by intracellular staining.

Cytokine Measurement by ELISA

Cytokine concentrations were measured by sandwich ELISA using the following capture and detection (biotinylated) antibody pairs from BD Pharmingen: IL-12/23p40, C15.6 and Cl7.8; IL-10, JES5-2A5 and JES5-16E3; IFN-γ, R4-6A2, and XMG1.2; IL-4, 11B11, and BVD6-24G2; TNF-α, G281-2626 and MP6-XT3 according to the manufacturer's instructions. Concentrations were compared to a standard curve (0-4000pg/ml) generated by serial dilution of recombinant protein standards purchased from

BD Pharmingen. Streptavidin alkaline phosphatase (AP) and p-nitrophenyl phosphate (PNPP) substrate were purchased from Southern Biotechnology (Birmingham, Alabama).

Flow Cytometry and Intracellular Staining

Macrophages were stained with FITC conjugated α-I-A^d (AMS-32.1) or PE-conjugated α-CD86 (GL1) (BD Pharmingen). T cells were stained with FITC-conjugated antibodies against CD25 (PC61), CD69 (H1.2F3), or CD62L (MEL-14) and a PE-conjugated antibody against Thyl.2 (53-2.1) (eBioscience). CFSE-stained T cells were also stained against Thy1.2 for gating. Intracellular staining was performed on secondarily stimulated T cells using Pharmingen Cytofix/Cytoperm kit with GolgiStop according to the manufacturer's instructions with some modifications. Briefly, cells were incubated in the presence of GolgiStop for 6 hours after reactivation. Cells were harvested, washed, and resuspended in Cytofix/Cytoperm solution for 20' at 4°C, then washed in Perm/Wash solution. Cells were stained with a PE-conjugated antibody against IL-4 (11B11) and a FITC-conjugated antibody against IL-10 (JES5-16E3) (BD Pharmingen). Cells were analyzed on a Becton Dickinson FACSCalibur flow cytometer. Quadrants were set to an appropriate isotype control antibody for analysis.

MTT Assay

MTT (1-(4,5-Dimethylthiazol-2-yl)-3,5-diphenylformazan) assays were performed to measure changes in cell viability between macrophages stimulated with LPS or LPS+IC. 2×10^5 BMMΦ were plated out overnight and stimulated for 24, 48, 72, and 96 hours in 500μl of media. At the specified time points, 250μl of media was

removed and 100µl of 5mg/ml of MTT (in PBS) was added and incubated at 37° for 2 hours. The conversion of MTT to purple formazan was measured by lysing the cells for 30 minutes at room temperature in 120µl of a solution of acidified isopropanol. Acidified isopropanol was prepared by adding 200µl of 2N HCl, 500µl of 10% SDS, and 300µl of water to 9ml of isopropanol. 100µl of cell lysate was then transferred to an assay plate and measured at 550λ. Each time point was performed in triplicate.

RNA Stability Assay

2×10^6 BMMΦ were stimulated for 2 hours with LPS or LPS+IC before the addition of actinomycin D to a final concentration of 0.5µg/ml. The degradation of HB-EGF mRNA was subsequently measured by QRT-PCR over the following 2 hours.

Electrophoretic Mobility Shift Assay

Probes to amplify potential Sp1 binding sites were generated from the following oligo pairs. Consensus: 5'-CTGCGGGGCGGGGCA-3' and 5'-TCTGCCCCGCCCC-3'; -348/-312: 5'-GGAAGGGGGCGGTGCCGGGCGGGGCGG and 5'-GGAGCCCCGCCCCGCCCGGCACCGCCCCC-3'; -1277/-1258: 5'-AAGTGGGGGTGGGGTG-3' and 5'- TCTCCACCCCACCCCC-3'; and -1828/-1809: 5'-CCCCACCCCCACCCCC-3' and 5'- CCCTGGGGGTGGGGGT-3'. Oligo pairs were combined at an equal molar ratio and annealed by heating to >95°C in a heating block then allowed to cool to room temperature over several hours. Probes were then radiolabeled using α-^{32}P dGTP by the Klenow fill-in method. Nuclear extracts were prepared from 1×10^7 RAW264.7 cells as previously described[101]. Briefly, RAW264.7

cells were stimulated for 45', washed twice with ice-cold PBS, then scraped from dishes and the cells pelleted by centrifugation. Nuclei were isolated by resuspending cells in 400µl of nuclei isolation buffer (10mM HEPES pH7.9, 10mM KCl, 0.1mM EDTA, 0.1mM EGTA, 1mM DTT, 0.5mM PMSF, 10µg/ml aprotinin, and 10µg/ml leupeptin) and incubating on ice for 15 minutes. 25µl of NP-40 was then added and nuclei pelleted by centrifugation at 12,000g for 40 seconds. Nuclei were washed with an additional 200µl of nuclei isolation buffer, then nuclear proteins extracted using 100µl of extraction buffer (20mM HEPES, 0.4M NaCl, 1mM EGTA, 1mM EDTA, 25% glycerol, 1mM DTT, 0.5mM PMSF, 10µg/ml aprotinin, and 10µg/ml leupeptin) and incubated on ice for 30 minutes. Insoluble nuclear material was then pelleted by centrifugation for 10 minutes at 14,000 RPM and supernatants containing soluble nuclear proteins collected. ^{32}P labeled double-stranded oligomers were incubated on ice for 1h with nuclear extracts, poly(DiDc), and BSA. Binding was competed with increasing concentrations (10×-50×) of cold unlabeled probe or consensus cold probe. DNA-Sp1 protein complexes were supershifted by incubating nuclear extracts with 1 or 3µg of antibody against Sp1 or Histone H3 for 30' on ice prior to incubation with labeled probe. DNA/Protein mixtures were run on 6% Acrylamide/0.25%TBE gels which were pre-run for one hour prior to loading.

Chromatin Immunoprecipitation (ChIP) Assay

ChIP assays were conducted using the ChIP Assay kit (Upstate Biotechnology) following the manufacturer's protocol with some modifications, as previously described[105]. Briefly, approximately 1×10^7 BMMΦ were stimulated in 100mm tissue

culture dishes for the time indicated in the figures, then fixed with formaldehyde at a final concentration of 1% for 10-15 minutes at room temperature. Cells were thoroughly washed with PBS containing protease and phosphatase inhibitors, then scraped and centrifuged. Fixed cells were resuspended in SDS lysis buffer containing inhibitors at a concentration of 10^7cells/ml and allowed to lyse on ice for 10 minutes. Lysed cells were separated into 200µl aliquots then DNA was sheared using a Cole Palmer ultrasonic processor (Cole-Parmer Instrument Company,Vernon Hills, IL). This resulted in relatively uniform DNA fragment size of approximately 300 bp[105]. Aliquots of the same time points were combined and diluted in ChIP dilution buffer. The remaining protocol of immunoprecipitation, washing, and elution, and purification of DNA was followed according to the manufacturer's protocol. HB-EGF (NC_000084) promoter primers used for ChIP analysis are presented in Table 4 (Chapter 4).

DNase Accessibility Assay

DNase accessibility assays were performed as previously described[106]. Briefly, 1×10^7 BMMΦ grown on 100mm tissue culture dished were stimulated with LPS+IC for the indicated times, then fixed with formaldehyde at a final concentration of 1%. Cells were thoroughly washed and scraped into cold PBS, then lysed in ice-cold Nuclei EZ lysis buffer (Sigma-Aldrich). Washed nuclei were resuspended in ice-cold DNase I buffer (100 mM NaCl, 50 mM Tris, pH 8.0, 3 mM $MgCl_2$, 0.15 mM spermine, and 0.5 mM spermidine) supplemented with 1 mM $CaCl_2$. DNase I (Roche Diagnostics) was added and incubated on ice for 1 hour. The reaction was stopped by adding DNase stop buffer (10mM EDTA, 20% SDS, and 0.4 M NaCl) and cross linking was reversed by incubation

at 65° for approximately 4 hours. Proteinase K and RNase A were added at 37° overnight. DNA was then purified by phenol/chloroform extraction and cold ethanol precipitation.

HB-EGF Promoter Reporter Construct

Approximately 3kb of the HB-EGF promoter was cloned using the following primers: Forward 5'-ACCTCGGAGACATGAGCTCTTAC-3' and reverse 5'-GCTACCCTCTCAATGAATTAAGCTA-3'. PCR was performed using Expand Long Template PCR System (Roche Diagnostics). The PCR product was ligated into the pCRII-TOPO vector (Invitrogen) for scale up. The cloned promoter fragment (-2704/+330, relative to transcriptional start site) was removed using NheI and EcoRV restriction enzymes, gel purified, then ligated into the pGL4.19[luc2CP/Neo] luciferase reporter vector (Promega Corporation, Madison, WI). The -1238/+330 promoter construct was made by KpnI digestion of the -2704/+330 construct, gel purification of the larger fragment and ligation. The -557/+330 promoter construct was made by digestion of the -2704/+330 construct with Tth111I and NheI restriction enzymes. The larger fragment was then gel purified and sticky ends were filled in using Klenow enzyme. The resultant fragment was then blunt-end ligated (Figure 7).

Mutation of the Sp1 site in the -557/+330 promoter construct was done using the QuikChange Site-Directed Mutagenesis kit II from Stratagene (La Jolla, CA) according to the manufacturer's instructions. The following primers were designed using Stratagene's QuikChange primer design program; Sense: 5'-GGGAGGGAAGGGGTAGGTGCCGGTAGGGTAGGGGCTCCCACTC-3' and

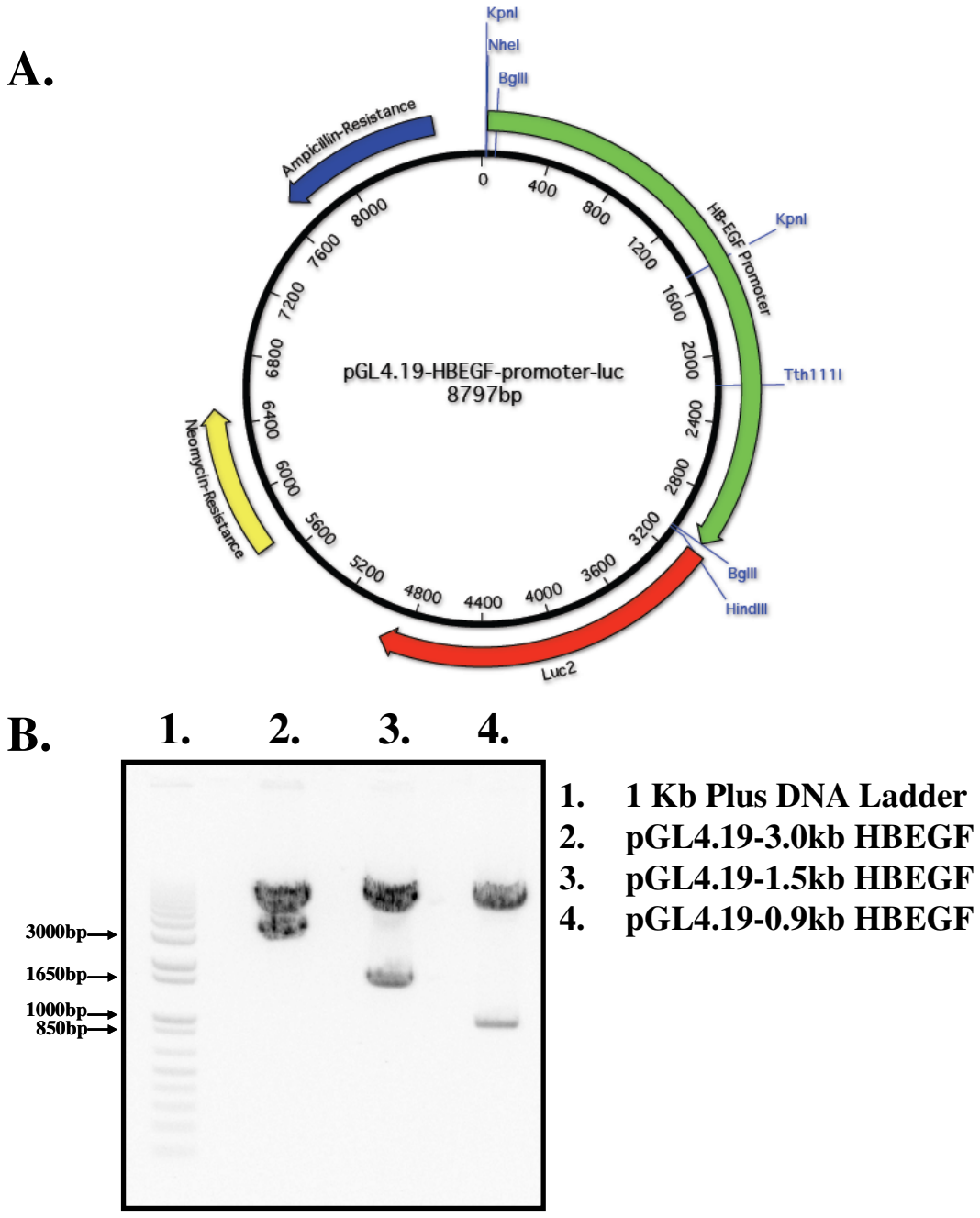

Figure 7: HB-EGF promoter luciferase plasmids.
(A) 3.0kb HB-EGF luciferase construct containing relevant restriction enzyme sites used in the construction and validation of 1.5kb and 0.9kb reporter plasmids. 1.5kb promoter plasmid was constructed by KpnI digestion followed by sticky-end ligation. 0.9kb promoter plasmid was constructed by NheI and Tht111l digestion, klenow fill-in, then blunt-end ligation. (B) Restriction enzyme analysis for validation of HB-EGF reporter constructs. 3.0kb and 1.5kb were digested using NheI and HindIII. 0.9kb was digested using KpnI and HindIII.

antisense: 5'-GAGTGGGAGCCCCTACCCTACCGGCACCTACCCCTTCCCTCCC. Mutations were confirmed by sequencing (Genewiz, Inc., South Plainfield, NJ).

Transient Transfection and Luciferase Activity

RAW264.7 cells were transiently transfected using the FuGENE HD transfection reagent according to the manufacturer's instructions. Briefly, 2μg of plasmid was added to 3μg of FuGENE diluted in 100μl of RPMI and incubated at room temperature for 30minutes. 20μl of the resultant transfection complex was added per well of a 48-well plate containing approximately 2×10^5 RAW cells. Each reporter construct was cotransfected with the pRL-Null *Renilla* luciferase plasmid at a ratio of 40:1.The following morning, media was replaced and cells were stimulated according to the figure for approximately 8 hours. Luciferase activity was assessed using the Dual-Luciferase Reporter Assay System (Promega). Firefly luciferase activity was measured for each HB-EGF reporter construct and normalized using *Renilla* luciferase activity.

5' Rapid Amplification of cDNA Ends (RACE) for HB-EGF

5' RACE was performed using the FirstChoice RLM-RACE from Ambion (Austin, Texas) according to the manufacturer's instructions using total RNA from 120' LPS+IC stimulated macrophages. Briefly, total RNA was treated with calf intestinal alkaline phosphatase to remove free 5'-phosphates from nucleic acids lacking a 5' cap. The 5' cap was then removed using tobacco acid pyrophosphatase. A RACE adaptor oligonucleotide was then ligated to the 5' end of full length RNA and reverse transcription performed. A nested PCR reaction was performed using RACE adaptor-

specific (provided) and HB-EGF specific oligonucleotides. The reverse (HB-EGF specific) oligonucleotides used were: (outer primer) 5'GGCATTTGCAAGAGGGAGTA-3' and (inner primer) 5'-GTGGGTAGCAGCTGGTTTGT-3'. The nested PCR reaction was attempted using the Fast Start High Fidelity PCR System (Roche, Mannheim, Germany) or Platinum PCR Supermix High Fidelity from Invitrogen, which were unsuccessful and successful, respectively. These PCR reactions are presented in Figure25A and labeled PCR 1-1 and 1-2 for the Fast Start High Fidelity PCR System and PCR 2-1 and 2-2 for the Platinum PCR Supermix High Fidelity. The nested PCR reaction 2-2 produced a major band of the expected length of approximately 450bp. The PCR product was directly ligated into the pCR4-TOPO plasmid using the TOPO TA cloning kit for sequencing from Invitrogen and transformed into Top10 chemically competent E. coli. Restriction digestion of clones with EcoRI revealed clones of three sizes, (Figure 25B) all of which were sequenced.

Tumor Associated Macrophage Isolation

Tumor associated macrophages were isolated from 15-20mm tumors. Tumors were excised from the hind leg of the mice and physically disrupted in a filter sterilized solution of RPMI containing 0.3% Type IV Collagenase (Worthington) and 200mg/ml DNase (Roche). Enzyme digestion of finely minced tumors was allowed to proceed for approximately 30'-45' at 37°C. Digested tumor was diluted in RPMI and passed through a 100μM nylon filter into a 50ml tube. After centrifugation, cells were resuspended in ACK lysis buffer to lyse contaminating red blood cells, then centrifuged and resuspended in RPMI and plated out onto ten 100mm tissue culture dishes. Cells were incubated for 1

hour at 37°C to select for adherent cells. Tissue culture dishes were thoroughly washed five times with warm RPMI and adherent cells were removed using CellStripper. Adherent cells were then counted and stained with PerCP-Cy5.5 α-CD11b (Clone M1/70) and FITC α-F4/80 (Clone BM8). Double positive cells were then sorted and allowed to recover for 1 hour at 37°C prior to stimulation.

Immunoprecipitation Kinase Assay

Immunoprecipitation kinase assays were performed similar to Upstate's immunoprecipitation radioactive kinase assay protocol, without using radioactivity. 2×10^6 cells were plated overnight then given immune complexes with or without LPS or left unstimulated for times indicated in figure 37. Cells were then washed with cold PBS and lysed with 200µl buffer A (50 mM Tris-HCl, ph 7.5, 1mM EDTA, 1mM EGTA, 0.1% (v/v) 2-metcaptoethanol, 1% Triton X-100, 5-mM) supplemented with a protease inhibitor cocktail (Roche) and phosphatase inhibitors (5mM sodium pyrophosphate, 0.5mM NaV, 50mM NaF, 10mM β-glycerophosphate). Insoluble material was removed by centrifugation for 10' at 10,000 RPM and lysates pre-cleared with Protein G-PLUS Agarose (Santa Cruz). 50µl of precleared cell lysate was added to 200µl of buffer A with 5µg of anti-MSK1 or anti-MSK2 at 4^oC overnight. MSK-Ab complex was precipitated by adding 100µl of 25% Protein G-PLUS Agarose slurry at 4^oC for 2 hours. Agarose beads were washed two times with buffer A then with assay dilution buffer I (20mM MOPS, pH 7.2, 5mM EGTA, 25mM β-glycerophosphate, 1mM $NaVO_4$ and 1mM dithiothreitol).

Beads were then resuspended in assay 20µl of ADBI, then 10µl of 500µM ATP and 10µl of 200 µg/ml recombinant human histone H3 (Upstate) was added. This was

then incubated at 30°C for 15 minutes with agitation every 5 minutes. The reaction was terminated by spinning down beads and adding supernatants to an equal volume of 2x sample buffer then boiling for 3 minutes. Samples were subject to PAGE and blotted for anti-phosphorylated histone H3 (S10).

siRNA Design and Transfection

Potential siRNA targets were found using Ambion's online siRNA target finder and the corresponding sense and antisense siRNA oligonucleotides used for the Silencer™ in vitro siRNA Construction Kit (Ambion) were designed. siRNAs were constructed according to the manufacturer's instructions. Briefly, two 29-mer DNA template oligonucleotides consisting of 21 nucleotides encoding the siRNA and 8 nucleotides complementary to the T7 Promoter Primer were annealed to the T7 promoter primer and filled in with DNA polymerase. Sense and antisense templates were transcribed by T7 RNA polymerase. These RNA transcripts were hybridized to create dsRNA. Leader sequences were removed using single-strand RNase and DNA templates removed with DNase and the remaining dsRNA purified. The resultant product is double stranded 21-mer. The following oligonucleotides were used to construct siRNAs for MSK2 and MSK1/2: MSK2, 5'-AAGTACAAGATGTTCTCGGGTCCTGTCTC-3' and 5'-AAACCCGAGAACATCTTGTACCCTGTCTC-3'; MSK1/2, 5'-AAACAGGACTCATCGTAGCCACCTGTCTC-3' and 5'-AATGGCTACGATGAGTCCTGTCCTGTCTC-3'.

$5x10^6$ macrophages cultured for 6 or 7 days were used for each transfection. Macrophages were resuspended in 100µl of Cell Line Kit T transfection solution

(Amaxa) with 1µl of 10µM (100nM final concentration) dsRNA. This suspension was added to transfection cuvettes and transfected with the Amaxa's nucleofector device (program T20). Cells were resuspended in warm media containing growth factors and then cell yield was determined. Cells were then added to preincubated media and cultured for 24 hours. Additional media was added and cultured for an additional 24 hours before silencing efficiency was determined by RT-PCR and cells assayed for cytokine production.

CHAPTER 3: CHARACTERIZATION OF THREE ACTIVATED MACROPHAGE POPULATIONS

Activated macrophages differ in cytokine production

We generated three distinct populations of activated macrophages *in vitro* from murine bone-marrow derived macrophages, and performed a series of parallel comparisons between them. As a first step, we measured cytokine production from each of these cells. Classically activated macrophages have long been associated with the secretion of IL-12[148], whereas MΦ-II were previously shown by the lab to produce high amounts of IL-10[92]. Others have also suggested that the AA-MΦ were also a good source of IL-10[149]. Cytokine production from these three populations of macrophages was compared. Ca-MΦ produced relatively high levels of IL-12/23P40 but low levels of IL-l0 (Figure 8A). Coupling macrophage activation with FcγR ligation by the addition of immune complexes (IC) resulted in a population of macrophages (MΦ-II) that produced high levels of IL-10 and low levels of IL-12/23p40 (Figure 8A), as previously reported[90]. Priming of these cells with IFN-γ was not necessary to see this reciprocal alteration in cytokine production caused by the addition of IC (Figure 8B).

IL-4 treated macrophages (AA-MΦ) failed to secrete detectable levels of either IL-12/23p40 or IL-10 (Figure 8A). Cytokine production by AA-MΦ was not significantly different from unstimulated macrophages. Because previous studies reported that macrophages isolated from infections in which IL-4 predominated were a rich source of IL-10[150], we primed macrophages with IL-4 overnight and then stimulated them with LPS the next morning and examined cytokine production. The stimulation of IL-4-primed

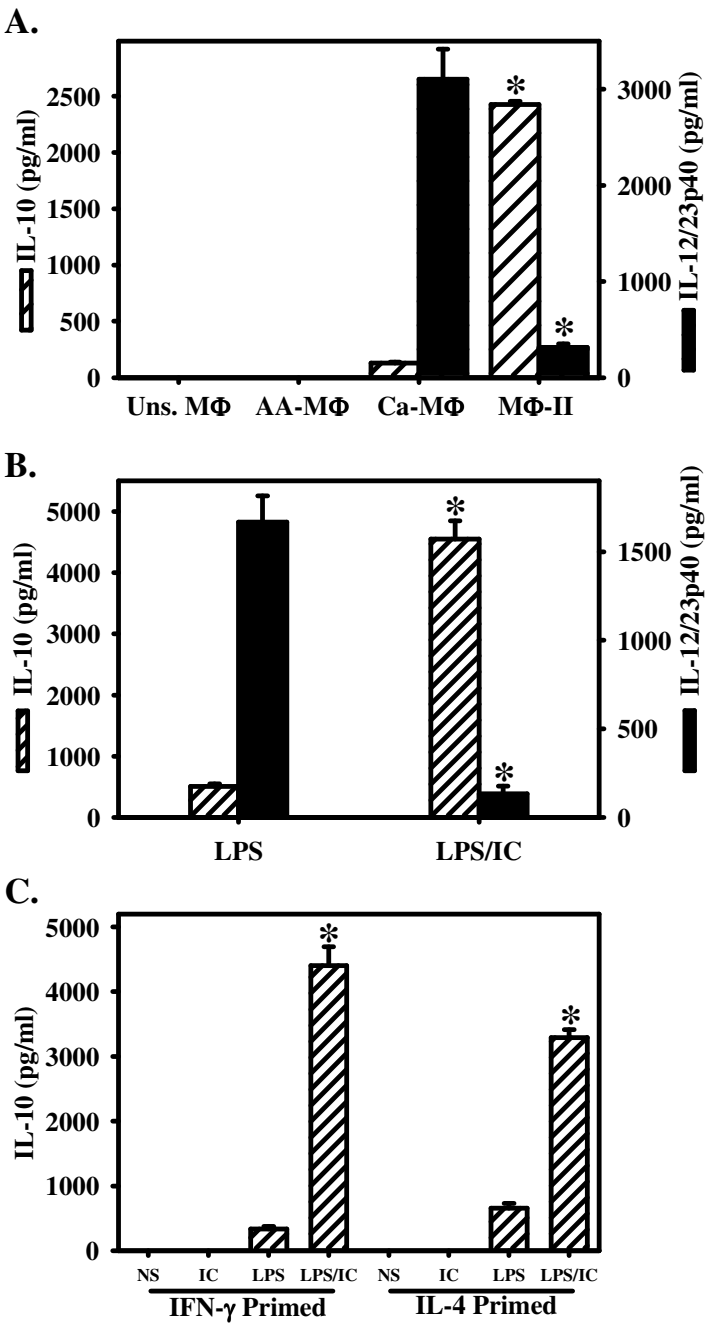

Figure 8: Cytokine profiles of activated macrophages.
(A) IL-10 (hatched bars, left axis) and IL-12/23p40 (solid bars, right) were measured by ELISA 16 h after macrophage activation. AA-MΦ were prepared by treating macrophages overnight with IL-4 (10U/ml). Ca-MΦ and MΦ-II were prepared by treated macrophages with IFN-γ (100U/ml) overnight, then stimulating with LPS or LPS/IC, respectively. (B) IL-10 (hatched bars) and IL-12/23P40 (black bars) levels in supernatants following a 16 hr stimulation of cells with LPS or LPS/IC. These cells were not primed with IFN-γ. (C) IL-10 levels in macrophages primed overnight with IFN-γ or IL-4, then left unstimulated or stimulated with immune complexes(IC), LPS, or LPS/IC. Figures are representative of at least three independent experiments. Error bars indicate mean± SD. *p<0.001

cells with LPS resulted in a modest increase in the production of IL-10 (Figure 8C). However, the level of this cytokine remained substantially below that of MΦ-II. IL-4 primed cells were also stimulated with LPS+IC. These IL-4 primed cells also responded to the addition of IC by secreting high levels of IL-10 (Figure 8C). Thus, all three populations of activated macrophages display distinct profiles of cytokine production, and yet these cells exhibit functional plasticity. Thus, the nature, order, and/or duration of stimulation can influence cytokine production, as previously reported[151].

Activated macrophages exhibit different patterns of arginine metabolism

Alterations in arginine metabolism have previously been described as one of the defining characteristics of murine alternatively activated macrophages. Therefore, we examined iNOS and arginase production in each of the three macrophage populations. First we measured the accumulation of NO_2^- in culture supernatants by the Greiss assay[146]. Both Ca-MΦ and MΦ-II produced relatively high levels of NO, whereas the AA-MΦ produced virtually no detectable NO (Figure 9A). We also measured the amount of urea generated by these three populations of macrophages. Ca-MΦ and MΦ-II possessed virtually no arginase activity above that of the basal level associated with unstimulated macrophages, therefore were unable to produce appreciable urea when lysates were incubated with L-arginine. The opposite was true of the AA-MΦ which produced high levels of urea (Figure 9B). Thus, with regard to arginine metabolism, AA-MΦ were distinct from the other two populations of macrophages. AA-MΦ failed to produce NO but readily catabolized arginine to urea, whereas the converse was true for Ca-MΦ and MΦ-II (Figure 9).

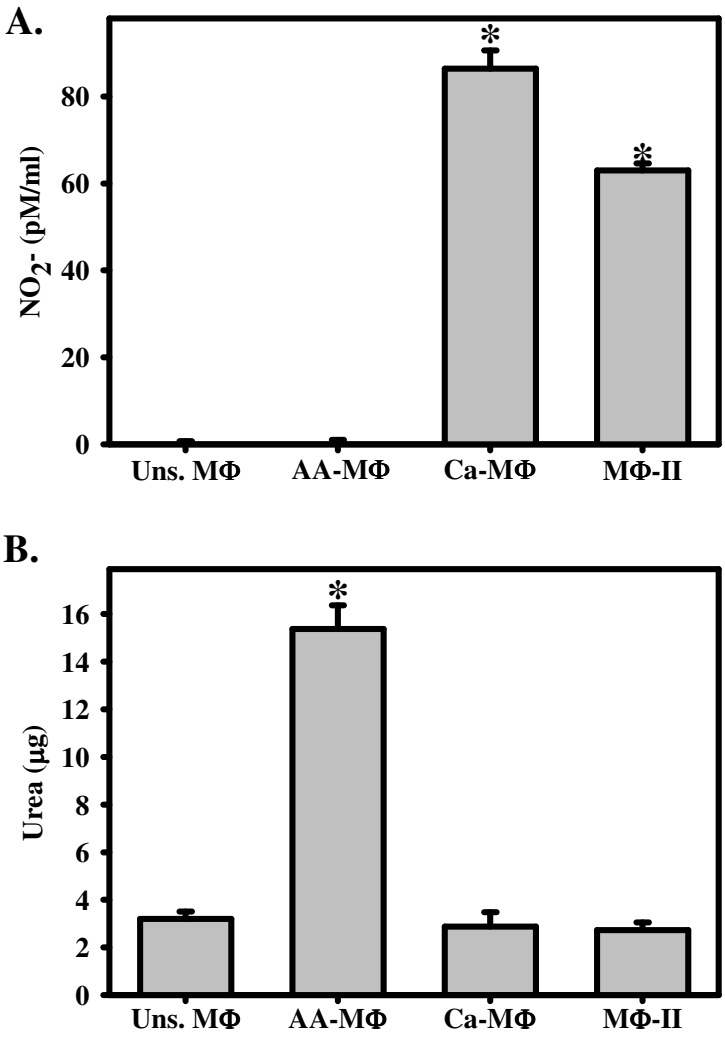

Figure 9: Activated macrophages exhibit different patterns of arginine metabolism. (A) NO_2^- accumulation after 24 hours of macrophage activation measuring iNOS activity. Equal volumes of cell supernatants were mixed with Greiss regeant for 10 minutes, and the absorbance at 540λ was measured. A solution of NO_2^- was used to construct a standard curve. (B) Arginase assay measuring the formation of urea after incubation of lysates from activated macrophages with arginine. Arginase enzyme was activated by heating for 10' at 55°C. The hydrolysis of arginine to ornithine and urea was conducted by incubating the lysates with L-arginine at 37°C for 60 min. The reaction was stopped and urea measured at 550 nm after addition of α-isonitrosopropiophenone followed by heating at 100°C for 30 min. Values were compared to a standard curve of urea concentrations. Figures are representative of at least three independent experiments. Error bars indicate ± SD. *$p<0.00001$

Biochemical Markers to discriminate between populations of macrophages

RNA was isolated from the three populations of activated macrophages 4 hours after stimulation, and analyzed by RT-PCR (Figure 10). We first examined iNOS and Arg-1 mRNA in each of the three populations. As previously reported, and consistent with the protein activity data above, macrophages exposed to the Th2 associated cytokine IL-4 produced mRNA for arginase but failed to produce iNOS mRNA[152]. Conversely, Ca-MΦ and MΦ-II express iNOS mRNA, but fail to express appreciable arginase (Figure 10). Ca-MΦ produce high levels of IL-12/23p40 but little detectable IL-10, whereas MΦ-II express high levels of IL-10 and less IL-12/23p40. Only the AA-MΦ expressed the previously described marker FIZZ1, a secreted protein that has been associated with allergic and pulmonary inflammation[153,154], confirming that FIZZ1 represents a reliable marker for murine AA-MΦ (Figure 10).

Since there have been no reported markers for MΦ-II we performed an initial microarray analysis using the Affimetrix GeneChip Mouse Genome 430 2.0. The analysis included a comparison between Ca-MΦ and MΦ-II, since these two populations of cells exhibited several biochemical similarities (Figure 10). Microarray analysis revealed a limited number of changes in gene expression between these two cell types. When a 2-fold difference in transcript levels was used as the cut-off, only 184 of the 39,000 possible transcripts represented on this chip (<0.5%) were consistently increased in MΦ-II relative to Ca-MΦ. Table 3 lists 29 genes of known biological function which were increased by 3-fold or more in MΦ-II, and which had a signal greater than 2000. These 29 genes are the only ones that fit these criteria. The data discussed in this publication have been deposited in NCBI's Gene Expression Omnibus (GEO,

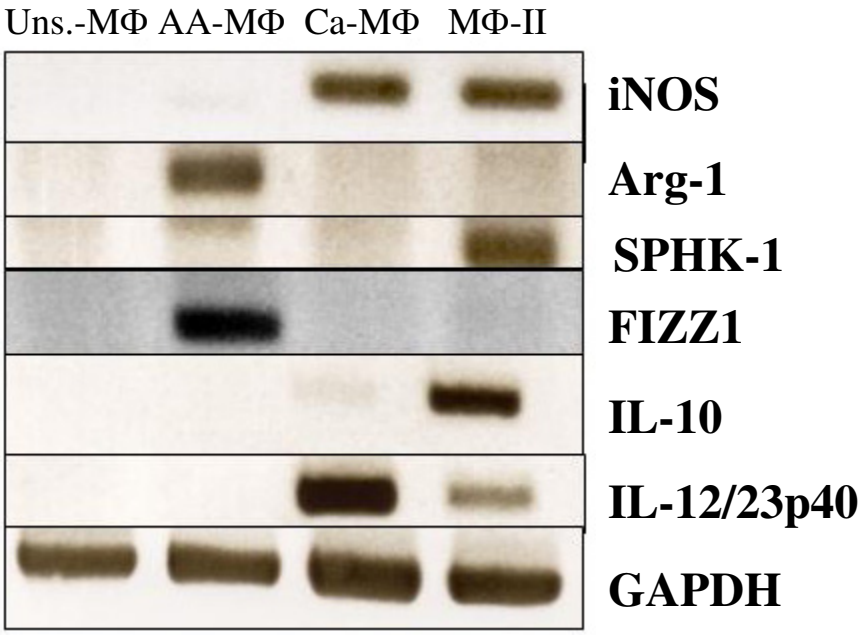

Figure 10: Activated macrophages have different mRNA expression profiles. RT-PCR was performed to examine the expression of iNOS, Arg-1, SPHK-1, FIZZ1, IL-10, and IL-12/23p40 mRNA levels in four different macrophage populations. cDNA from unstimulated macrophages and the three activated macrophage populations, was reverse transcribed from total RNA four hours after stimulation. GAPDH mRNA was used to normalize loading. Figures are representative of at least three independent experiments.

Gene Symbol	Gene Name	Average Signal	Average Fold Change
Bcar3	breast cancer anti-estrogen resistance 3	3479.25	3.031
Bhlhb2	basic helix-loop-helix domain containing, class B, 2	2579.85	4.203
Dusp4	dual specificity phosphatase 4	2713.25	3.375
Emp1	epithelial membrane protein 1	6476.5	4.297
Fabp4	fatty acid binding protein 4	5134.4	7.222
Fosb	FBJ osteosarcoma oncogene B	2357.35	3.711
Gadd45g	growth arrest and DNA-damage-inducible 45 gamma	2487.2	5.78
Gas2l3	growth arrest-specific 2 like 3	6283.1	5.291
Hbegf	heparin-binding EGF-like growth factor	6600.95	7.956
Hmox1	heme oxygenase (decycling) 1	2805.8	4.297
Ifnb1	interferon beta 1	3703.8	3.186
Il10	interleukin 10	12817.6	3.249
Impact	imprinted and ancient	2049.6	3.516
Klf9	Kruppel-like factor 9	2844.65	3.639
Mafb	v-maf musculoaponeurotic fibrosarcoma oncogene family, protein B	3254.3	4.76
Ndrg1	N-myc downstream regulated gene 1	8642.7	3.28
Ndrl	N-myc downstream regulated-like	6851.45	3.186
Plau	plasminogen activator, urokinase	5734.55	3.155
Plk2	polo-like kinase 2	3925.6	6.981
Rgc32	response gene to complement 32	2356.9	6.28
Rhov	ras homolog gene family, member V	4564.9	7.423
Ris2 (cdt1)	chromatin licensing and DNA replication factor 1	3508.2	3.14
Samd8	sterile alpha motif domain containing 8	2713.4	3.155
Sgk	serum/glucocorticoid regulated kinase 1	6724.3	3.155
Slc6a8	solute carrier family 6 (neurotransmitter transporter, creatine), member 8	2382.25	3.015
Snx30	sorting nexin family member 30	6079.5	4.06
Sphk1	sphingosine kinase 1	2449.95	3.257
Tnfsf14	tumor necrosis factor (ligand) superfamily, member 14	2281.05	8.657
Vps18	vacuolar protein sorting 18	5875.6	4.972

Table 3: Increases in gene expression in MΦ-II relative to Ca-MΦ. Includes genes with known biological function that exhibited a signal greater than 2000 and an average fold change of 3 or more.

number GSE4811.

From this analysis, several genes that were up-regulated in MΦ-II were examined. Sphingosine kinase-1 was shown to be upregulated by more than 3-fold in MΦ-II, relative to Ca-MΦ at 2 h poststimulation. We therefore compared SPHK-1 mRNA levels in the three macrophage populations. Only the Type II activated macrophages expressed detectable levels of SPHK-1 mRNA by conventional PCR four hours after stimulation (Figure 10). This observation was extended by quantitative real-time PCR (QRT-PCR) (Figure 11A). This analysis revealed that SPHK-1 mRNA was robustly induced in MΦ-II, with mRNA levels increasing substantially over time, relative to unstimulated cells (Figure 11A). There was some induction of SPHK-1 mRNA in Ca-MΦ, however this induction was modest relative to MΦ-II. Thus, high SPHK-1 expression may be useful to identify MΦ-II in tissue.

Since mice have two forms of sphingosine kinase-1, SPHK1a and SPHK1b, we decided to determine which of these two isoforms was up-regulated by the type II activated macrophage. These isoforms differ in both in their enzymatic activity, but also in their characteristics. The SPHK1a exhibits higher enzymatic activity, stability, and is localized to the cytoplasm, while SPHK1b is relatively unstable and localized to membrane fractions[155,156]. The expression of SPHK1 was monitored by isoform specific primers after stimulation with LPS or LPS+IC (Figure 12). The expression of SPHK1a was strongly induced after stimulation with LPS+IC, whereas there was a relatively modest increase after stimulation with LPS alone (Figure 12A). Neither stimulation condition resulted in an appreciable change in the expression of SPHK1b (Figure 12B).

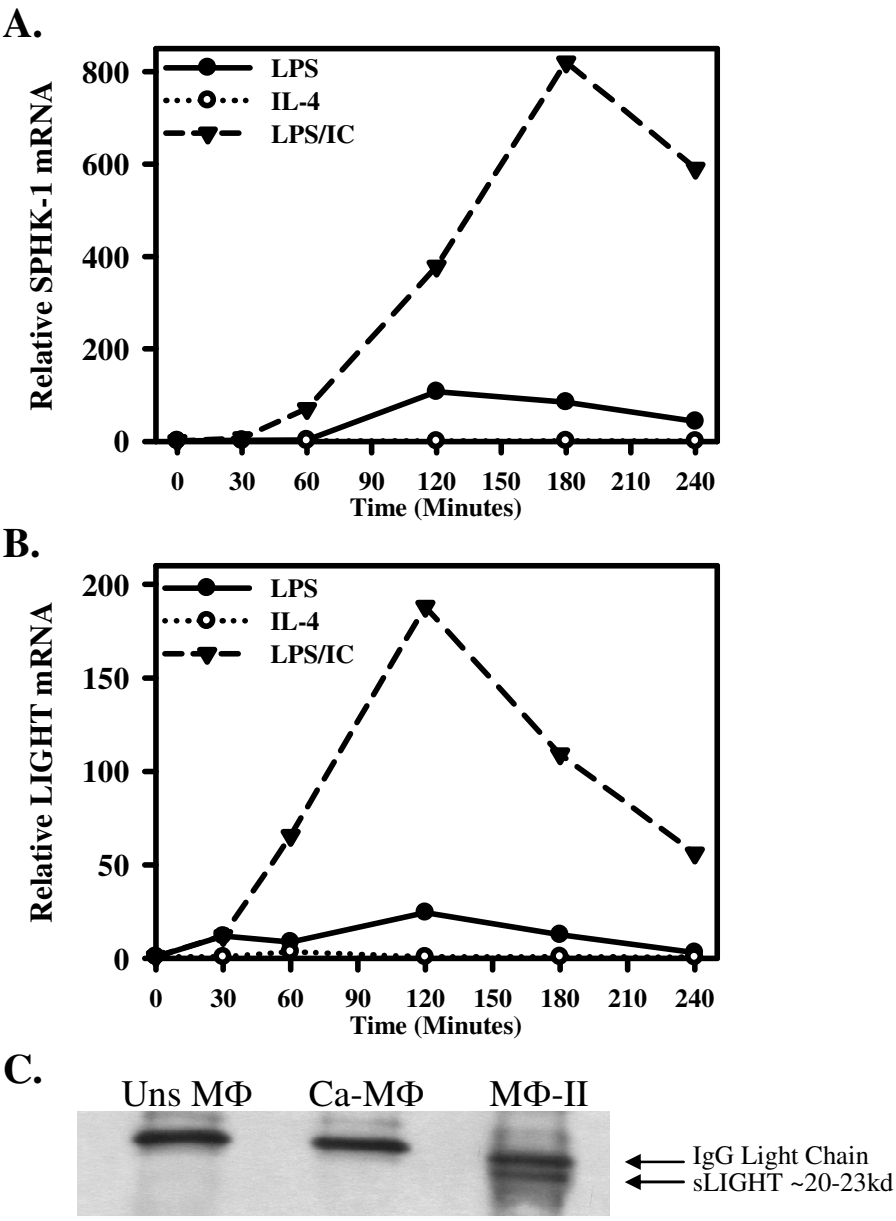

Figure 11: Type-II activated macrophages upregulate sphingosine kinase-1 (SPHK-1) and TNFSF14/LIGHT.

(A) SPHK-1 mRNA was measured by QRT-PCR after macrophage activation by LPS (closed circles), LPS and immune complexes (LPS/IC, closed triangles), or IL-4 (open circles). (B) Relative LIGHT mRNA was measured by QRT-PCR after macrophage activation by LPS (closed circles), LPS/IC (closed triangles), or IL-4 (open circles). Fold values are relative to unstimulated control. (C) Immunoprecipitation of soluble LIGHT from 6h cell supernatants of unstimulated macrophages, Ca-MΦ, and MΦ-II. Western blot analysis for LIGHT using a rat α-LIGHT monoclonal antibody, showing the soluble form of LIGHT present as a 20-23kd protein. Figures are representative of at least three independent experiments.

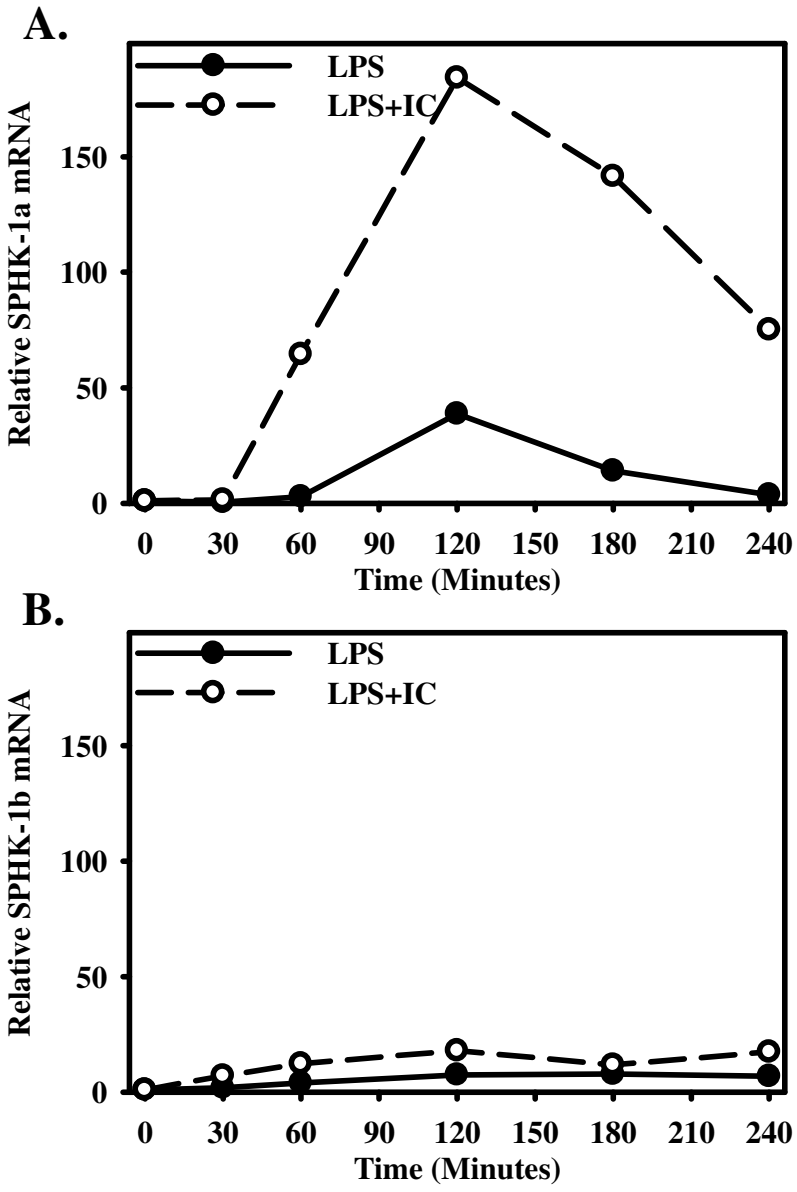

Figure 12: Expression of Sphingosine Kinase-1 splice variants SPHK1a and SPHK1b.

Macrophages were stimulated with LPS or LPS+IC and relative SPHK1a (A) and SPHK1b (B) mRNA levels were measured by QRT-PCR after 0', 30', 60', 120', 180', and 240'. Values are relative to mRNA levels present at 0'. Figures are representative of two independent experiments.

Type II Activated Macrophages express LIGHT, a member of the TNF superfamily

From the microarray analysis, another marker for MΦ-II emerged. This was murine LIGHT or TNFSF14. It was found to be present at more than 8.5-fold higher levels in the MΦ-II relative to Ca-MΦ. In order to confirm LIGHT mRNA induction in MΦ-II, QRT-PCR was performed to compare mRNA levels in the three macrophage populations. In the MΦ-II, LIGHT mRNA increased by approximately 200-fold over unstimulated cells, peaking at 2 hours post-stimulation (Figure 11B). Classically activated macrophages had a slight induction of LIGHT mRNA, but these levels were always at least 10-fold lower than these observed in MΦ-II (Figure 11B). There was no evidence for LIGHT induction in AA-MΦ and in fact the addition of IL-4 marginally decreased LIGHT mRNA levels in AA-MΦ.

It has previously been reported that LIGHT may be secreted or cleaved from the surface of cells in a soluble form. In order to address this possibility, macrophages were primed with IFN-γ, and then stimulated for 6 hours with LPS or LPS+I.C. IL-4 treated macrophages were not addressed because the expression of LIGHT was not induced in this population (Figure 11b). LIGHT was then immunoprecipitated from the supernatants of stimulated cells with a monoclonal antibody specific for the extracellular domain of LIGHT. A ~20-25 kD band, which corresponds to the molecular mass of soluble LIGHT (sLIGHT), was detected only in the supernatants of MΦ-II (Figure 11C). This suggests that MΦ-II are the primary macrophage producers of LIGHT, and that this molecule is either rapidly cleaved from the surface of these cells or secreted as soluble LIGHT by MΦ-II.

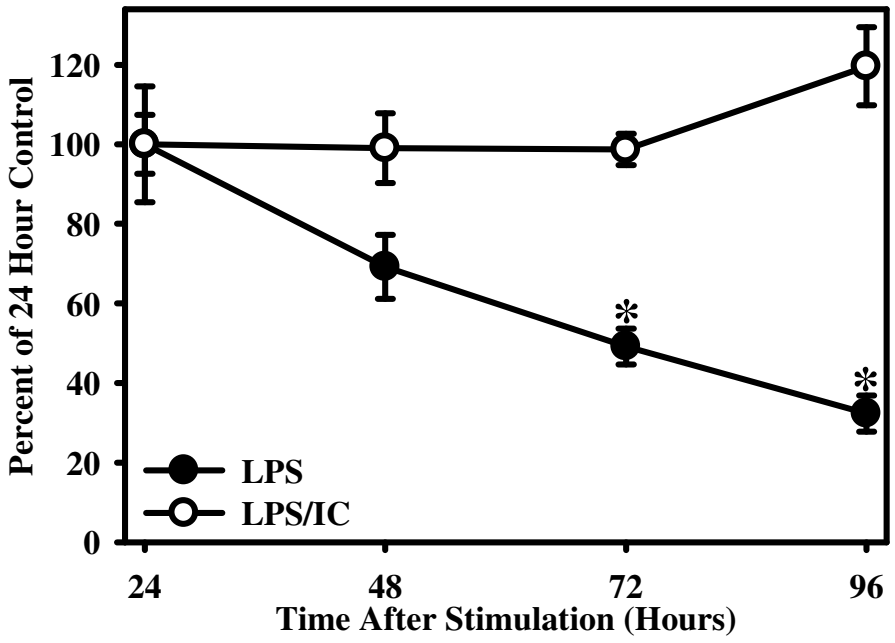

Figure 13: Macrophages stimulated with LPS+IC retain viability.
MTT assays were performed to measure the conversion of MTT to purple formazan. 2×10^5 BMMΦ were stimulated with LPS or LPS/IC, then assayed every 24 hours. For each time point, macrophages were incubated with MTT for 2 hours, lysed, then absorbance measured at 550λ. Each time point was performed in triplicate and normalized to the absorbance at 24 hours. Asterisk indicates $p<0.001$.

Type II Activated Macrophages Retain Long-Term Viability

It has previously been reported that the induction of sphingosine kinase is important for retaining cell viability in endotoxin stimulated macrophages. In these studies, the use of a sphingosine kinase specific siRNA sensitized the macrophage cell line RAW264.7 cells, as well as primary macrophages to LPS-induced apoptosis[157]. As we see relatively high induction of sphingosine kinase in macrophages stimulated with LPS+IC, we wanted to address whether stimulation of macrophages in the presence of immune complexes enhances the viability of macrophages over LPS stimulated cells. Macrophages were stimulated with LPS or LPS+IC for a 24, 48, 72, or 96 hours. Changes in cell viability were measured by MTT conversion to formazan (Figure 13). Over this period of time, macrophages stimulated with LPS lost viability. However, when macrophages were stimulated with LPS+IC, they retained their viability over 96 hours (Figure 13). Although this is certainly not definitive, the induction of sphingosine kinase by MΦ-II may contribute to sustained viability of these cells.

Antigen presentation by activated macrophages

Activated macrophages are able to present antigen to T cells[91]. We wished to examine the antigen presenting potential of each of the three macrophage populations. One of the defining characteristics of efficient APCs is the expression of MHC class II and B7 costimulatory molecules. BMMΦ were primed with IFN-γ overnight or left unprimed. Primed cells were then stimulated for 24 hours with LPS (Ca-MΦ), or LPS + IgG-OVA immune complexes (MΦ-II). AA-MΦ were stimulated with IL-4. These cells were then stained with FITC-conjugated α-I-A^d or PE-conjugated α-CD86. Expression

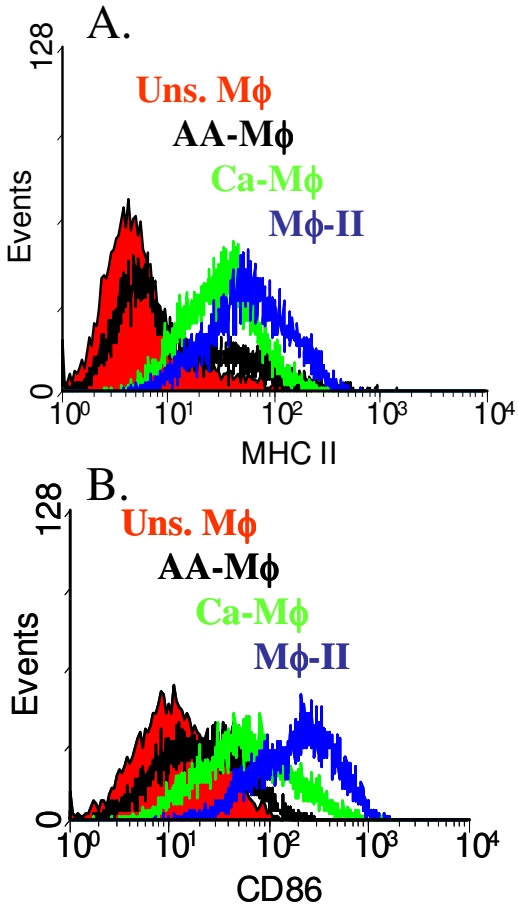

Figure 14: Activated macrophages express different levels of MHC class II and B7 costimulatory molecules.
Flow cytometry profiles for (A) MHC class II and (B) B7.2 (CD86) on activated macrophages 24 hours after stimulation. Macrophages were primed with IFN-γ and stimulated with LPS (Ca-MΦ) or LPS+IC (MΦ-II), primed with IL-4 (AA-MΦ), or left unstimulated (Uns. MΦ). Macrophages were stained with FITC conjugated α-I-A^d or PE-conjugated α-CD86. Changes in expression are assessed by comparison against unstimulated macrophages. Figures are representative of at least three independent experiments.

in activated cells was compared to that of unstimulated macrophages. MΦ-II had the highest expression of MHC class II (Figure 14A) and CD86 (Figure 14B). Ca-MΦ also up-regulated MHC class II and CD86, although not to the level of MΦ-II. In contrast, AA-MΦ only minimally up-regulated MHC class II and CD86 expression. Thus, the three macrophage populations express distinct levels of these molecules and therefore may have different potential to present antigen to T cells.

Each of the macrophage populations were analyzed for their ability to present ovalbumin antigen (OVA) to naïve OVA-specific DO11.10 T cells. For these studies BMMΦ were primed overnight with IFN-γ (100 U/ml) or IL-4 (10 U/ml, AA-MΦ). Cells primed with IL-4 overnight were confirmed to have high arginase and FIZZ1 expression (data not shown). Cells were washed and stimulated with LPS+OVA (Ca-MΦ), or LPS+IgG-OVA (MΦ-II), or OVA alone (AA-MΦ and unstimulated macrophages). $CD3^+$ T cells were isolated from total splenocytes from DO11.10 mice and added to macrophages 2 hours after activation. T cells and macrophages were co-cultured for 24 hours, and then stained for CD25, CD69, and CD62L expression. CD25 and CD69 typically increase with T cell activation, whereas CD62L decreases[158-160]. The expression of each marker was assessed by flow cytometry, gating on $Thyl.2^+$ cells. As expected, unstimulated macrophages were poor APCs, driving minimal up-regulation of CD25 (Figure 15, left panels) and CD69 (Figure 15, center panels) by T cells. They also induced only minimal down-regulation of CD62L (Figure 15, right panels). T cells co-cultured with MΦ-II showed the greatest signs of activation, expressing the highest levels of CD25 and CD69 expression and the lowest expression of CD62L (Figure 15). Thus, despite the potent production of IL-10 from MΦ-II, these cells are very effective

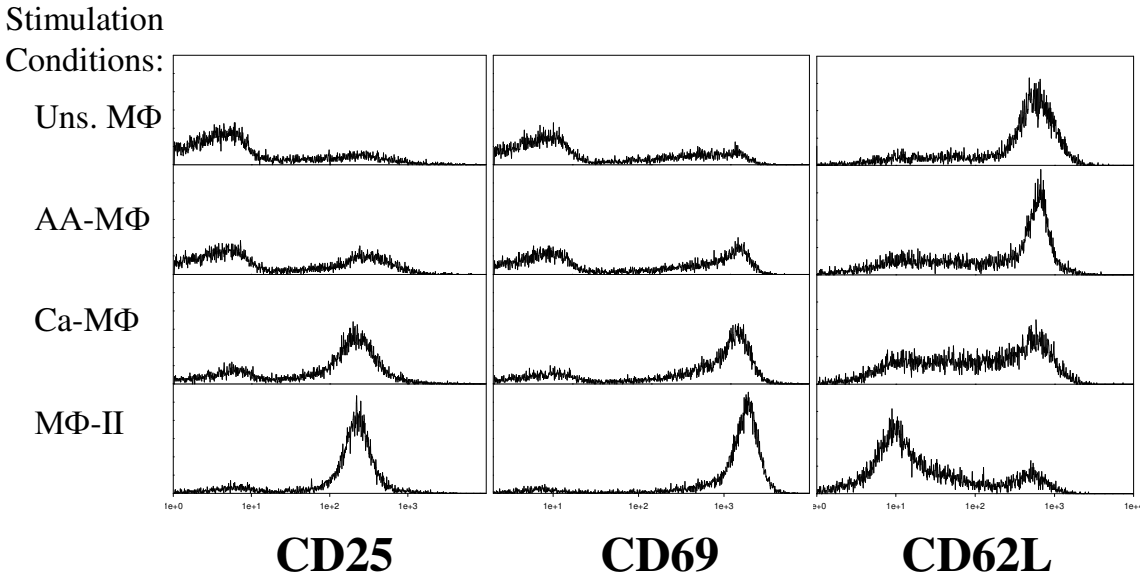

Figure 15: Activated macrophages drive different levels of T cell activation. DO11.10 T-cells were stained after 24 hours of co-culture with unstimulated (top panels), alternatively activated (upper middle panels), classically activated (lower middle panels), and type-Il activated macrophages (bottom panels) in the presence of antigen. T cells were selected by gating for Thyl.2^{+} cells, then measured for CD25 (left), CD69 (center), and CD62L (right) expression. Figures are representative of at least three independent experiments.

activators of naïve T cells. The co-cultivation of T cells with Ca-MΦ was also able to induce T cell activation markers, albeit slightly less than MΦ-II. There was a slight decrease in the up-regulation of CD25 and CD69 and less of a down-regulation of CD62L (Figure 15). Alternatively activated macrophages induced only minimal signs of T cell activation, which were similar to unstimulated macrophages. Thus, MΦ-II appear to be very efficient antigen presenting cells, and this is in stark contrast to AA-MΦ which were poor at inducing T cell activation.

Activated macrophages drive different levels of T-cell proliferation

To directly compare T cell activation by these three populations of macrophages, $CD3^+$ T-cells were CFSE stained, and added to each population of macrophages 2 hours after stimulation in the presence of antigen. Macrophages and T cells were co-cultured for 96 hours and stained with PE-conjugated α-Thy 1.2. Proliferation of $Thyl.2^+$ cells was assessed by flow cytometry. As expected, resting macrophages given antigen alone were able to drive only minimal levels of T cell proliferation, as shown by minimal dilution of the CFSE stain (Figure 16A). AA-MΦ were equally poor at driving T cell proliferation (Figure 16A). Both CA-MΦ and MΦ-II induced a robust primary T cell response characterized by several rounds of T cell proliferation (Figure 16A). Thus, MΦ-II are particularly effective as APCs, inducing the rapid expression of early activation markers (Figure 15) supporting T cell proliferation (Figure 16). AA-MΦ, in contrast, are relatively poor at inducing T cell activation markers and they fail to support the proliferation of naïve T cells. Even after stimulation with LPS, IL-4 primed macrophages failed to support substantial amounts of T cell proliferation (Figure 16B).

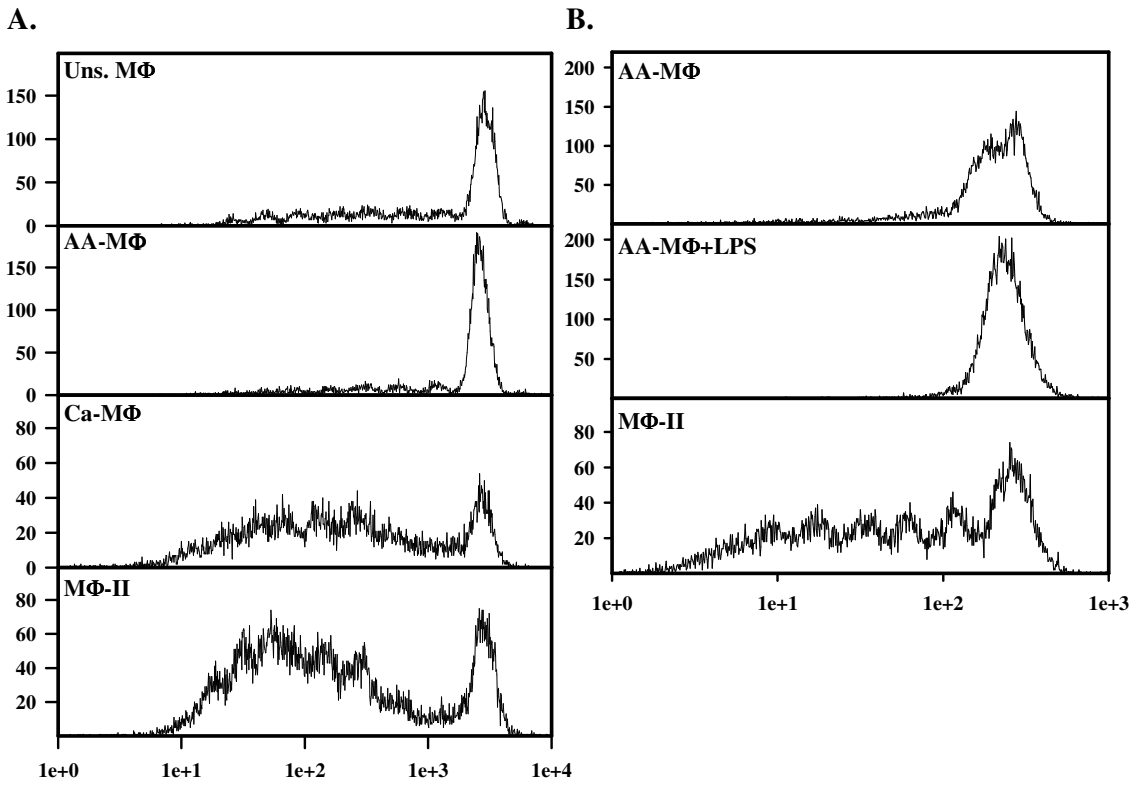

Figure 16: Activated macrophages drive different levels of T cell proliferation. (A) Naïve T cells were isolated from total splenocytes from DO11.10 mice, CFSE stained, then co-cultured in the presence of unstimulated (top panel), alternatively activated (upper middle panel), classically activated (lower middle panel), or type-II activated macrophages (bottom panel) in the presence of 150 μg/ml OVA. CFSE profiles of Thy1.2^{+} T cells were measured after 96 hours of co-culture. (B) AA-MΦ given OVA alone (upper panel) or OVA+LPS (10ng/ml, center panel). MΦ-II were used as antigen presenting cells as in (A.) as a control. Figures are representative of at least three independent experiments.

T-cell Biasing by Activated Macrophage Populations

We also examined secondary T cell responses to antigen and APCs. For these assays, T cells were stimulated with each of the macrophage populations and antigen for 7 days. T cells were washed and restimulated under non-biasing conditions with plate bound anti-CD3 for 24 hours. Cytokine levels were measured by ELISA. Although cytokine production from T cells activated by MΦ-II has previously been examined[91], a comparison between the three cell types has not been reported. T-cells activated by Ca-MΦ (LPS+OVA) produced relatively high levels of IFN-γ and less IL-4, whereas T-cells activated by MΦ-II produced relatively high levels of IL-4 and significantly reduced levels of IFN-γ (Figure 17A), as previously reported[91]. We measured IL-10 production from these T cells. MΦ-II give rise to T cells that produced high levels of IL-10 in the secondary response, whereas Ca-MΦ induced a population of T cells that produced only modest levels of IL-10, as measured by ELISA (Figure 17B). T cells biased by MΦ-II also had high levels of IL-10 mRNA 24 hours after restimulation (Figure 17C). These differences in cytokine production are not due to an overall lack of antigen presentation, since Ca-MΦ induced relatively high levels of IFN-γ production from T cells (Figure 17A). AA-MΦ failed to induce IL-10 production in the secondary response, possibly due to the lack of significant levels of proliferation in the primary response. Flow cytometry and intracellular cytokine staining was used to measure cytokine production on the single cell level (Figure 18). Following T cell activation by Ca-MΦ, there was only a small percentage of T-cells in the population that produced IL-4 (5.8%) or IL-10 (1%) (Figure 18, left panel). There were few if any double producers. In contrast, following activation with MΦ-II a substantial portion of the T cell population produced IL-4 (31.6%) or IL-10

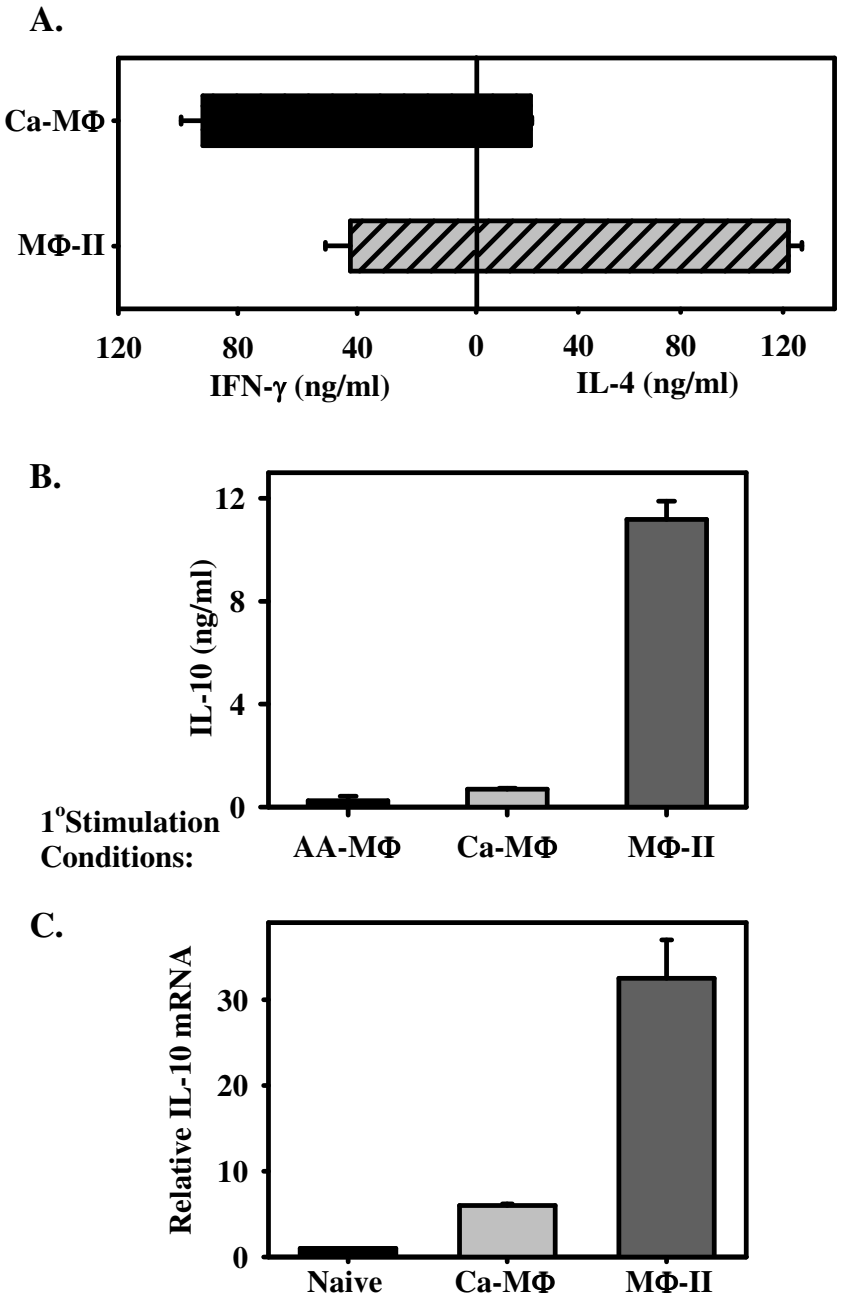

Figure 17: Cytokine profiles of T cells after secondary stimulation.
T cells were co-cultured with AA-MΦ, Ca-MΦ, or MΦ-II for one week, washed, then restimulated with plate-bound α-CD3 (5 μg/ml). (A) T cell cytokine production following primary stimulation with Ca-MΦ (top) or MΦ-II (bottom), as previously described. (B) IL-10 from T cells restimulated for 24 hours as measured by ELISA. (C) QRT-PCR measuring IL-10 mRNA 24 hours after restimulation with α-CD3 after primary stimulation with Ca-MΦ or MΦ-II. mRNA levels are presented relative to naïve T-cell IL-10 mRNA. Figures are representative of at least three independent experiments. Error bars indicate ± SD.

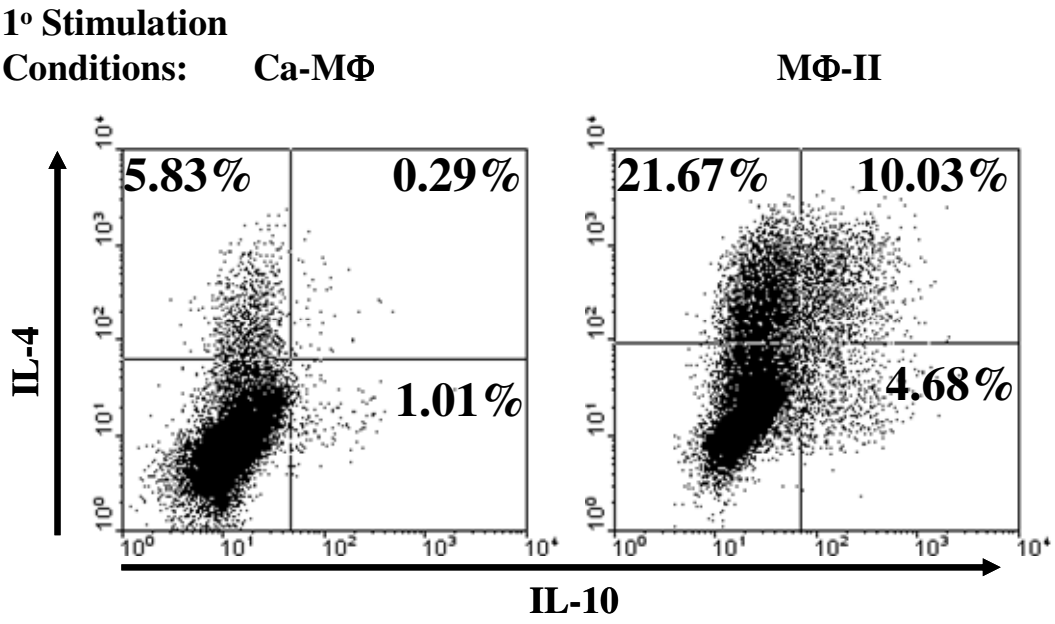

Figure 18: Intracellular staining for IL-4 and IL-10 after secondary stimulation. T cells were re-stimulated for 6 hours in the presence of GolgiStop (monensin) with plate-bound α-CD3e after biasing and activation by Ca-MΦ (Left Panel) or MΦ-II (Right Panel). Cells were fixed/permeablized using the Cytofix/Cytoperm reagent and stained using a PE-conjugated antibody against IL-4 and a FITC-conjugated antibody against IL-10. Quadrants are set using appropriate isotype controls. Figures are representative of at least three independent experiments.

(14.7%), with 10% of total T cells producing both IL-4 and IL-10 (Figure 18, right panel).

Discussion

The classical activation of macrophages leads to the production of a variety of lipid mediators, cytokines and chemokines. These mediators make classically activated macrophages important effector cells that can efficiently kill intracellular microorganisms. These same mediators, however, make these cells potent inflammatory cells that can mediate autoimmune pathologies. The thorough characterization of classically activated macrophages has been greatly aided by the reliable generation of these cells in vitro, simply by priming cultured macrophages with IFN-γ and then stimulating them with TNF or TLR activators. These defined in vitro studies have told us a great deal about the activation response and the biochemistry of the mediators produced during it. Alternatively Activated macrophages (AA-MΦ) were first identified following the addition of IL-4 to cultures of resident macrophages. These cells were shown to express higher levels of the mannose receptor[69]. Subsequent studies have identified a number of reliable "markers" for the AA-MΦ, including FIZZ1 and YM1/2[153,161]. Many of the studies to characterize the AA-MΦ were performed on macrophages isolated from mice, following experimental trematode[20] or nematode[162] infections. These studies showed that AA-MΦ are physiologically distinct from classically activated macrophages, in that they up-regulate the ECM associated proteins fibronectin and βIG-H3[163], the chemokine AMAC-1 (alternative macrophage associated chemokines 1)[164], and the receptor for β-glucan, Dectin-1[165]. The expression of arginase by murine AA-

macrophages restricts the availablility of L-arginine, a substrate for iNOS. This not only prevents NO production by these cells, but also gives them the ability to contribute to the formation of the extracellular matrix through the production of proline[166]. It should be noted that human monocytes may not respond to Th2 cytokines in the same way as murine bone marrow derived macrophage cells, because they fail to upregulate arginase activity when treated with IL-13[167]. Alternatively activated macrophages may provide immunity during helminth infections[168], but they can also contribute to disease pathology in a murine model of experimental schistosomiasis[20]. Despite all we now know about these cells from disease models, a careful parallel comparison with other macrophages following defined in vitro activation conditions has not been performed previously.

The type II activated macrophage (MΦ-II) remains poorly characterized, relative to these other macrophage populations. The lab has previously reported on the alterations in cytokine production by these cells [90,91] and on functional properties that are distinct from classically activated macrophages[92]. These cells develop during some *Leishmania* infections and contribute to disease progression[56]. We show that MΦ-II lack arginase and are thus unable to produce urea from arginine. In this respect, they are similar to Ca-MΦ but markedly different from AA-MΦ. MΦ-II express high levels of co-stimulatory molecules and are efficient antigen presenting cells, another property that distinguishes them from AA-MΦ. Finally, neither MΦ-II nor Ca-MΦ expresses FIZZ1 or YM1, two markers for AA-MΦ. Thus, there are clear biochemical and functional distinctions between these two populations of macrophages. We also compared MΦ-II with Ca-MΦ by microarray analysis and found that there were only a limited number of transcripts that were different between these two populations.

We identified two potential "markers" for MΦ-II . We show that MΦ-II up-regulate LIGHT (homologous to Lymphotoxins, shows inducible expression, and competes with herpes simplex virus glycoprotein D for HVEM/TNF-related 2). LIGHT may not only be a marker for MΦ-II, but it may also bear functional activity. LIGHT has been shown to costimulate T-cell responses through HVEM (TR2)[169], which is ubiquitously expressed on most lymphocyte populations[170]. LIGHT can also transmit costimulatory signals into T-cells through interactions with the soluble receptor TR6, enhancing activation in response to suboptimal TCR interactions[171,172]. Thus, LIGHT may play a role as an additional costimulatory molecule contributing to T-cell activation and proliferation in response to MΦ-II. In addition to LIGHT, Sphingosine kinase-1 may be another previously undescribed marker for the MΦ-II. Sphingosine kinases catalyze the production of sphingosine-1 phosphate from sphingosine. Mice have two isoforms, SPHK1a and SPHK1b, of which it appears that only SPHK1a is appreciably expressed in MΦ-II. These two proteins can differ with respect to enzymatic activity, stability, and cellular location[156]. SPHK1 has been shown to be necessary for C5a-triggered intracellular Ca(2+) signals[173]. Although this does not necessarily fit our model of MΦ-II being anti-inflammatory macrophages, this enzyme may be an important mediator of calcium fluxes in these macrophages. It has also been proposed that SPHK1 may play a role in retaining cell viability of endotoxin stimulated macrophages[157]. We show that macrophages stimulated with LPS+IC, as compared to macrophages stimulated with LPS alone, have markedly enhanced cell survival. This may be a contribution of high SPHK1 expression. In T cells SPHK1 controls the overproduction of the Th1-associated

cytokines, IL-2, TNF-α, and IFN-γ[174]. Thus, the induction of sphingosine kinase may be an important negative-regulator of inflammatory cytokines and chemokines in the MΦ-II.

In summary this side-by-side comparison of three distinct populations of activated macrophages has allowed us to characterize each with regard to physiology and functionality, and gives us the potential to develop a specific panel of markers for these macrophage populations. These specific "signatures" for each of the various activated macrophage populations may allow us to identify specific populations of macrophages associated with different disease states.

Future research should focus on several aspects of the biology of the type II activated macrophages. We show that naïve T-cells activated and biased by the presence of MΦ-II produce high levels of the Th2 associated cytokine IL-4 and IL-10. These biased T-cells cells should in turn be used to activate macrophages, with the hypothesis that MΦ-II can drive Th2 differentiation which could in turn drive alternative macrophage differentiation. Simple expression analysis for the various markers for alternative activation could be used to determine the activation status of these cells. Additionally, the role of SPHK1 has not fully been assessed. Although we hypothesize that SPHK1 may contribute to enhanced viability of MΦ-II, this may not be the case. Enzymatic activity should be assessed by looking at accumulation of sphingosine-1 phosphate and comparing MΦ-II to Ca-MΦ. Furthermore, there are several inhibitors of SPHK available which could be added at various times to look for a role in retaining cell viability. Most importantly, the full potential of the microarray has not fully been exploited. The genes present in table 4 have not been fully assessed as potential markers for MΦ-II.

CHAPTER 4: REGULATION OF HEPARIN-BINDING EGF-LIKE GROWTH FACTOR BY THE TYPE II ACTIVATED MACROPHAGE

The induction of Heparin-Binding Epidermal Growth Factor-Like Growth Factor (HB-EGF) mRNA and protein

We previously performed microarray analyses on macrophages stimulated with LPS in the presence of immune complexes (IC), and compared this to macrophages stimulated with LPS alone. Stimulation in the presence of IC activated a specific subset of genes relative to those stimulated with LPS alone([175] and GEO dataset GDS2041, Table 3). One gene, Heparin-Binding Epidermal Growth Factor (HB-EGF), was found to be induced by an average of approximately 8-fold over macrophages stimulated with LPS alone[175] (Table 3). Due to the strong signal, high fold-change over LPS stimulated macrophages, and the potential importance of HB-EGF to macrophage biology, we decided to further examine the induction of HB-EGF mRNA in these cells. Macrophages stimulated with LPS+IC synthesized HB-EGF mRNA (Figure 19A). Macrophages stimulated with LPS alone also increased HB-EGF mRNA production, however this increase was relatively modest compared to those stimulated with LPS+IC. At the peak of mRNA induction at 90 min, LPS+IC simulated macrophages expressed 7- to 8-fold more HB-EGF mRNA than cells stimulated with LPS alone, and these elevated levels were maintained for three hours post-stimulation (Figure 19A). Elevated HB-EGF mRNA levels were confirmed and visualized by conventional PCR (Figure 20A). In addition, stimulation with endogenous TLR4 ligand low molecular weight hyaluronic acid (LMW- HA), also a

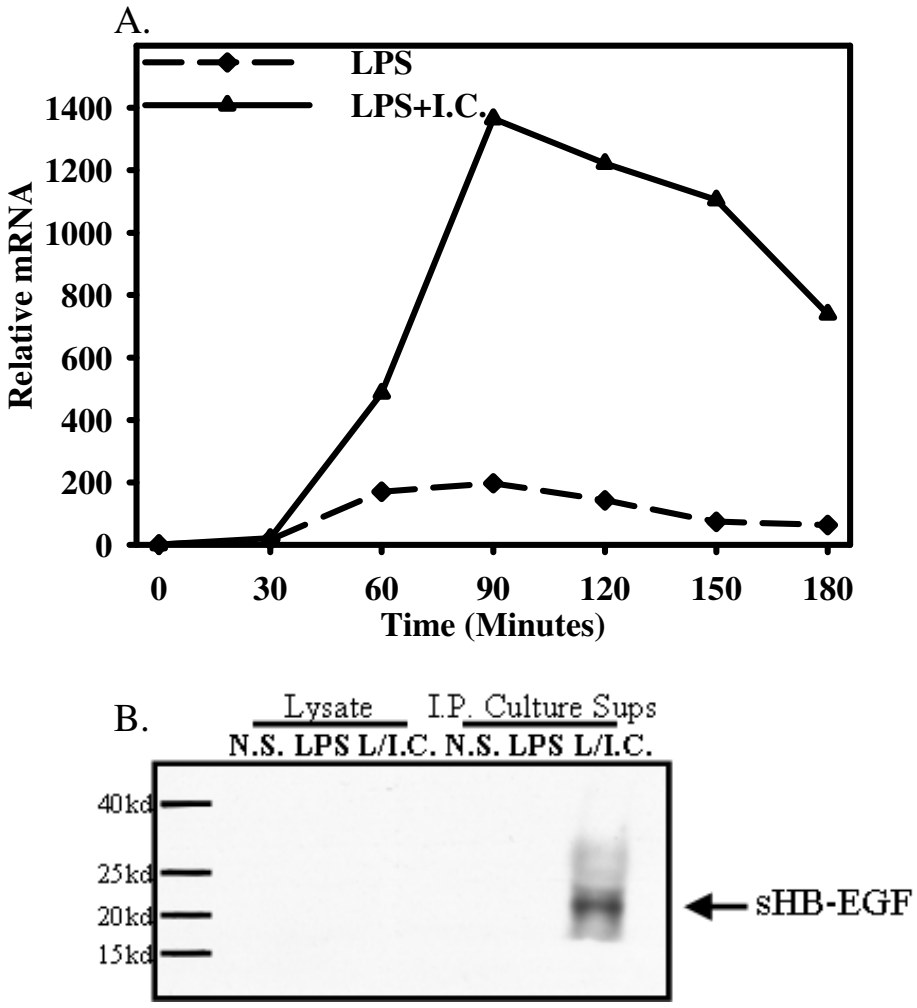

Figure 19: Heparin-binding EGF-like growth factor is induced in bone-marrow derived macrophages in response to LPS and immune complexes (IC).
(A) Real-time (QRT-PCR) of HB-EGF expression in bone-marrow derived macrophages (BMMΦ) after stimulation with LPS (10ng/ml) alone or LPS+IgG-OVA immune complexes (IC). QRT-PCR for HB-EGF mRNA is expressed as a fold change over unstimulated conditions (0'). (B) Western blot for HB-EGF in cell lysates or immunoprecipitated from cell culture supernatants of unstimulated (NS) macrophages or macrophages stimulated with LPS (10ng/ml) or LPS+IC for 16h. Figures are representative of at least three independent experiments.

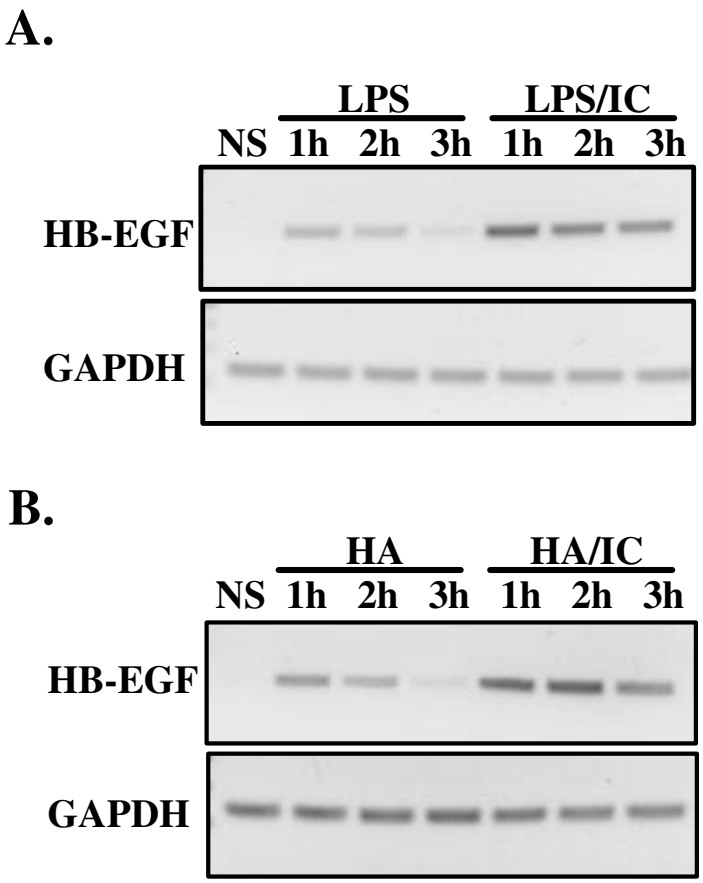

Figure 20: Immune complexes enhance TLR agonist induced HB-EGF expression. (A) RT-PCR measuring HB-EGF mRNA from macrophages stimulated with LPS (10ng/ml) or LPS/IC. (B) RT -PCR measuring HB-EGF mRNA from macrophages stimulated with hyaluronic acid (HA, 10μg/ml) or HA/IC. RT-PCR for GAPDH is present as a loading control. Figures are representative of at least three independent experiments.

TLR4 ligand, yielded similar results when combined with immune complexes (Figure 20B).

Like other members of Epidermal Growth Factor (EGF) family, HB-EGF is synthesized as a membrane associated precursor (proHB-EGF) that is subsequently cleaved, yielding a soluble and active growth factor[176]. To determine whether HB-EGF is secreted or retained on the cell surface, macrophages were stimulated for 24 hours with LPS+IC, then cell culture supernatants and cell lysates were analyzed by immunoprecipitation using a polyclonal antibody specific for HB-EGF. Immunoprecipitated HB-EGF was subject to SDS-PAGE. A band corresponding to processed sHB-EGF, with a molecular weight of approximately 20kd, was detected in culture supernatants of macrophages stimulated with LPS+IC at 24 hours (Figure 19B). Macrophages stimulated with LPS alone did not secrete sHB-EGF. Furthermore, proHB-EGF was not detected in cell lysates from any of the cells. Thus, HB-EGF is synthesized by macrophages stimulated with LPS+IC and is rapidly cleaved to yield the soluble secreted form.

The induction of HB-EGF is due to increased transcription and not to changes in mRNA stability

Other groups have reported that high levels of HB-EGF mRNA are due to changes in mRNA stability. Sorensen et al. reported that the 3'UTR of HB-EGF contains 6 AU rich elements (ARE), which are essential for full induction of HB-EGF[137]. To determine whether the high levels of HB-EGF mRNA were due to changes in mRNA stability we performed an mRNA stability assay. First, macrophages were pre-treated

with increasing concentrations of the transcriptional inhibitor actinomycin D, then stimulated with LPS+IC. HB-EGF mRNA was measured by QRT-PCR (Figure 21A). With increasing concentrations of actinomycin D, HB-EGF mRNA levels declined to basal levels, indicating that new transcription was essential for HB-EGF induction. Maximal inhibition was achieved at 0.5-1 μg/ml actinomycin D. To analyze mRNA stability, macrophages were stimulated with LPS or LPS+IC for two hours, and then 0.5 μg/ml actinomycin D was added. HB-EGF mRNA levels were measured by QRT-PCR for 2 hours thereafter (Figure 21B). Although macrophages stimulated with LPS+IC had approximately 5 fold greater levels of HB-EGF mRNA than LPS stimulation alone, the rate at which the mRNA was degraded was similar to that of macrophages stimulated with LPS alone. Therefore, the high degree of HB-EGF mRNA induction in macrophages stimulated with LPS+IC relative to cells stimulated with LPS alone was not due to alterations in mRNA stability.

The role of MAPK and Syk activation in HB-EGF and IL-10 induction

The lab has previously demonstrated that IL-10 was induced by stimulation of macrophages with TLR agonists in combination with IC, and that this induction was dependant upon the activation of the MAPKs ERK1/2 and p38[106]. In MΦ-II, HB-EGF follows a similar pattern of induction as IL-10, in that i) it is induced very early after activation, and ii) LPS alone induces only modest induction, whereas stimulation (with LPS) in the presence of immune complexes induces robust induction. We therefore wished to investigate whether ERK and p38 were also involved in the induction of HB-EGF. Macrophages were pretreated for one hour with increasing concentrations of the

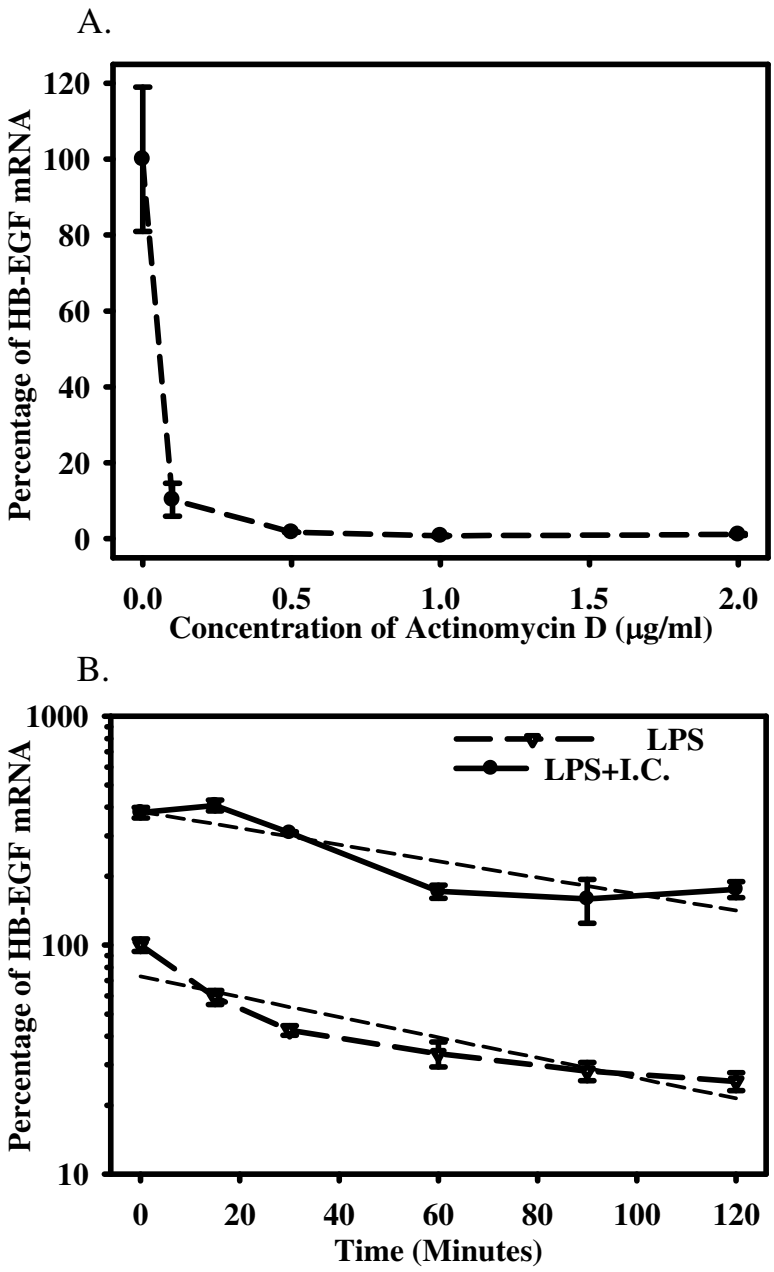

Figure 21: The induction of HB-EGF depends on new transcription and not on alterations in mRNA stability.
(**A**) BMMΦ were pretreated for 1h with increasing concentrations of actinomycin D (0-2.0μg/ml) then stimulated with LPS(10ng/ml)+IC for 2h. Relative HB-EGF mRNA was measured by QRT-PCR and presented as a percentage of HB-EGF mRNA present in macrophages stimulated in the presence of the vehicle control (0μg/ml). (**B**) mRNA stability was examined in which BMMΦ were stimulated for 2h with LPS(10ng/ml) or LPS+IC before the addition of 0.5μg/ml of actinomycin D. Relative levels of HB-EGF mRNA were measured by QRT-PCR for 2h after stimulation. Error bars indicate ± standard deviation. Figures are representative of at least three independent experiments.

MEK1,2 inhibitor (U0126, 0-4.0μM) before stimulation in the presence of immune complexes. HB-EGF mRNA was measured by QRT-PCR 2 hours after activation (Figure 22A, left) and IL-10 cytokine levels were measured by ELISA after 8 hours (Figure 22A, right). As previously reported, increasing concentrations of U0126 inhibited the super-induction of IL-10 (Figure 22A, right). HB-EGF mRNA production followed a similar pattern of inhibition in response to comparable concentrations of U0126 (Figure 22A, left). Similar results were obtained when the p38 MAPK was inhibited by SB203580. Both IL-10 (Figure 22B, right) and HB-EGF (Figure 22B, left) were inhibited at comparable inhibitor concentrations. As a control, the JNK inhibitor II only minimally decreased IL-10 and HB-EGF production when used at concentrations sufficient to significantly inhibit the secretion of TNF-α (Figure 22C).

We next investigated the necessity for Syk in HB-EGF induction. This signaling molecule has been shown by us to be necessary for full activation of ERK by immune complexes and the production of IL-10 by immune complexes[117]. Inhibition of FcγR signaling was achieved by treating BMMΦ with increasing concentrations of the Syk inhibitor 3-(1-Methyl-1H-indol-3-yl-methylene)-2-oxo-2,3-dihydro-1H-indole-5-sulfonamide before activation with LPS+IC. HB-EGF was measured by QRT-PCR 2h after activation. IL-10 was measured by ELISA from cell culture supernatants 8h after activation. Treatment of macrophages with increasing concentrations of the Syk inhibitor greatly diminished their production of both HB-EGF (Figure 23A) and IL-10 (Figure 23B), indicating that both IL-10 and HB-EGF superinduction by immune complexes requires Syk mediated FcγR signaling. Thus, the MAPKs ERK1/2 and p38 are required for the optimal induction of both HB-EGF and IL-10 in MΦ-II.

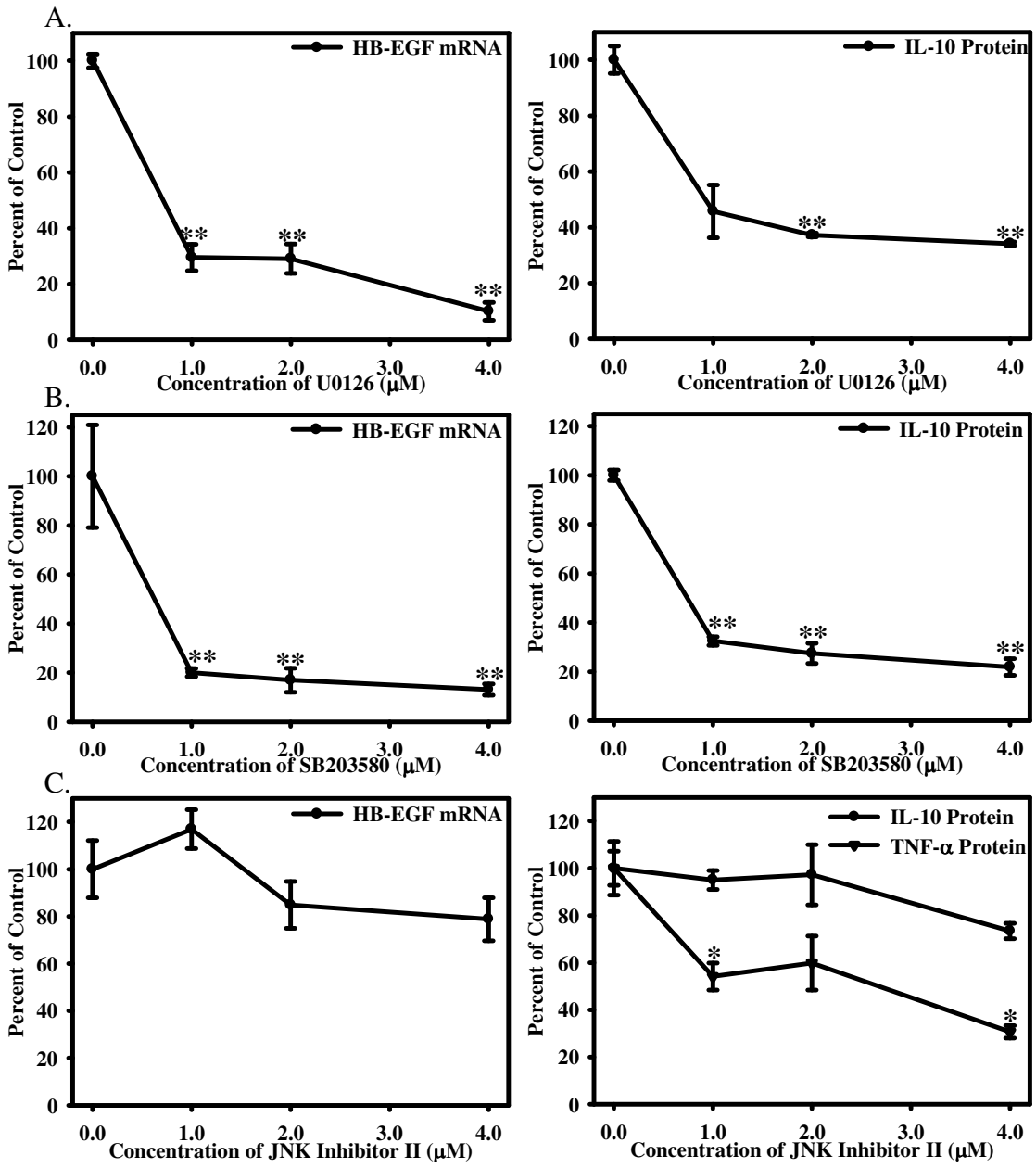

Figure 22: Immune complex mediated induction of HB-EGF requires the activity of ERK1/2 and p38.

BMMΦ were pretreated with increasing concentrations of the inhibitors of the ERK1/2 pathway (**A**, U0126 0-4.0μM), p38 (**B**, SB203580 0-4.0μM), JNK(**C**, JNK Inhibitor II 0-4.0μM). BMMΦ were then stimulated with LPS (10ng/ml)+IC for 2h. HB-EGF mRNA was measured by QRT-PCR and expressed relative to vehicle controls (**A-D**, left panels). IL-10 protein was measured by ELISA after 8h of stimulation and expressed as a percentage of protein relative to vehicle controls (**A-D**, right panels). Figures are representative of at least three independent experiments. Error bars indicate ± standard deviation. Asterisk indicates (*)$p<0.05$ and (**$p<0.01$) as compared to vehicle alone control.

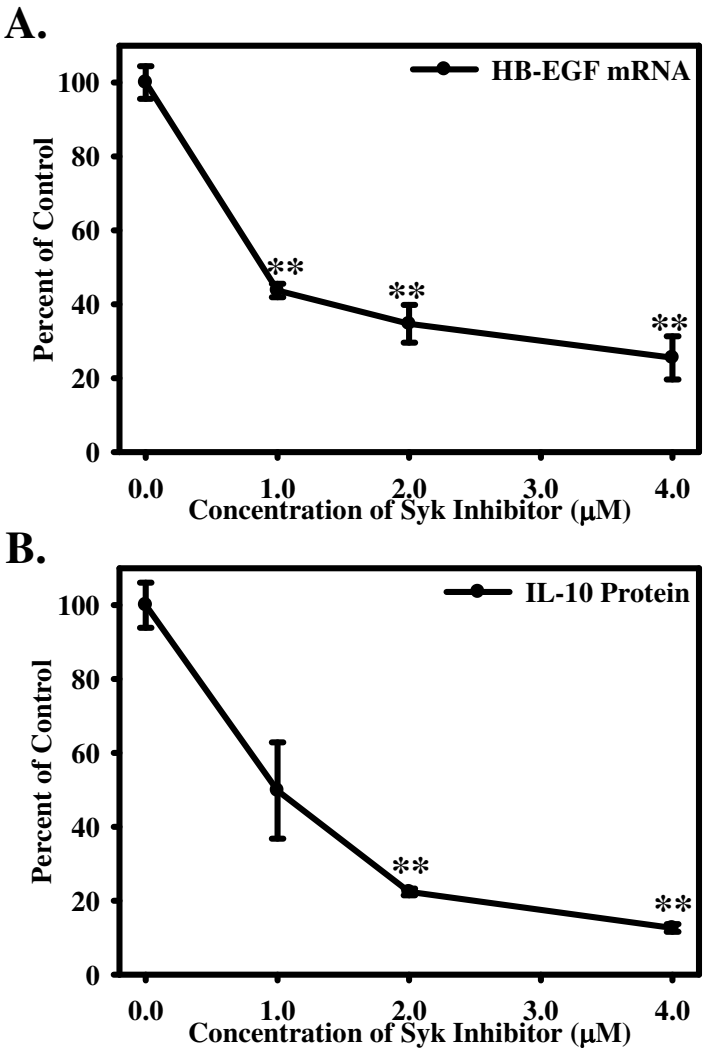

Figure 23: Immune complex mediated induction of HB-EGF requires Syk activity. BMMΦ were pretreated with increasing concentrations of the inhibitor of Syk (Syk Inhibitor 0-4.0μM). BMMΦ were then stimulated with LPS (10ng/ml)+IC for 2h. (A) HB-EGF mRNA was measured by QRT-PCR and expressed relative to vehicle controls. (B) IL-10 protein was measured by ELISA after 8h of stimulation and expressed as a percentage of protein relative to vehicle controls. Figures are representative of at least three independent experiments. Error bars indicate ± standard deviation. ** indicates $p<0.01$ as compared to vehicle alone control.

The induction of HB-EGF mRNA is not dependant upon IL-10

The sensitivity of HB-EGF induction to inhibition of ERK and p38 suggested that HB-EGF was induced by mechanisms that are similar to those of IL-10. An alternative interpretation would be that IL-10 is required for HB-EGF induction. We considered this to be unlikely due to rapid induction of HB-EGF mRNA following stimulation, but to directly address this possibility HB-EGF induction in macrophages deficient in IL-10 was examined. Both wild-type and IL-$10^{-/-}$ macrophages produced comparable levels of HB-EGF mRNA in response to stimulation by LPS+IC (Figure 24A).

Additionally, to block the production of IL-10, macrophages were pretreated with increasing concentrations of the translation inhibitor, cycloheximide. As expected, stimulation of macrophages with LPS+IC led to high levels of IL-10 protein, which were diminished to undetectable levels with increasing concentrations of cycloheximide (0.00 to 0.50μg/ml, Figure 24B, solid). Parallel to this, HB-EGF mRNA was measured two hours after stimulation with LPS+IC by QRT-PCR. Increasing concentrations of cycloheximide failed to significantly diminish HB-EGF mRNA (Figure 24B, bars), while blocking the production of IL-10 protein. Thus, the production of HB-EGF by MΦ-II does not depend on IL-10 production.

5' RNA Ligase Mediated Rapid Amplification of cDNA Ends (5'-RLM-RACE) for HB-EGF

In order to be sure of the position of transcription factors along the HB-EGF promoter relative to the transcriptional start site, 5' rapid amplification of cDNA ends

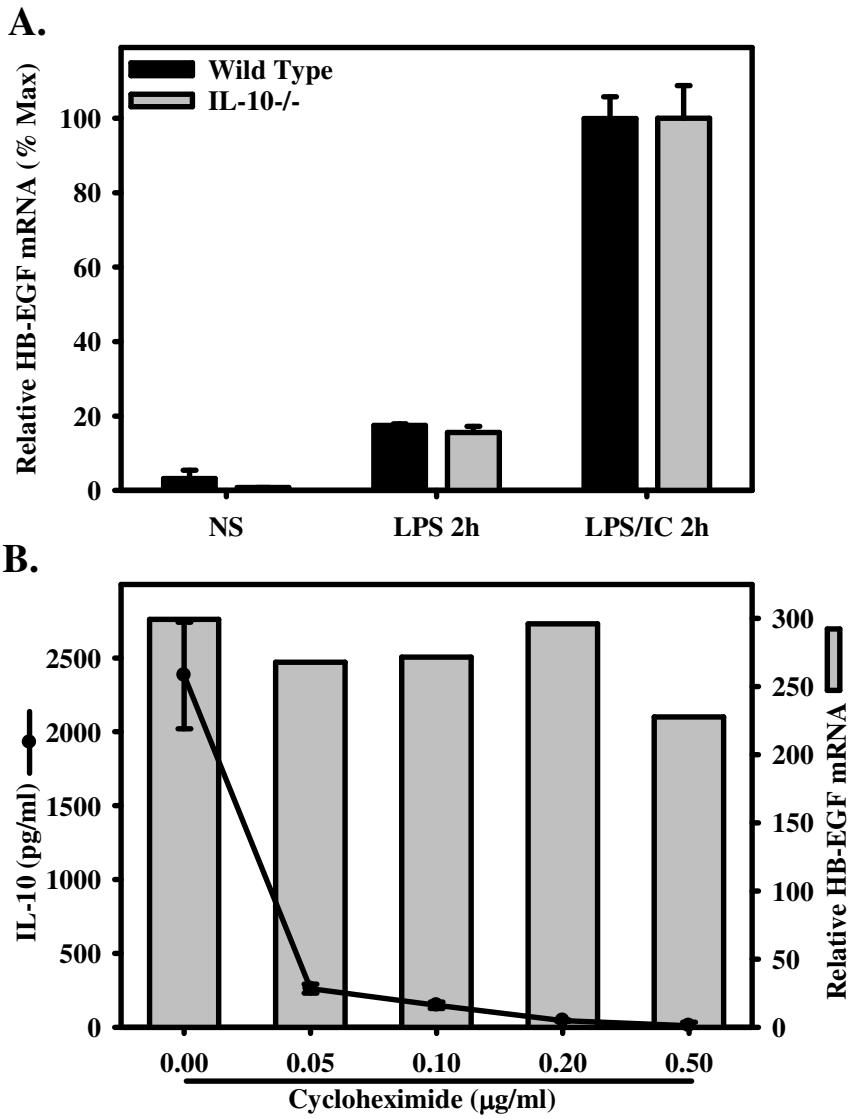

Figure 24: Immune complex-mediated induction of HB-EGF mRNA does not require IL-10 protein synthesis.
(A) BMMΦ from wild-type or IL-$10^{-/-}$ mice were stimulated with LPS (10ng/ml) or LPS+IC and HB-EGF mRNA was measured at 2h after stimulation. (B) BMMΦ were pretreated for 1h with increasing concentrations of actinomycin D (0-0.5µg/ml) then stimulated with LPS+IC. IL-10 protein was measured by ELISA 8h after stimulation (line) and HB-EGF mRNA was measured by QRT-PCR after stimulation for 2h (bar). mRNA levels are presented relative to unstimulated controls. Error bars indicate ± standard deviation. Figures are representative of at least three independent experiments.

was performed. The transcriptional start site was previously determined for differentiating myotubes[142], but not for activated macrophages. The nested PCR reaction produced a band of the expected size of approximately 450bp. EcoRI digestion of TOPO TA clones from the nested PCR reaction revealed clones of three different sizes (Figure 25). Of the 20 digested plasmids, 8 were self ligations, 8 contained the expected product size of approximately 450bp, one contained a product of approximately 350bp, and 3 contained a product of approximately 250bp. All three of these plasmids were sequenced. The major clone contained the previously reported sequence. The second clone contained a product missing approximately the first 120bp of the first exon and is likely to simply be a partially degraded mRNA. The third clone was missing the central 233bp of the first exon, which contains the translational start site for HB-EGF. Although not confirmed, this most likely represents a nonsense and therefore non-functional mRNA. Despite the presence of the two minor clones, these results essentially confirm the previously reported transcriptional start site for HB-EGF (Figure 25).

Sp1 transcription factor binds to the HB-EGF promoter in situ and in vitro

The robust induction of HB-EGF mRNA in macrophages stimulated with LPS+IC prompted us to determine which transcription factors may play a role in HB-EGF transcription. Preliminary promoter analysis using Transfac (default 85% cutoff; http://www.gene-regulation.com/pub/databases.html [177]) revealed 3 potential Sp1 binding sites within the first 2kb of the HB-EGF promoter (Table 4). In order to determine the binding of Sp1 to the HB-EGF promoter *in situ* in live cells, a ChIP assay was performed. BMMΦ were stimulated with LPS+IC, and then processed for ChIP analysis using an

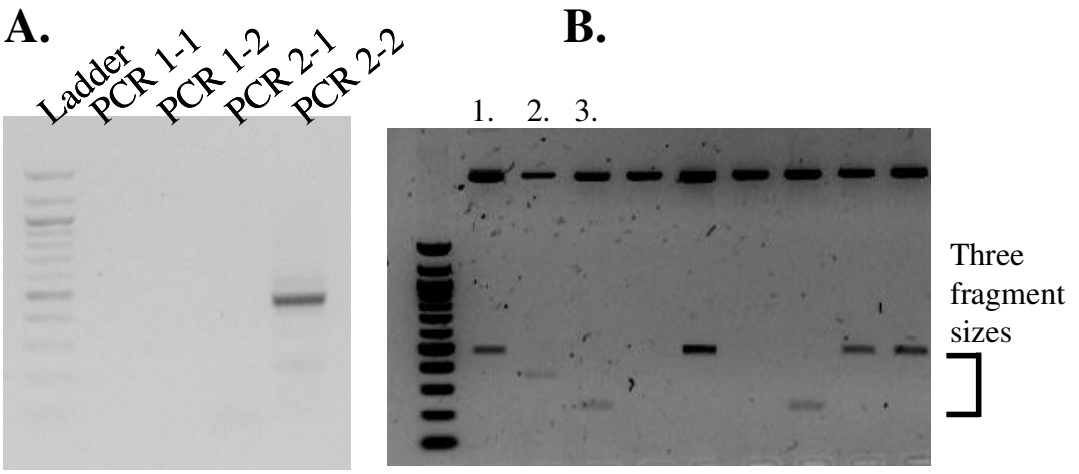

C.

Fragment 1

CGCGGATCCGAACGCTGCGTTTGCTGGCTTTGATGAAAAGTCGGCCCGGGGAGCT
GCACGCGGCTGGCTGGTCGGCCTGACAGACCTTCAAGGGCTGGAGTGGACGCGCGGA
CCGACTCTGAACAGACAGACGAACCGCGGCCGCAAGGTTCCCAGAC**AGG**ATCTCACC
CAGAGGCAGGCAGCGGACAGTGCCTTAGTGGAACCTCGCTGTCCTCCACCGCCTGGCC
CCGGTGCAGGCGTCCAGTGGCCGCCGCATCCAAAGTGATCGCTGCCTCCCCGTCTCCG
CCAGGCTCGGGACC**ATG**AAGCTGCTGCCGTCGGTGATGCTGAAGCTCTTTCTGGCCGC
AGTGTTGTCCGCGTTGGTGACCGGTGAGAGTCTGGAGCGGCTTCGGAGAGGTCTGGCG
GCAGCAACCAG**CAA**CCCTGACCCTCCCACTGGATCC**ACAAACCAGCTGCTACCCAC**

Fragment 2

CGCGGANCCNGACGCTGCGTTTGCTGGCTTTGATGAAA**AGG**ATCTCACC**CAG**AGGC
AGGCAGCGGACAGTGCCTTAGTGGAACCTCGCTGTCCTCCACCGCCTGGCCCCGGTGCA
GGCGTCCAGTGGCCGCCGCATCCAAAGTGATCGCTGCCTCCCCGTCTCCGCCAGGCTCG
GGACC**ATG**AAGCTGCTGCCGTCGGTGATGCTGAAGCTCTTTCTGGCCGCAGTGTTGTCC
GCGTTGGTGACCGGTGAGAGTCTGGAGCGGCTTCGGAGAGGTCTGGCGGCAGCAACCA
G**CAA**CCCTGACCCTCCCACTGGATCC**ACAAACCAGCTGCTACCCAC**

Fragment 3

CGCGGANCCNGACGCTGCGTTTGCTGGCTTTGTTGAAAAGTCGGCCCGGGGAGCTG
CACGCGGCTGGCTGGTCGGCCTGACAGACCTTCAAGGGCTGGAGTGGACGCGCGGACC
GACTCTGAACAGACAGACGAACCGCGGCCGCAAGGTTCCCAGAC**AGG**ATCTCACC**CAG**
CAACCCTGACCCTCCCACTGGATCC**ACAAACCAGCTGCTACCCAC**

Figure 25: 5'-RLM-RACE for HB-EGF.
The RACE adaptor is ligated to the 5' end of full-length mRNA, reverse transcribed, followed by a nested PCR using external and internal RACE adaptor and gene specific primers. (A) Nested PCR using Fast Start High Fidelity PCR System (1) and Platinum PCR Supermix High Fidelity (2). Nested reactions are labeled 1-2 and 2-2. (B) TA cloning of product from nested PCR excised using EcoRV. (C) Sequences of fragments from (B). **Blue** text denotes RACE adaptor, **green** texts denotes internal gene specific reverse primer, **red underlined** text denotes translation start site, **red** text denotes where fragment 3 begins, and **underlined black** text marks where clone 3 is missing sequence.

anti-Sp1 antibody. An analysis of the the HB-EGF promoter (-2000/+292) using 13 primer pairs (Figure 26A) revealed Sp1 binding to three regions of the Sp1 promoter (amplicons 3,8, and 11), each of which contain a predicted Sp1 binding site. Table 4 contains these primers pairs and a schematic of these predicted Sp1 binding sites. A kinetic analysis of these regions revealed a rapid, although transient, binding of Sp1 to the HB-EGF promoter which peaked at approximately 45 minutes (Figure 26B, amplicons 3, 8, 11). As a control, an upstream region (-2000/-1849) of the HB-EGF promoter was also analyzed. It failed to efficiently recruit Sp1 (Figure 26B, amplicon 13).

EMSAs were performed in order to determine if the predicted promoter elements could be directly bound by Sp1. For these assays, the macrophage-like RAW264.7 cell line was used. These cells respond similarly to primary macrophages in their HB-EGF induction, following stimulation with LPS or LPS+IC (see Figure 27A). Nuclear proteins were mixed with a consensus probe or with a probe corresponding to a potential Sp1 binding site within -1566/-1548 of the HB-EGF promoter (relative to the transcriptional start site). By EMSA, Sp1 bound to both probes following the addition of nuclear extracts from either stimulated or resting cells (Figure 27A). In Figure 27, the asterisks indicate bands corresponding to Sp1 bound to these probes. Free probe without nuclear extracts (FP) did not reveal this band. Despite the dramatic differences in HB-EGF production following stimulation, there were no detectable differences in the amount of Sp1 binding when extracts from unstimulated RAW264.7 cells, or cells stimulated with LPS or LPS+IC were added. All of these extracts contained Sp1 that was competent to bind to these probes (Figure 27A). Two additional probes corresponding to the other Sp1 binding sites were also confirmed to have Sp1 binding activity in vitro (Figure 27B-C).

Amplicon	Primers		
1	5'-GGTTCCCAGACAGGATCTCA-3' 5'-AGAAAGAGCTTCAGCATCACC-3'	**7**	5'-GTCGAGGTTAGCTGGTTGGA-3' 5'-CCAGCAACAGCAAAGGAAGT-3'
2	5'-CTTCCCCGGAGCCTTATTC-3' 5'-TGAGATCCTGTCTGGGAACC-3'	**8**	5'-ATGAAGAGGGGAAGCCAGAT-3' 5'-TGCTGGGTAGGGAGTTTGAC-3'
3	5'-CCCTACACCCACACTCCAGT-3' 5'-GAATAAGGCTCCGGGGAAG-3'	**9**	5'-CCTCTTCTGACCTCTGTGGG-3' 5'-ATCTGGCTTCCCCTCTTCAT-3'
4	5'-CAGATCACCTTTCGCTAGGC-3' 5'-ACTGGAGTGTGGGTGTAGGG-3'	**10**	5'-ATACTGAGCACCCAAGGTGG-3' 5'-CCCACAGAGGTCAGAAGAGG-3'
5	5'-ACTTCCTTTGCTGTTGCTGG-3' 5'-GCCTAGCGAAAGGTGATCTG-3'	**11**	5'-GAGAGCAGGGTGTGAATGGT-3' 5'-CCACCTTGGGTGCTCAGTAT-3'
6	5'-GTCGAGGTTAGCTGGTTGGA-3' 5'-CCAGCAACAGCAAAGGAAGT-3'	**12**	5'-GGTTCTCTGCAGTTCTGGGA-3' 5'-ACCATTCACACCCTGCTCTC-3'
		13	5'-CTTCTTTTTTCTCTTTCTTTGA-3' 5'-TCCCAGAACTGCAGAGAACC-3'

Table 4: Schematic diagram and table of primers used for analysis of the HB-EGF promoter. Arrowheads indicate predicted Sp1 binding sites.

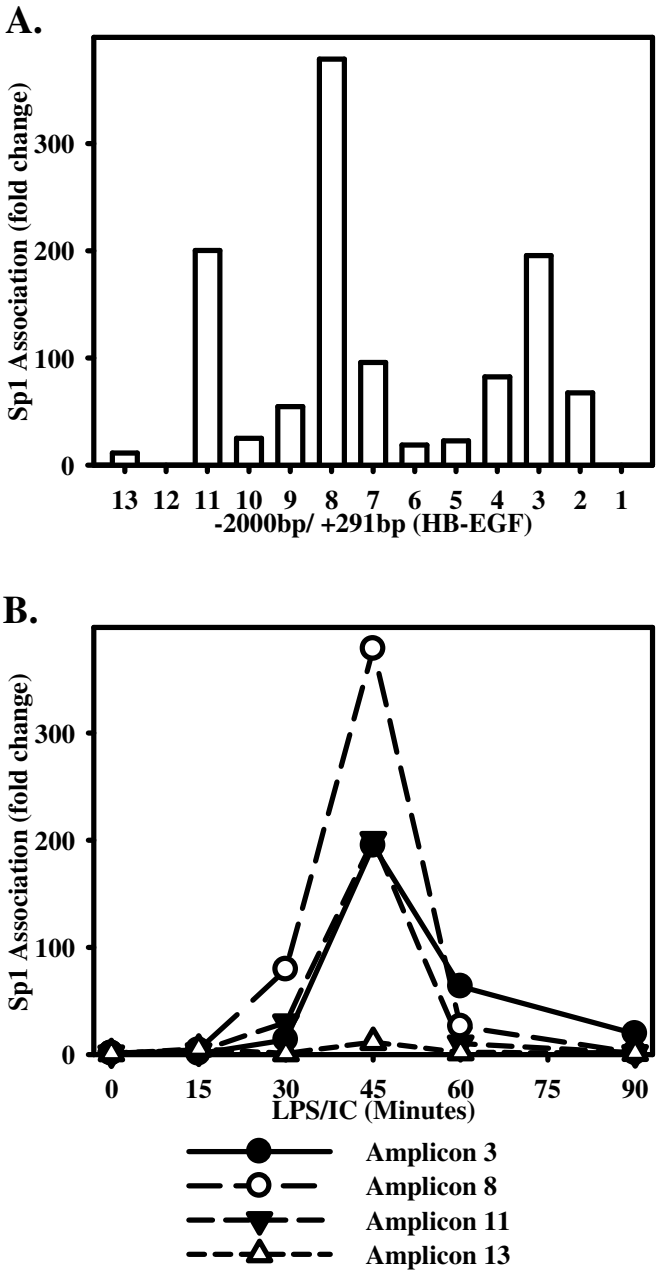

Figure 26: Sp1 is recruited to the HB-EGF promoter in situ by BMMΦ after stimulation with LPS+IC.

(**A**) BMMΦ were stimulated with immune complexes (IC) and 10 ng/ml LPS (IC/LPS) for 0 and 45 minutes. Cross-linked chromatin fragments were immunoprecipitated with anti-Sp1 antibody. Immunoprecipitated DNA was purified and examined for the presence of HB-EGF promoter sequences corresponding to each of the 13 amplicons with the corresponding primers present in table 4 as measured by QRT-PCR. The data were normalized to inputs at each time point and plotted graphically as fold changes relative to the data at 0 min. (**B**) BMMΦ were stimulated with immune complexes (IC) and 10 ng/ml LPS (IC/LPS) for 0, 15, 30, 45, 60 and 90 min and processed for ChIP as in (**A**). DNA was purified and examined for the presence of HB-EGF promoter sequences corresponding to amplicons 3, 8, 11, and 13 by QRT-PCR. Figures are representative of at least two independent experiments.

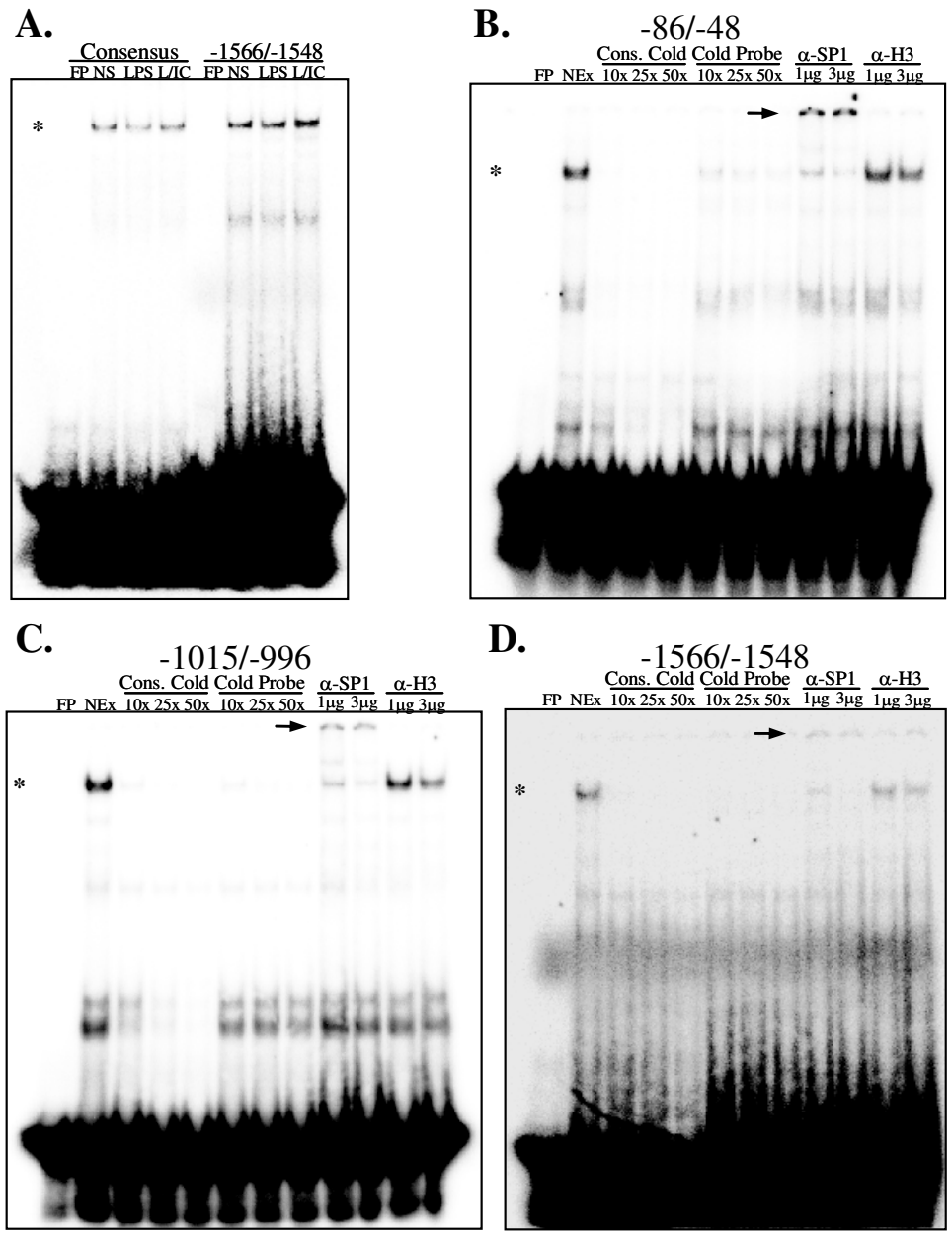

Figure 27: Sp1 binds potential Sp1 sites of the HB-EGF promoter in vitro.
(A) ^{32}P labeled double-stranded oligomers corresponding to a consensus Sp1 binding sequence or the -1566/-1548 of the HB-EGF promoter were incubated on ice for 1h with nuclear extracts from unstimulated (NS), LPS or LPS+IC stimulated (45') RAW264.7 cells. FP=Free Probe. Labeled probes corresponding to the -86/-48 (B), -1015/-996 (C), and the -1566/-1548 (D) potential Sp1 sites of the HB-EGF promoter were incubated with nuclear extracts from RAW264.7 cells stimulated with LPS+IC for 45'. Binding was competed with increasing concentrations (10×-50×) of cold unlabeled probe or consensus cold probe. DNA-Sp1 protein complexes were supershifted by incubating nuclear extracts with 1 or 3μg of antibody against Sp1 or Histone H3 for 30' on ice prior to incubation with labeled probe (B-D). *Indicates Sp1-DNA complexes. Arrowheads indicate supershifted Sp1-DNA complexes.

This binding was competed for by increasing molar ratios of a cold probe (10x-50x) corresponding to this site or to a cold consensus probe. In all cases (Figure 27B-D), the addition of an antibody against Sp1 (1μg or 3μg) prior to the addition of labeled probe resulted in a supershift (arrow). Thus, the EMSA confirms that all three sites identified by ChIP can bind to Sp1 in vitro. However, there was a clear and important distinction between the results obtained with ChIP and with EMSA. Resting cells did not exhibit significant Sp1 ChIP activity at the HB-EGF promoter (Figure 26B, Time 0), whereas by EMSA their nuclei clearly contained Sp1 that was fully competent to bind DNA, and this binding was comparable to that of stimulated cells.

Activity of an HB-EGF Reporter Construct in Response to stimulation

In order to address which promoter elements were necessary for the transcription of HB-EGF, reporter plasmids containing portions of the HB-EGF promoter were transfected into RAW264.7 cells. The lab and others have previously used this cell line to study the regulation of IL-10[94,101]. By RT-PCR, RAW264.7 cells respond similarly to primary bone-marrow derived macrophages in the induction of HB-EGF mRNA. Similar to primary macrophages, stimulation with LPS alone resulted in modest levels of HB-EGF mRNA, which were dramatically increased when combined with immune complexes (Figure 28A). Three HB-EGF promoter reporter plasmids were constructed, including the first ~2700 bases of the HB-EGF promoter (-2704/+330), as well as two truncations (-1238/+330 and -557/+330) (Figure 28B). The -2704/+330 plasmid contains three potential Sp1 binding sites, while the -1230/+330 and the -557/+330 plasmid contained two and one binding sites, respectively. Luciferase activity was unchanged

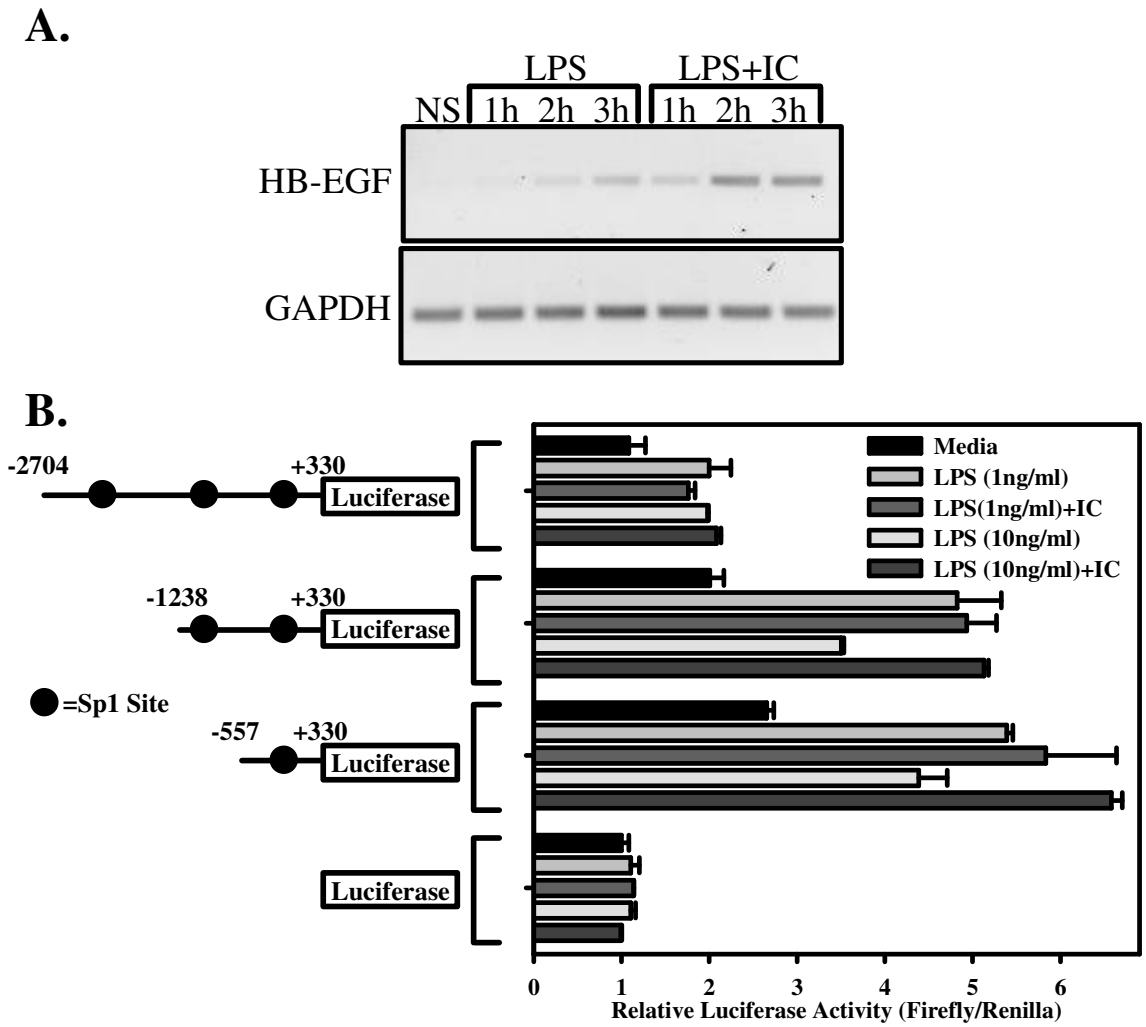

Figure 28: Luciferase activity of RAW264.7 cells transfected with wild-type and mutant HB-EGF reporter vectors after stimulation with LPS or LPS+IC.
(A) RAW264.7 cells were stimulated with LPS or LPS+IC for 1, 2, or 3h or left unstimulated (NS). HB-EGF and GAPDH mRNA were measured by RT-PCR. GAPDH is present as a loading control. (B) Schematic illustration of luciferase reporter constructs of the HB-EGF promoter. pGL4.19 luciferase reporter constructs containing -2704/+330, -1238/+330, -557/+330 or none of the HB-EGF promoter were transfected into RAW264.7 cells overnight then stimulated with LPS(1 or 10ng/ml) or LPS+IC for 8 hours. Each sample was measured for firefly luciferase activity and normalized to renilla luciferase activity (transfected at a ratio of 40:1). Values are represented as fold changes relative to unstimulated cells transfected with the empty vector. Figures are representative of at least three independent experiments. Error bars indicate ± standard deviation of experiments performed in triplicate.

following stimulation of RAW cells transfected with empty pGL4.19 vector (Figure 28B). Transfection of the -2704/+330 plasmid resulted in only minor increases over the level of activity of the empty vector. However, truncation of the promoter (to -1238) strongly enhanced the activity of the promoter upon stimulation (Figure 28B). The most severely truncated HB-EGF promoter analyzed (-557) displayed similarly increased levels of luciferase activity upon stimulation (Figure 28B). Importantly, both of these vectors (-1238 and -557) responded equally well to stimulation with LPS or LPS+IC. Thus, luciferase activity did not accurately reflect HB-EGF mRNA induction, since the combination of LPS+IC did not result in a super-induction of luciferase activity.

Since both the -1230/+330 and the -557/+330 promoter plasmids responded similarly to stimulation with LPS+IC, we investigated whether the Sp1 binding site located within -83/-54 was required for the response to LPS+IC. This region actually contains 3 potential Sp1 binding sites directly adjacent to each other (Figure 29A). In order to assess the importance of this region, we used site-directed mutagenesis to modify two nucleotides of the conserved core binding site of GGGCGG to GGTAGG (Figure 30A) at each of these sites. Transfection of the -557/+330 led to a constitutive enhancement in luciferase activity that was further enhanced upon stimulation with LPS+IC for 8h (Figure 29B). However, both the constitutive activity as well as the induced activity were nearly completely nullified by mutating these sites (Figure 29B). Thus, this site binds Sp1, and this binding is required for the activity of the HB-EGF promoter.

Enhanced HB-EGF Promoter Accessibility in Response to LPS+IC

A.

-83/-54 WT-Sp1 AAGGGGGCGGTGCCGGGCGGGGCGGGGCTC
-83/-54 MT-Sp1 AAGGGGTAGGTGCCGGTAGGGTAGGGGCTC
* * *

B.

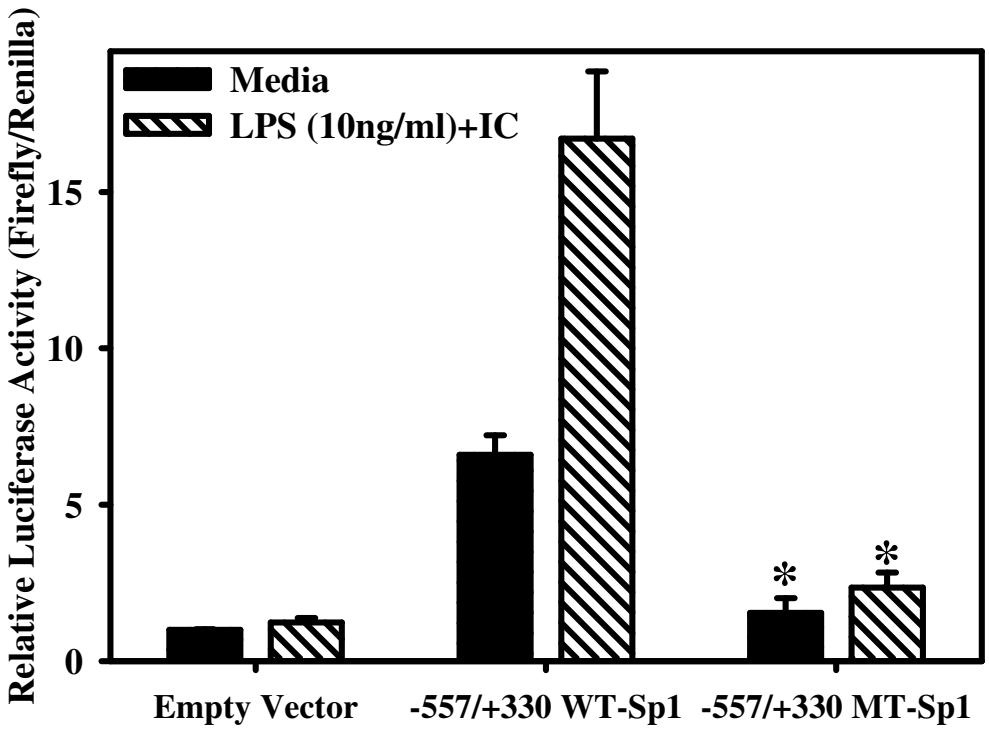

Figure 29: Sp1 site located at -83/-54 is required for HB-EGF promoter activity. (A) Schematic of the mutations made in the Sp1 site contained in the -557/+330 vector. The central GC of the three conserved core GGGCGG sequences was mutated to TA by site-directed mutagenesis. (B) RAW264.7 cells were transfected with the empty vector or the -557/+330 HB-EGF reporter vector containing the wild-type or mutant Sp1 binding site overnight then stimulated with LPS(10ng/ml)+IC for 8h. Samples were analyzed as described in B, and represented as fold changes from unstimulated cells transfected with the empty vector. Error bars indicate ± standard deviation. Asterisk indicates a p-value of <0.001 as comparing media or LPS+IC conditions from wild-type to mutant -557/+330 transfected cells. Figures are representative of at least three independent experiments. Error bars indicate ± standard deviation of experiments performed in triplicate.

To explain the seemingly discordant data concerning the constitutive DNA binding ability of Sp1 by EMSA, the increase in the recruitment to the HB-EGF locus by ChIP, as well as the difference between luciferase activity and mRNA production, we decided to determine whether HB-EGF was regulated, at least in part, at the level of chromatin and locus accessibility. We examined the sensitivity of DNA to cleavage by DNase before and after stimulation of macrophages with LPS+IC (Figure 30). Chromatin sensitivity to DNase was measured at amplicons 3, 8, and 11 and compared with a region of the TdT gene, which is not expressed in macrophages[178]. At 0' (unstimulated cells), all of these regions were relatively resistant to DNase cleavage. Within minutes of stimulation, all three regions studied showed a dramatic increase in accessibility to the DNase enzyme. Although each region showed slightly different kinetics, the extent of the accessibility increase was comparable in all three regions (Figure 30). This was not the case for the TdT gene, which showed essentially no changes in accessibility over this period of observation (Figure 30). These data suggest that although Sp1 is constitutively found in the nucleus in a form that is able to bind to its cognate sequences, in unstimulated cells this binding does not occur. Changes in HB-EGF promoter accessibility allow for the association of Sp1 to the HB-EGF promoter following stimulation.

Requirement of ERK activity for efficient Sp1 recruitment and promoter accessibility

Our previous observations indicated that ERK activity is required for efficient recruitment of Sp1 to the IL-10 promoter[105] due to ERK dependent phosphorylation of histone H3, which results in enhanced promoter accessibility. In order to determine

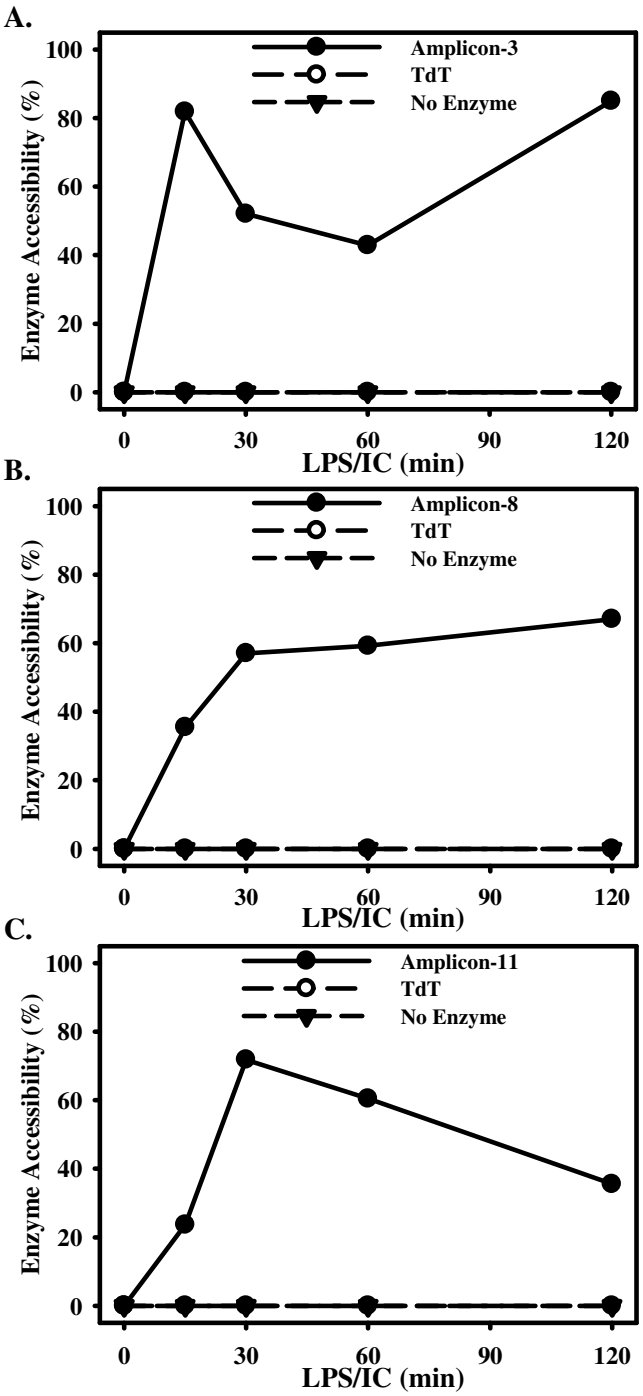

Figure 30: Changes in DNase I accessibility at the HB-EGF promoter.
BMMΦ were stimulated with LPS+IC for 0, 15, 30 60, or 120 minutes then fixed with formaldehyde. Nuclei were isolated and treated with DNase for 1h on ice. DNA was then purified and subject to QRT-PCR. Data are presented as a percentage of DNase accessibility to amplicons 3 (**A**), 8 (**B**) and 11 (**C**) as normalized to undigested DNA then to unstimulated control. The lymphocyte specific TdT gene is present as a negative control for changes in DNase sensitivity. Figures are representative of at least three independent experiments.

whether ERK activity was required for efficient Sp1 recruitment to the HB-EGF promoter, macrophages were pretreated with the ERK inhibitor U0126 and Sp1 recruitment to the HB-EGF promoter was measured by ChIP (Figure 31). Similar to the observations made in figure 5, stimulation of macrophages with LPS+IC resulted in a strong recruitment of Sp1 to all three regions of the HB-EGF promoter at 45' (amplicons 3, 8, and 13). Blocking the ERK pathway with U0126 completely diminished Sp1 binding at all three of these sites (Figure 31).

Blocking the ERK pathway also prevented stimulation-dependent increases in DNA accessibility at the HB-EGF promoter. Similar to figure 30, when macrophages were treated with LPS+IC, the HB-EGF promoter became more accessible to DNase activity at amplicons 3 (Figure 32A), 8 (32B), and 11 (32C). Inhibition of the ERK pathway with U0126, however, greatly diminished the stimulus-dependent increase in accessibility at the HB-EGF promoter (Figure 32A-C). Thus, both Sp1 association and DNase accessibility were dependent on the activation of ERK.

Induction of HB-EGF by various IL-10 promoting stimuli are ERK dependent

We wished to determine whether IL-10 and HB-EGF were coordinately regulated in macrophages that were induced to over-produce IL-10 by stimuli other than immune complexes. Macrophages were incubated with prostaglandin E(2), dibutyryl cAMP, or 4T1 tumor cell culture supernatants alone or in combination with LPS. Stimulation of macrophages with LPS in the presence of immune complexes (Figure 34A) prostaglandin E(2) (Figure 34B), dibutyryl cAMP (Figure 34C),or 4T1 culture supernatants (Figure 34D) enhanced the production of both IL-10 (left panels) and HB-EGF (right panels)

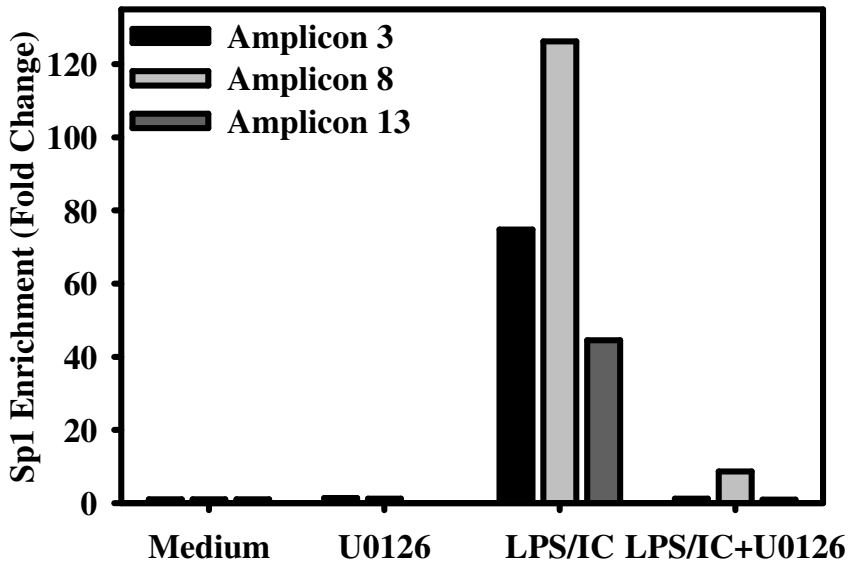

Figure 31: ERK dependent association of Sp1 with the HB-EGF promoter. BMMΦ were treated with vehicle alone or 5μM U0126 for 1h, then left unstimulated (Medium) or stimulated with LPS(10ng/ml)+IC for 45 minutes. Cells were then fixed and processed for Sp1 ChIP as described in figure 26. Sp1 association is expressed as fold enrichment from unstimulated vehicle control for amplicons 3, 8, and 13, each of which contain Sp1 binding sites. Figures are representative of at least two independent experiments.

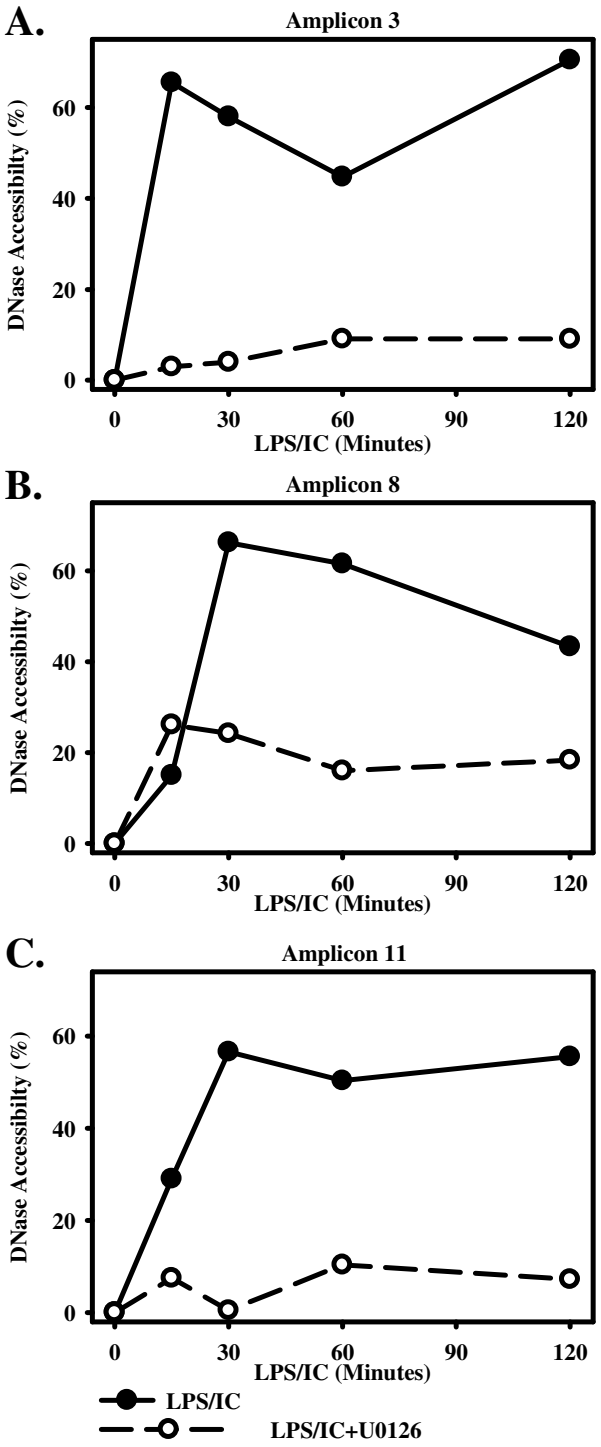

Figure 32: Erk dependent accessibility to the HB-EGF promoter.
BMMΦ were treated with vehicle alone or 5μM U0126 for 1h, then left unstimulated (0') or stimulated with LPS(10ng/ml)+IC for 15', 30', 60', or 120'. Cells were then fixed and processed for DNase accessibility as described for figure 30. DNase accessibility is presented as a percentage of digested DNA as normalized to unstimulated and undigested controls for amplicons 3 (A), 8 (B), and 11 (C). Figures are representative of at least two independent experiments.

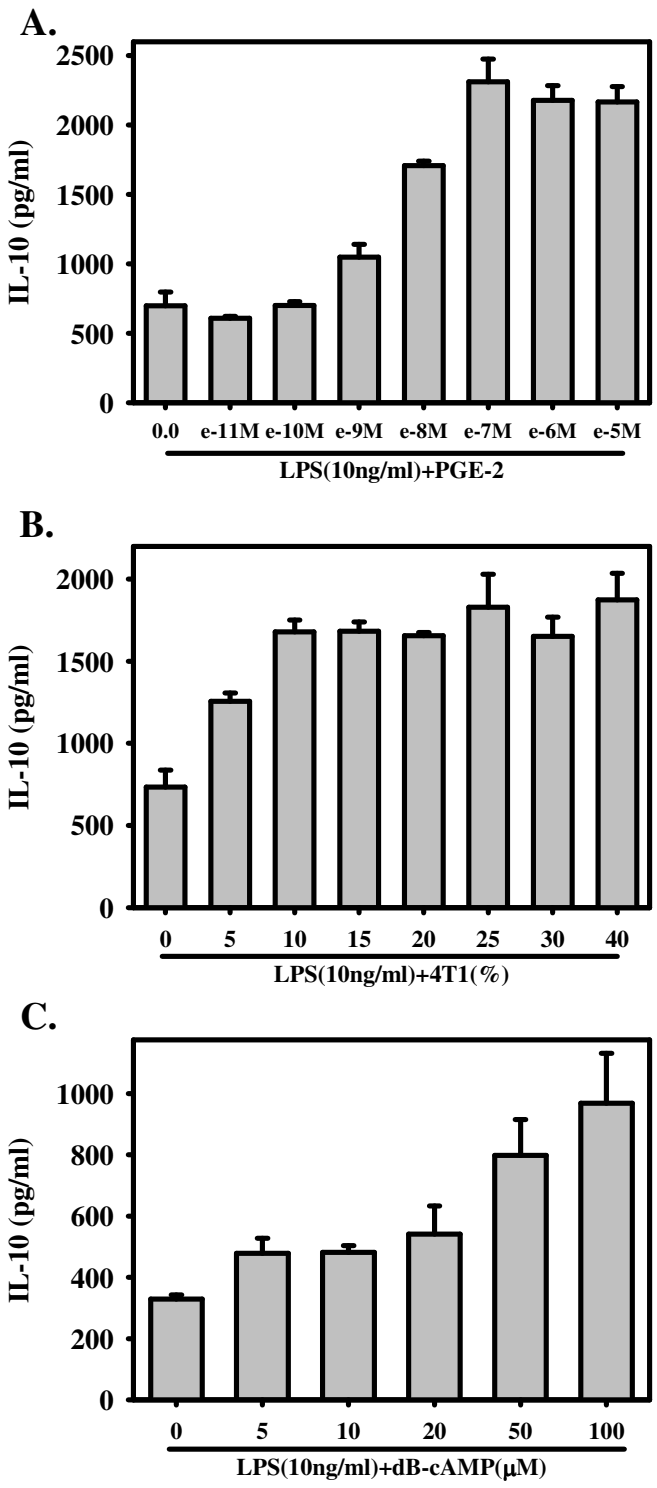

Figure 33: LPS induced IL-10 production is enhanced by a number of stimuli. Macrophages were stimulated with LPS with increasing concentrations of Prostaglandin E(2) (PGE-2, **A**), 4T1 culture supernantants (4T1%, **B**), and dibutyryl-cAMP (dB-cAMP, **C**). Macrophage culture supernantants were collected after 8 hours and the concentration of IL-10 determined by ELISA. Error bars indicate ± standard deviation of experiments performed in triplicate.

mRNA, as measured by real-time PCR. None of these three stimuli when used alone induced either IL-10 or HB-EGF (solid line). It was only when they were combined with a stimuli such as LPS (dashed lines) that the dramatic induction was observed. We next examined whether ERK activity was required for the enhanced production of HB-EGF in response to PGE-2, dibutyryl cAMP, or 4T1 culture supernatants. In the presence of U0126 there was a dramatic inhibition of HB-EGF mRNA induction (Figure 35) regardless of the stimulation conditions. Thus, both IL-10 and HB-EGF are induced by a variety of stimuli and in all cases this induction depends on the activation of ERK.

HB-EGF and Cytokine Levels Expressed by Tumor Associated Macrophages (TAMs)

It has previously been observed that tumor associated macrophages express elevated levels of IL-10 both constitutively and after stimulation[144,179]. As we have established that there appears to be a mechanism of coordinate regulation between IL-10 and HB-EGF (Figure 34), we wished to investigate if whether tumor associated macrophages expressed elevated levels of IL-10, did they also express elevated levels of HB-EGF. $CD11b^+$ / $F4/80^+$ double positive cells were sorted from adherent cells isolated from homogenized 15-20mm B16 melanomas. Cells were then stimulated with LPS for 90' or left unstimulated. HB-EGF (Figure 36A), IL-10 (36B), and TNF-α (36C) levels were assessed by QRT-PCR and compared to mRNA levels from peritoneal macrophages of age-matched controls or tumor-bearing mice. TAMs expressed elevated levels of IL-10 as well as elevated levels of HB-EGF, with or without stimulation with LPS. TAMs were devoid of TNF-α, even after stimulation with LPS (Figure 37C).

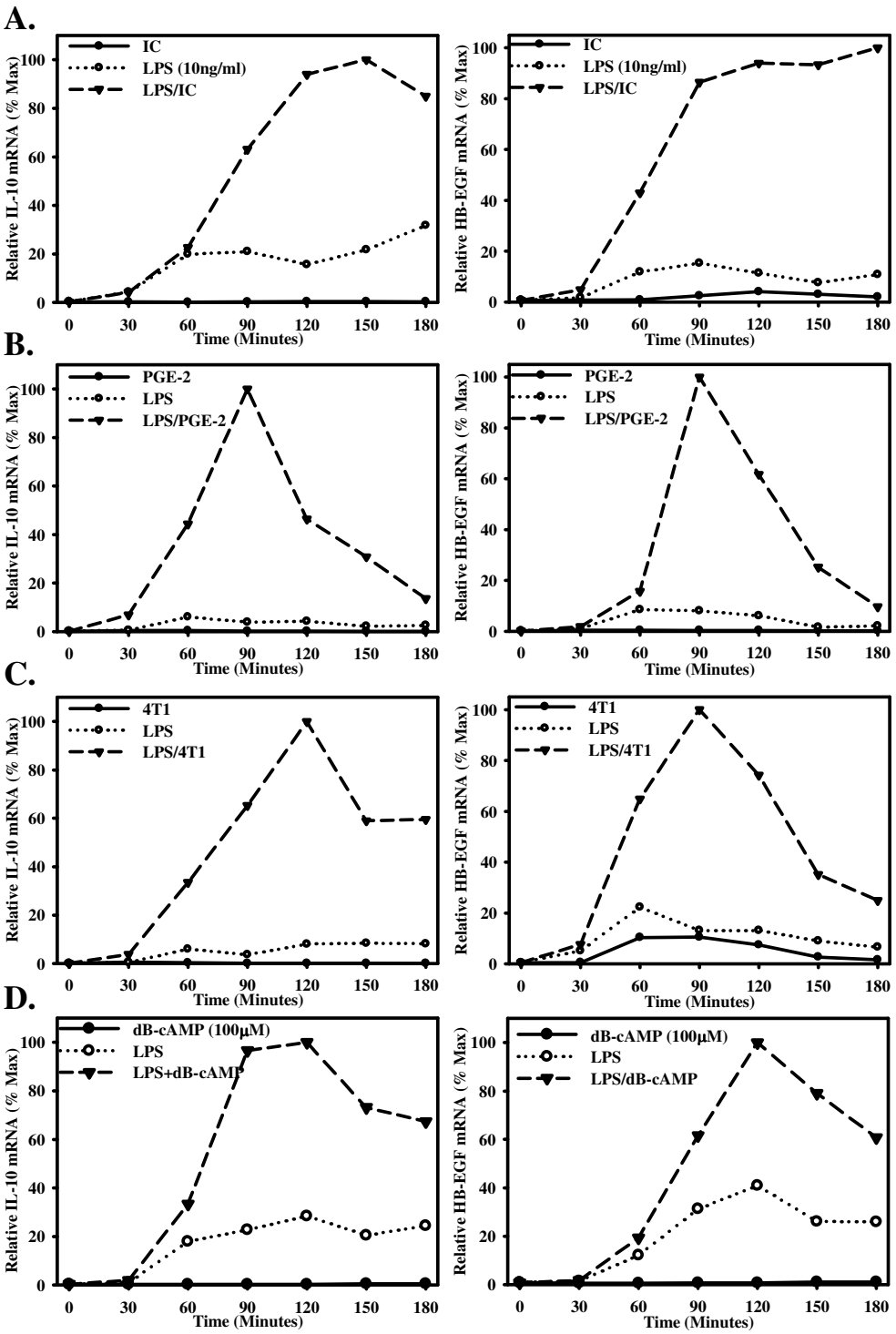

Figure 34: Conditions which promote IL-10 also promote HB-EGF.
BMMΦ were stimulated with immune complexes (**A**, IC), 10^{-8}M prostaglandin E2 (**B**, PGE-2), 27% 4T1 culture supernatants (**C**, 4T1), or 100μM dibutyrl cAMP (**D**, dB-cAMP) in the presence or absence of LPS(10ng/ml). IL-10 (left) and HB-EGF (right) mRNA was measured at 0', 30', 60', 90', 120', 150' and 180' by QRT-PCR and expressed as relative to the maximum level of HB-EGF mRNA during the stimulation conditions. Figures are representative of at least three independent experiments.

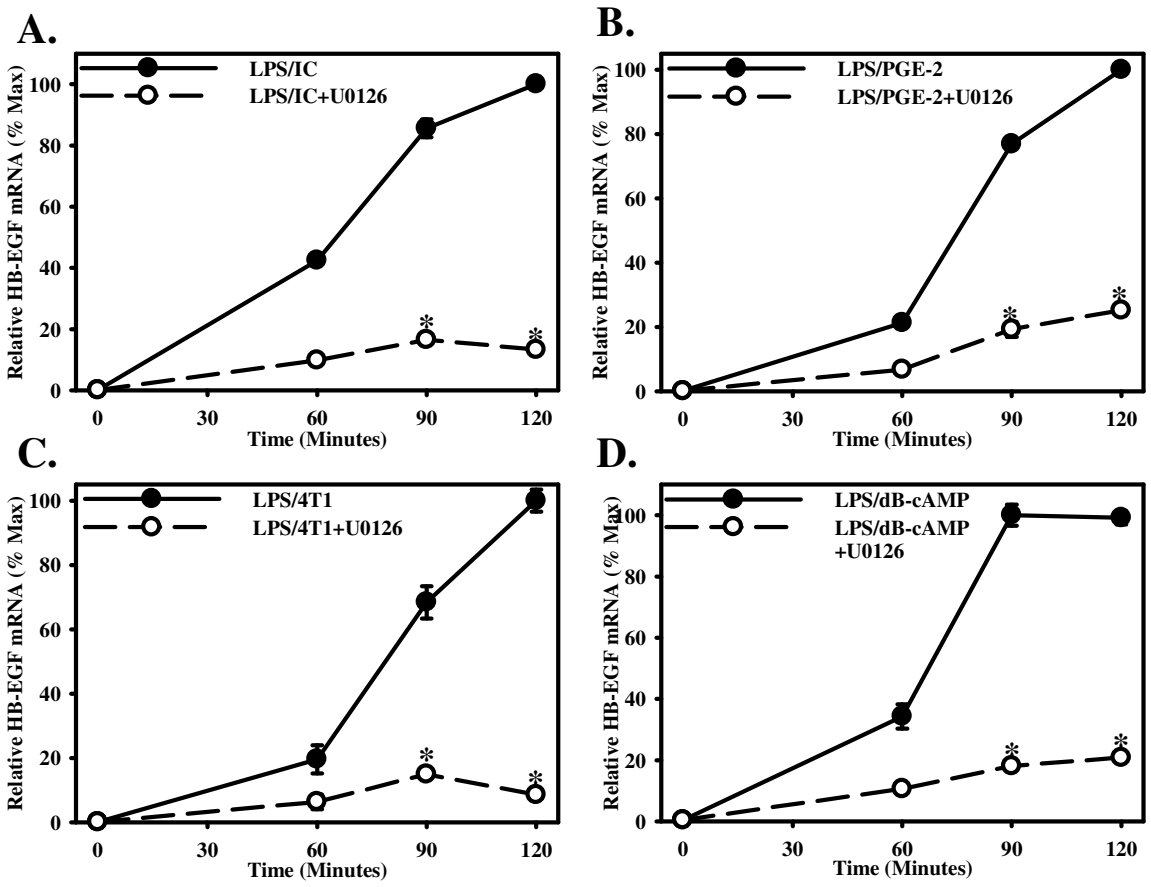

Figure 35: ERK dependent regulation of HB-EGF in response to multiple stimulation conditions.

BMMΦ were pretreated for 1 hour with 5μM U0126 or vehicle alone, then stimulated with LPS+IC (A), LPS+PGE-2 (B), 4T1 culture supernatants (C) or LPS+dB-cAMP (D) for 60', 90', or 120', as in figure 34. HB-EGF mRNA was measured by QRT-PCR and expressed relative to the maximum level of HB-EGF mRNA during the stimulation conditions. Figures are representative of at least three independent experiments. Asterisk indicates p-values <0.01.

Discussion

We have identified the production of heparin-binding EGF-like growth factor and describe its regulation in MΦ-II. HB-EGF is a growth factor involved in a number of both physiological and pathological conditions[119]. We show that there are many similarities between IL-10 and HB-EGF production, suggesting a common mechanism of gene expression. For the induction of both HB-EGF and IL-10, two of the three major MAPKs, p38 and ERK, are required. Blocking either of them prevents the transcription of both genes.

ERK activation results in increased accessibility of the HB-EGF promoter to the transcription factor Sp1, which binds to the HB-EGF promoter. This conclusion was reached after studies to analyze the binding of Sp1 to the HB-EGF promoter yielded dramatically different results, depending on the assays that were employed. The EMSA assays indicated that Sp1 is resident in the nucleus of unstimulated cells, and that it could constitutively bind to elements in the HB-EGF promoter in the absence of stimulation. This constitutive binding to unstimulated cells, however, was not observed by ChIP analysis. A potential explanation for these differences lies in the increased accessibility of the HB-EGF promoter to transcription factors following stimulation. Increased accessibility would also explain the discordant luciferase data in which LPS alone induced as much luciferase as did LPS+IC. Regulation at the level of chromatin accessibility would not be obvious during EMSA or luciferase assays, where naked DNA was used as the probe or readout. This increased accessibility of the HB-EGF promoter following stimulation was confirmed by DNase accessibility assays. Following stimulation the HB-EGF promoter became more accessible to DNase cleavage, whereas

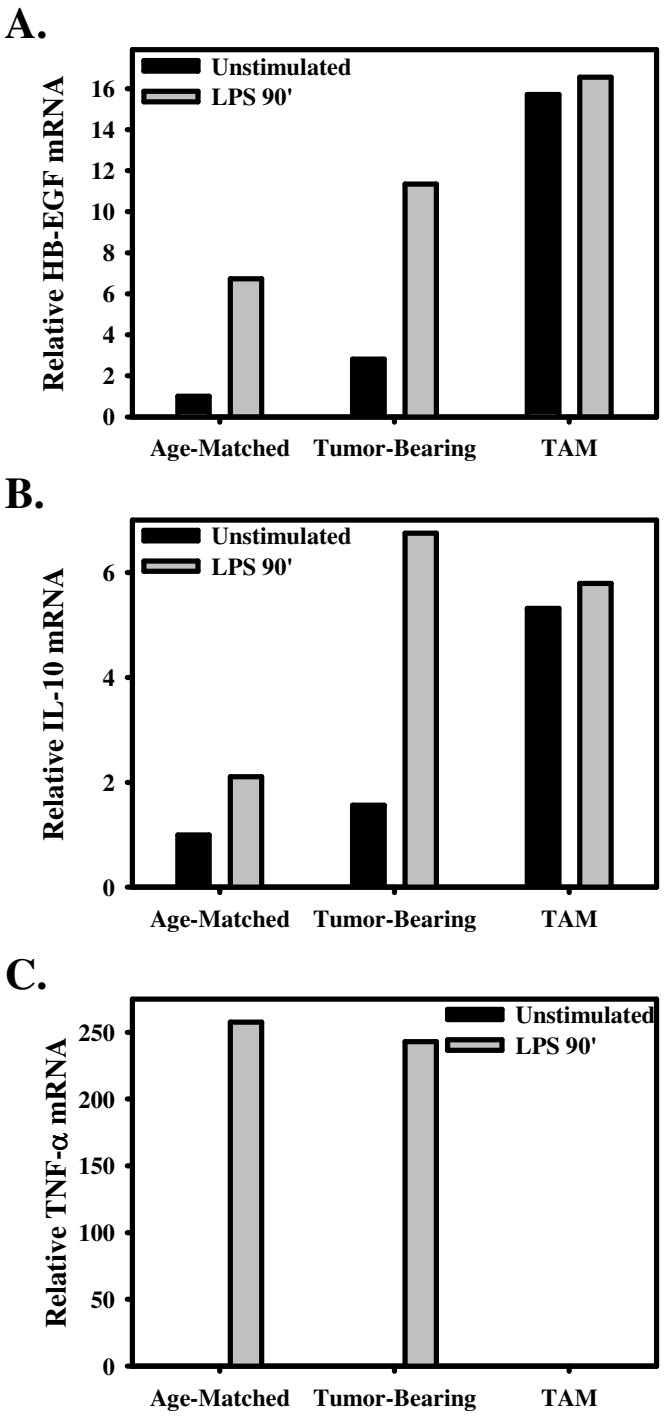

Figure 36: HB-EGF and cytokine mRNA levels from tumor associated macrophages.

Peritoneal macrophages from age-matched controls and tumor bearing mice, as well as sorted $CD11b^+$ and $F4/80^+$ cells (TAM) from melanomas were left unstimulated or stimulated with LPS for 90'. QRT-PCR was performed to assess message levels for HB-EGF, IL-10, and TNF-α. Values are relative to unstimulated macrophages from age-matched controls.

the accessibility of a control gene that was not transcribed in macrophages was unaltered. This increased accessibility did not occur when ERK was inhibited. Thus, an important component of the regulation of HB-EGF gene expression involves alterations in promoter accessibility, and ERK activation is involved in these alterations.

By EMSA and ChIP assays, we show that Sp1 can bind to three positions along the HB-EGF promoter. Luciferase reporter assays were performed to determine which site was most closely associated with transcriptional activation. The binding of Sp1 to the 3'-most site, located adjacent to the transcriptional start site, appeared to be required for the activity of the HB-EGF promoter. This site was sufficient to induce maximal luciferase activity. Surprisingly, an analysis of an extended promoter, including the 5'-most site, not only failed to contribute to transcription but substantially diminished luciferase activity. The logical interpretation of these results is that a repressor element was located within this site.

We examined three other conditions in which the production of IL-10 was induced and demonstrate that HB-EGF production was similarly regulated in an ERK dependant fashion. Prostaglandin E(2) (PGE-2) has been previously shown to enhance the endotoxin-driven production IL-10 from macrophages and monocytes[180]. We show that HB-EGF production is also enhanced under these conditions. Similar to what the lab has observed for immune complexes, PGE-2 alone induced no HB-EGF but rather reprogrammed macrophages to produce HB-EGF in response to stimulation with LPS (Figure 34). The same observations were made with supernatants from the mammary tumor cell line 4T1, and stimulation in the presence of dibutyryl cAMP. In all cases, HB-EGF induction required co-stimulation with LPS and was dramatically inhibited by the

addition of the MEK1/2 inhibitor, U0126. Thus, the activation of ERK in macrophages results in a phenotype that is quite distinct from classically activated macrophages. ERK activation results in macrophages that are not only immunosuppressive though the production of IL-10, but may also contribute to angiogenesis via HB-EGF.

Tumor-associated macrophages have been linked enhanced tumor survival and progression through a number of mechanisms. This includes immunosuppression via IL-10[179] and angiogenesis through a number of mechanisms[145]. Tumor associated macrophages are not only a rich source of IL-10, but are also thought to produce a number of tumor promoting growth factors[145]. Elevated expression of HB-EGF has been found in many human tumors, and high levels have been found to correlate with poor prognosis[133]. In vitro and in vivo studies indicate that the expression of HB-EGF in the developing tumor microenvironment can contribute to angiogenesis, and thus to metastasis[130]. We propose that the coexpression of IL-10 and HB-EGF by macrophages may be a mechanism to explain this. Conditions common in the tumor microenvironment, such as the secretion of PGE-2 by tumor cells, appear to prime macrophages to produce both IL-10 and HB-EGF. Importantly, we show that both IL-10 and HB-EGF are dependent on the activation of ERK. These findings suggest that the inhibition of ERK may prevent both the immunosuppressive and the angiogenic activities of these macrophages.

Future research should focus on the production of IL-10 and HB-EGF by tumor-associated macrophages and the specificity of the ERK-dependant enhancement of their production. We have investigated the expression of IL-10, HB-EGF, and TNF-α by tumor associated macrophages of the B16 melanoma model. We show a constitutive

enhancement in IL-10 and HB-EGF expression as compared to unstimulated macrophages from control peritoneal cells. Their expression remains unchanged by stimulation with LPS, unlike control cells. The constitutive enhancement of IL-10 expression by tumor associated macrophages has previously been reported. However, unlike what we have seen, stimulation with LPS leads to a marked up-regulation of IL-10 as compared to control cells. Therefore, the tumor microenvironment appears to prime these cells produce IL-10 even in response to an inflammatory stimulus. Therefore, future research should study an established model in which the expression of IL-10 has previously been investigated. Additionally, procedures used to enrich macrophages from tumors need to be revisited. The procedures used were most likely were not ideal for retaining the viability of macrophages and thus reproducible responsiveness to stimulation.

CHAPTER 5: ROLE OF THE MITOGEN AND STRESS ACTIVATED PROTEIN KINASES (MSKS) AND PHOSPHOINOSITIDE 3-KINASE IN THE REGULATION OF IL-10

Stimulation of Macrophages Modulates the Kinase Activity of the MSKs

In order to determine the potential role of the MSKs in the regulation of IL-10, we first wished to determine if the MSKs were activated during stimulation conditions that promoted IL-10. As previously observed, the IL-10 promoter is phophorylated at histone H3 at serine 10 when macrophages are stimulated with immune complexes alone or in combination with LPS[106]. Therefore, we wished to determine if the MSKs were activated under these conditions. In order to address this, an immunoprecipitation kinase assay was performed. Macrophages were left unstimulated or stimulated with immune complexes (IC) alone or the combination of LPS+IC, then cell lysates were taken at given time points. MSK1 or MSK2 was immunoprecipitated and combined with the substrate, recombinant histone H3, in the presence of ATP. Western blots were performed using phospho-histone H3 (serine 10) specific antibodies in order to determine if MSK1 or MSK2 was activated. These immunoprecipitated kinases were able to phosphorylate histone H3. Additionally, immune complexes seem to modulate the activity of MSKs. MSK1 has a high level of basal activity that seems to be increased with the addition of immune complexes with or without the presence of LPS. As to be expected, the activity seems to be more robust in the presence of LPS as it is also an activator of the MAPKs. MSK2 does not seem to have any detectable basal level of activity. However, in the presence of immune complexes MSK2 is activated. Importantly, this seems to have

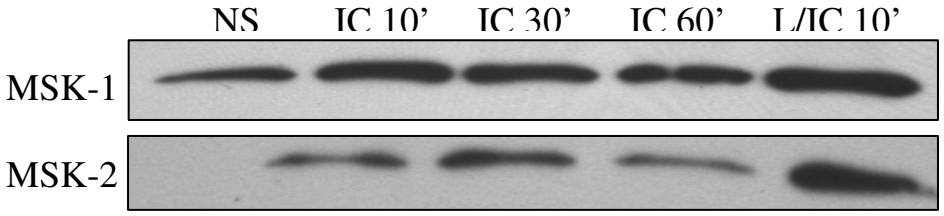

Figure 37: Kinase assay for MSK activity measuring phosphorylation of histone H3. Macrophages were stimulated with immune complexes (IC) with or without LPS or not stimulated (NS) then lysed in the presence of protease and phosphatase inhibitors at the given times. Total MSK1 or MSK2 was immunoprecipitated from cell lysates then incubated with ATP and recombinant human histone H3 for 15' at 30°C. Samples were subject to SDS-PAGE and western blotting was performed using an antibody specific for phosphorylated histone H3 (Ser^{10}).

kinetics similar to the pattern of phosphorylation at the IL-10 locus in that there is an increase in activity to at least 30 minutes, but at 60 minutes this activity appears to be tapering off. As expected, the presence of LPS increases the induced MSK2 activity (Figure 37).

Use of the Inhibitor H89 and MSK1/2 siRNA Blocks IL-10 Production

In order to first assess the potential role of the MSKs in the super-induction of IL-10, we first used the inhibitor H89. This inhibitor has previously been shown to primarily inhibit the activity of certain isoforms of PKA and PKC[181]. However, this inhibitor has also been shown to have a potent inhibitory effect against the MSKs, but not the MAPKs or RSKs[114]. Although this inhibitor is helpful for potentially ruling out the MSKs in IL-10 production, it can not be used to definitively implicate the MSKs in the production of IL-10. Macrophages pre-treated with H89 decreased IL-10 production in a dose dependant manner, with IL-10 levels after stimulation with LPS/IC nearing that of LPS alone (Figure 38A). IL-12/23p40 production was increased by the presence of H89 (Figure 38B).

In order to more directly address whether the MSKs played a role, an siRNA (small interfering RNA) approach was employed. Although either MSK1 or MSK2 may be involved in the chromatin remodeling at the IL-10 locus via phosphorylation of histone H3, the possibility exists that MSK1 and MSK2 are redundant or interchangeable kinases in the regulation of IL-10. If the expression of either MSK1 or MSK2 is knocked down by siRNA transfection, IL-10 production may still be induced despite the lack of one kinase. To this address this possibility, an siRNA target was based within the highly

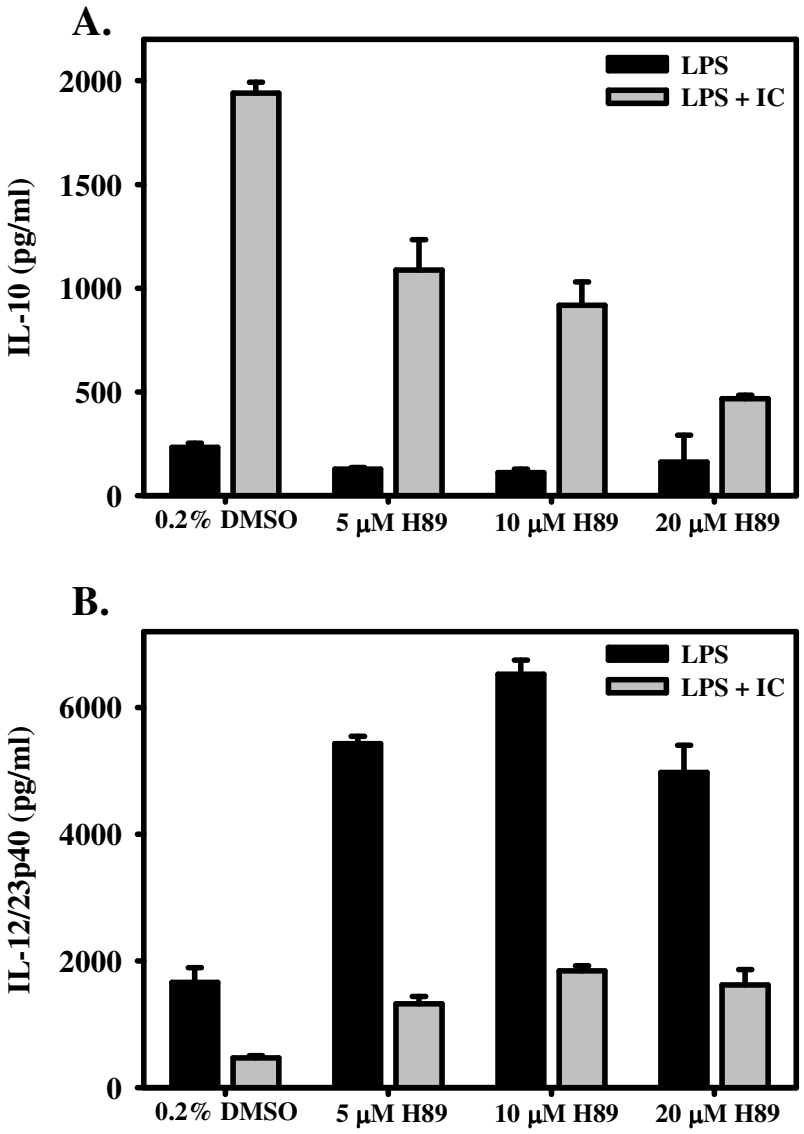

Figure 38: Cytokine production in the presence of the inhibitor H89.
Macrophages were pretreated with increasing concentrations of the inhibitor H89 (5-20μM) or vehicle control (0.2% DMSO) for 1h, then stimulated with LPS (10ng/ml) or LPS/IC overnight. Supernatants were collected and assayed for IL-10 (A) or IL-12/23p40 (B) concentrations as measured by ELISA.

A.

MSK-2 1621 ggcaggcgtggtgcaccgcgacctg***aaacccgagaacatcttgtac***gcggacgacactcc 1680

B.

MSK-1 2079 agaccccgtgcttcaccctccactacgcagcaccggagctcttgacgcac***aatggctacg*** 2138
MSK-2 1752 agac**T**cc**T**tgcttcac**A**ct**G**ca**G**tacgc**T**gcacc**c**gagct**GC**tg**G**c**A**ca**GC**a**G**ggctacg 1811
MSK-1 2139 ***atgagtcctgt***gacctgtggagcttgggtgtcatcctgtatacaatgctgtcagggcagg 2198
MSK-2 1812 atgagtcctg**C**ga**T**ct**A**tggagc**C**tgggtgtcat**T**ctgta**C**a**TG**atgctgtc**T**gg**C**cagg 1871
MSK-1 2199 tgccattcca 2208
MSK-2 1872 t**T**cc**C**ttcca 1881 Identities: 104/130 (80%)

Figure 39: siRNA design for MSK2 and MSK1/2.
(A) MSK2 cDNA sequence 1621-1680. Bold and italicized denotes the target of the siRNA against MSK2. (B) Alignments made between MSK1 (2079-2208) and MSK2 (1752-1881) cDNA in a region of significant homology. Bold and underlined denotes nucleotides that differ from MSK2 to MSK1. Bold and italicized denotes the target for the siRNA against MSK1 and MSK2. The 21 base target is based on the MSK1 template, however 18 bases are conserved in MSK2 with 17 bases conserved consecutively.

conserved region in the cDNA sequences of MSK1 (2079-2208) and MSK2 (1752-1881) (Figure 39B). The 21 base target was based on the MSK1 template, however 18 bases are conserved in MSK2 with 17 bases conserved consecutively. Additionally, another siRNA target was found for MSK2 (Figure 39A) which does not have any significant homology to MSK1. Macrophages were transfected with each of these siRNAs as well as a negative control scramble siRNA for 48 hours then assayed for cytokine production upon stimulation with LPS with or without immune complexes overnight. Concentrations of IL-10 and IL-12/23p40 were determined by ELISA. Macrophages transfected with only MSK2 siRNA did not seem to have modified cytokine production from the negative control (scramble), however those transfected with MSK1/2 siRNA had severely limited IL-10 production (Figure 40A). Silencing of MSK2 transcript with MSK2 siRNA and MSK1 and MSK2 transcript with MSK1/2 siRNA was confirmed with real time PCR. As mentioned above, both MSK1 and MSK2 could potentially be interchangeable in their role in IL-10 production. Knocking out just one kinase with siRNA against MSK2 may not be enough to effect IL-10 production significantly, so knocking out both MSK1 and MSK2 may only be enough to effect IL-10 production.

MSK1/2 Double Knockout Macrophages Retain Their Ability to Produce IL-10

As there is the possibility of off-target silencing when using siRNA, we obtained macrophages from MSK1/2 double knockout mice[182]. Macrophages stimulated with LPS+IC retained their ability to produce high levels of IL-10 in both wild type and MSK1/2$^{-/-}$ cells (Figure 41A), without any significant difference between the them. These knockout cells, however, did have enhanced IL-12 production from LPS and LPS+IC

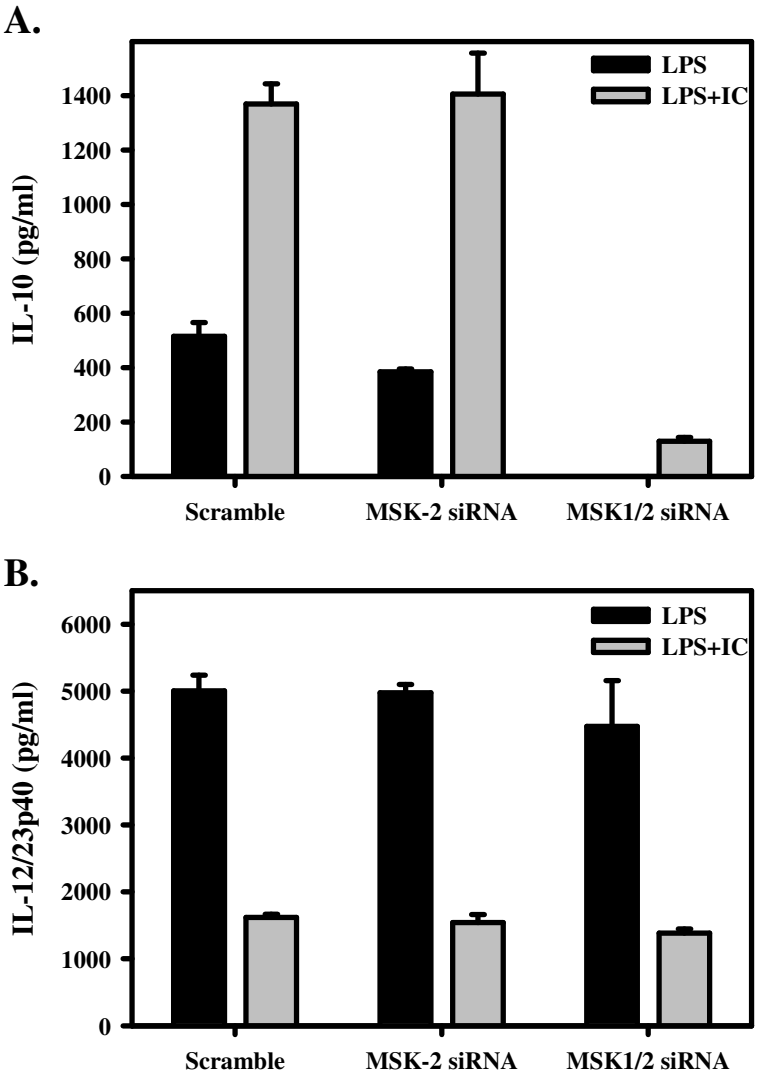

Figure 40: Cytokine production after transfection with siRNA for MSK1/2. BMMΦ were transfected with siRNA for MSK2, MSK1/2, or a control scrambled double-stranded RNA for 48 hours, then stimulated with LPS (10ng/ml) or LPS+IC overnight. Cell culture supernatants were then tested by ELISA for IL-10 (A) or IL-12/23p40 (B).

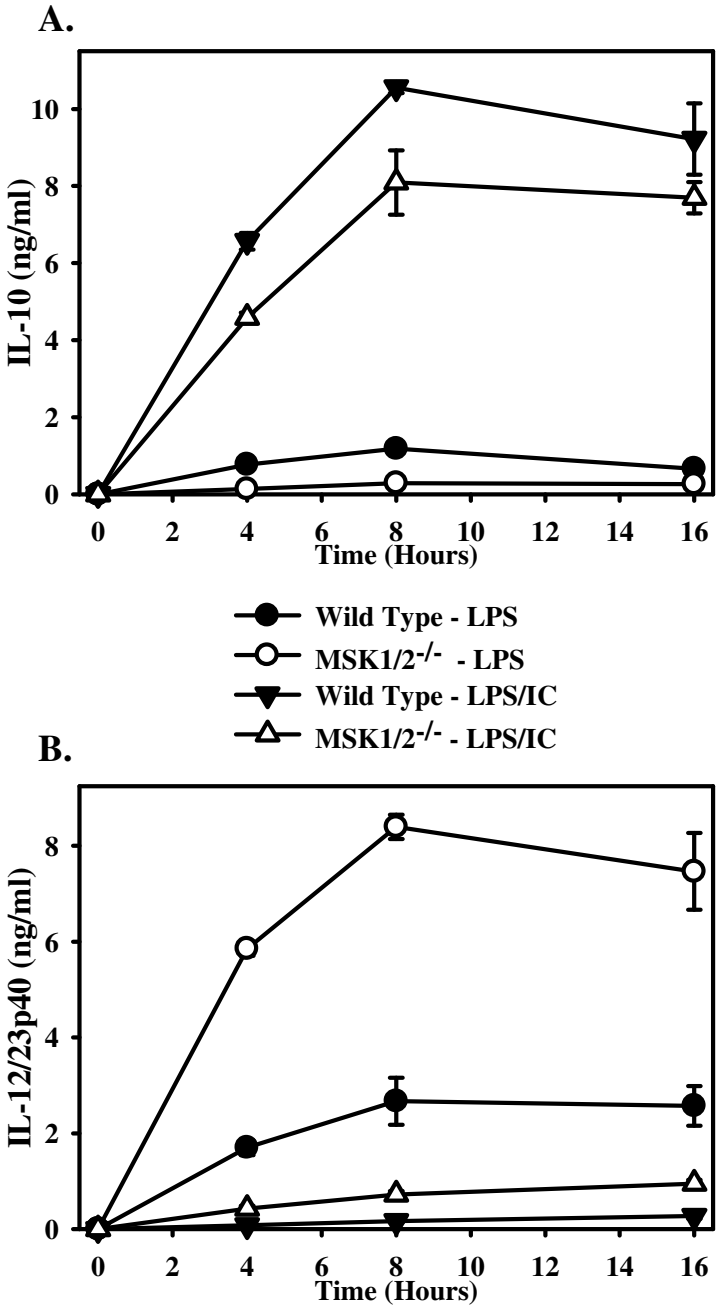

Figure 41: Cytokine production from MSK1/2 double knockout cells (MSK1/2-/-). Wild type and MSK1/2$^{-/-}$ BMMΦ were stimulated with LPS or LPS+IC for 4, 8, or 16 hours before supernatants were collected. Supernatants were assayed for IL-10 (A) or IL-12/23p40 (B) concentrations by ELISA. Experiments are representative of 2 two independent experiments.

stimulated macrophages (Figure 41B). Therefore, based on the knockout data, we conclude that the MSKs do not seem to play any direct role in superinduction of IL-10 due to LPS+IC stimulation.

The Role of Phosphoinositide 3-kinase in the Regulation of IL-10

Previous work in the lab has shown the requirement for Fcγ-receptor mediated Syk activation in the regulation of IL-10 by MΦ-II though the activation of ERK[117]. Crosslinking of the FcγR by immune complexes initiates the activation of Syk, which in turn leads to the activation of Ras and PI3K (Figure 2)[16]. Both of these pathways are able to mediate the activation of the MAPK by FcγR crosslinking. Previous unpublished observations showed no role for Ras activity in regulating IL-10, leading to the possibility that PI3K may instead play a role in regulating MAPK activity and thus IL-10. In order to address this, macrophages were pretreated with increasing concentrations of the PI3K inhibitor LY294002 (1-20μM), then stimulated with LPS or LPS+IC. LPS+IC mediated IL-10 production was severely attenuated by the presence of the LY294002 in a dose dependant fashion (Figure 42A). Additionally, LPS mediated IL-12/23p40 was moderately enhanced by the presence of the inhibitor (Figure 42B). Therefore, PI3K does appear to play a role in the regulation of IL-10. The role of PI3K in the reciprocal regulation of these two cytokines will be the subject of future investigations in the lab.

Discussion

Previous work in the lab has shown that ERK-mediated phosphorylation of histone H3 leads to enhanced accessibility to the IL-10 promoter and thus enhanced IL-

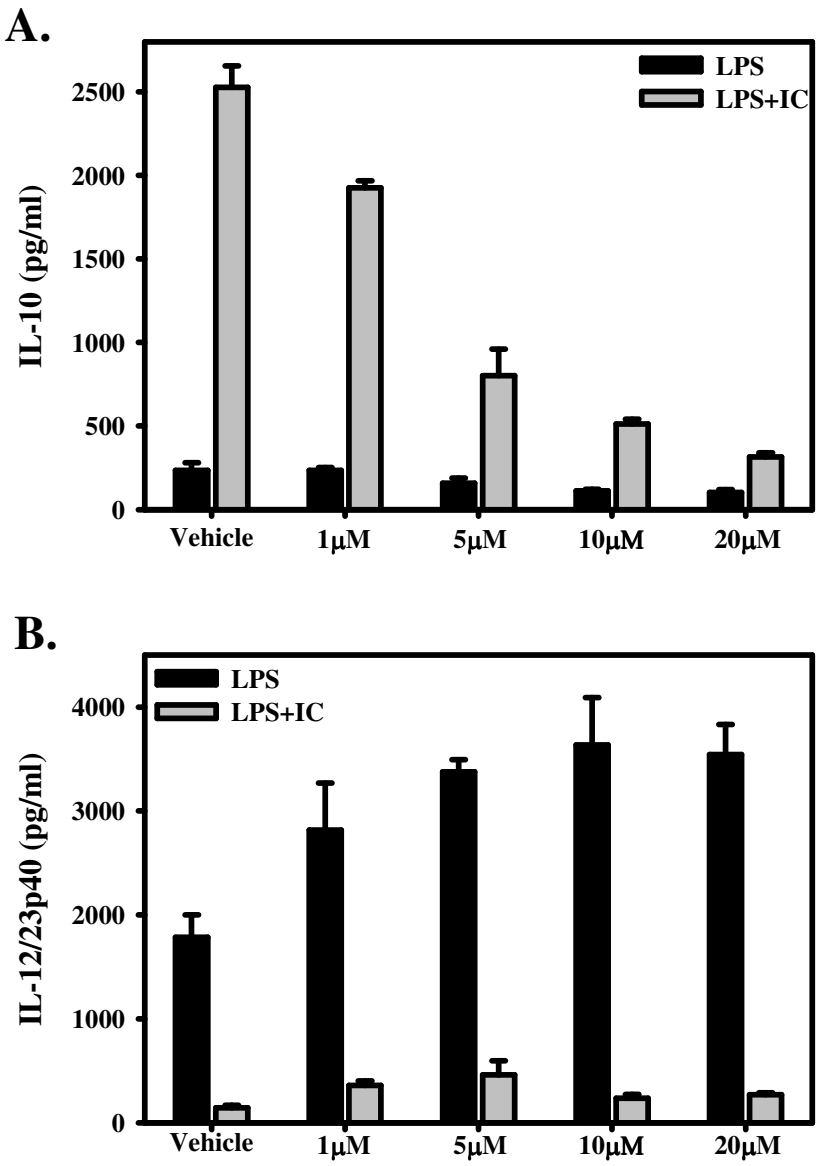

Figure 42: Production of IL-10 by MΦ-II is severely attenuated by the presence of the phosphoinositide 3-kinase inhibitor LY294002.
Macrophages were pretreated for 1 hour with increasing concentrations of PI3K inhibitor LY294002 or vehicle control, then stimulated with LPS or LPS+IC overnight. Supernatants were assayed for IL-10 (A) and IL-12 (B) concentrations by ELISA. Figures are representative of at least three independent experiments.

10 production[106]. Histone H3, however, is not phosphorylated directly by ERK, but is instead phosphorylated by a MAPK associated protein kinase (MK). Potential MKs that have been proposed to modify histones include RSK2, MSK1, and MSK2. As discussed above, there is some controversy as to the actual histone kinase, as studies using RSK-2 knockouts did not appear to be reproducible[115]. Therefore, we focused on MSK-1 and MSK2. The kinase activity of these proteins is enhanced by the presence of immune complexes. MSK1 appears to have a great deal of constitutive activity that is moderately enhanced by the presence of immune complexes, while MSK2 does not appear to have any constitutive activity but is enhanced by the presence of immune complexes. Both the inhibitor H89, as well as the MSK1/2 siRNA severely attenuated the production of IL-10 after stimulation with LPS+IC. These studies suggested that MSK1 or 2 may play a role in the regulation of IL-10. Most importantly, however, the lack of MSK1/2 activity in knockout cells did not significantly affect IL-10 production after stimulation with LPS+IC. Therefore, we concluded that neither MSK1 nor MSK2 appears to play a role in the regulation of IL-10. They do, however, appear to play a role in regulating excessive IL-12/23p40 production in response to LPS.

Recently, it was recognized that the HIV Tat (Transactivator of transcription) protein interacts with RSK2 and activates RSK2 kinase activity and is responsible for hyperphosphorylation of histone H3 within the integrated HIV promoter[183]. It is of note that Tat activity has been shown by several groups to be associated with the production of IL-10 by monocytes and macrophages[184]. Therefore, it may be possible that Tat activates RSK2 which may in turn hyperphosphorylates the promoter of the host gene IL-10, allowing for IL-10 production. Therefore, further work on the role of the histone kinases

in the regulation of IL-10 should focus on the role of RSK2. The RSK inhibitors BI-D1870 and SL0101, which have been used to establish RSK2 in regulating dendritic cell phagocytosis[185], should first be used to establish whether RSK plays a role in IL-10 production and histone phosphorylation. If this is the case, addressing whether conditions which enhance the activity of RSK2, possibly though expression of the Tat protein or by transfection, may represent a novel way to modulate IL-10 production by macrophages.

Additionally, the lab had previously shown a role for Syk in regulating ERK activity after engagement of the Fcγ receptors by the presence of IgG-immune complexes[117]. Syk mediates its activity through the activation of SOS which in turn activates Ras or through the activation of PI3K. Our unpublished results have shown that Ras activity is not required in the regulation of IL-10, therefore the activation of PI3K may be required for the activation of ERK via Syk. In the presence of LY294002, a specific inhibitor of PI3K, we show that the production of IL-10 after stimulation of macrophages with LPS+IC is severely attenuated, leading us to believe that PI3K is required. Future research should focus on the role of PI3K, possibly by assessing ERK after stimulation with immune complexes in the presence of LY294002 or the traditional inhibitor wortmannin.

Reference List

1. Gordon, S. Pattern recognition receptors: doubling up for the innate immune response. *Cell* **111**, 927-930 (2002).

2. Ehlers, M. R. CR3: a general purpose adhesion-recognition receptor essential for innate immunity. *Microbes. Infect.* **2**, 289-294 (2000).

3. Akira, S., Uematsu, S. & Takeuchi, O. Pathogen recognition and innate immunity. *Cell* **124**, 783-801 (2006).

4. Poltorak, A. *et al.* Defective LPS signaling in C3H/HeJ and C57BL/10ScCr mice: mutations in Tlr4 gene. *Science* **282**, 2085-2088 (1998).

5. Schwandner, R., Dziarski, R., Wesche, H., Rothe, M. & Kirschning, C. J. Peptidoglycan- and lipoteichoic acid-induced cell activation is mediated by toll-like receptor 2. *J. Biol. Chem.* **274**, 17406-17409 (1999).

6. Alexopoulou, L., Holt, A. C., Medzhitov, R. & Flavell, R. A. Recognition of double-stranded RNA and activation of NF-kappaB by Toll-like receptor 3. *Nature* **413**, 732-738 (2001).

7. Hemmi, H. *et al.* A Toll-like receptor recognizes bacterial DNA. *Nature* **408**, 740-745 (2000).

8. Echchannaoui, H. *et al.* Toll-like receptor 2-deficient mice are highly susceptible to Streptococcus pneumoniae meningitis because of reduced bacterial clearing and enhanced inflammation. *J. Infect. Dis.* **186**, 798-806 (2002).

9. Chamaillard, M. *et al.* An essential role for NOD1 in host recognition of bacterial peptidoglycan containing diaminopimelic acid. *Nat. Immunol.* **4**, 702-707 (2003).

10. Girardin, S. E. *et al.* Nod1 detects a unique muropeptide from gram-negative bacterial peptidoglycan. *Science* **300**, 1584-1587 (2003).

11. Yoneyama, M. *et al.* The RNA helicase RIG-I has an essential function in double-stranded RNA-induced innate antiviral responses. *Nat. Immunol.* **5**, 730-737 (2004).

12. Kang, D. C. *et al.* mda-5: An interferon-inducible putative RNA helicase with double-stranded RNA-dependent ATPase activity and melanoma growth-suppressive properties. *Proc. Natl. Acad. Sci. U. S. A* **99**, 637-642 (2002).

13. Takaoka, A. *et al.* DAI (DLM-1/ZBP1) is a cytosolic DNA sensor and an activator of innate immune response. *Nature* **448**, 501-505 (2007).

14. Tsan, M. F. & Gao, B. Endogenous ligands of Toll-like receptors. *J. Leukoc. Biol.* **76**, 514-519 (2004).

15. Kawai, T. & Akira, S. TLR signaling. *Cell Death. Differ.* **13**, 816-825 (2006).

16. Nimmerjahn, F. & Ravetch, J. V. Fcgamma receptors as regulators of immune responses. *Nat. Rev. Immunol.* **8**, 34-47 (2008).

17. Nimmerjahn, F. & Ravetch, J. V. Fcgamma receptors: old friends and new family members. *Immunity.* **24**, 19-28 (2006).

18. Nimmerjahn, F., Bruhns, P., Horiuchi, K. & Ravetch, J. V. FcgammaRIV: a novel FcR with distinct IgG subclass specificity. *Immunity.* **23**, 41-51 (2005).

19. Bogdan, C., Rollinghoff, M. & Diefenbach, A. Reactive oxygen and reactive nitrogen intermediates in innate and specific immunity. *Curr. Opin. Immunol.* **12**, 64-76 (2000).

20. Hesse, M. *et al.* Differential regulation of nitric oxide synthase-2 and arginase-1 by type 1/type 2 cytokines in vivo: granulomatous pathology is shaped by the pattern of L-arginine metabolism. *J. Immunol.* **167**, 6533-6544 (2001).

21. Saura, M. *et al.* An antiviral mechanism of nitric oxide: inhibition of a viral protease. *Immunity.* **10**, 21-28 (1999).

22. Szabo, S. J. *et al.* A novel transcription factor, T-bet, directs Th1 lineage commitment. *Cell* **100**, 655-669 (2000).

23. Zheng, W. & Flavell, R. A. The transcription factor GATA-3 is necessary and sufficient for Th2 cytokine gene expression in CD4 T cells. *Cell* **89**, 587-596 (1997).

24. Lee, G. R., Fields, P. E. & Flavell, R. A. Regulation of IL-4 gene expression by distal regulatory elements and GATA-3 at the chromatin level. *Immunity.* **14**, 447-459 (2001).

25. Fields, P. E., Lee, G. R., Kim, S. T., Bartsevich, V. V. & Flavell, R. A. Th2-specific chromatin remodeling and enhancer activity in the Th2 cytokine locus control region. *Immunity.* **21**, 865-876 (2004).

26. Ouyang, W. *et al.* Inhibition of Th1 development mediated by GATA-3 through an IL-4-independent mechanism. *Immunity.* **9**, 745-755 (1998).

27. Segal, B. M., Dwyer, B. K. & Shevach, E. M. An interleukin (IL)-10/IL-12 immunoregulatory circuit controls susceptibility to autoimmune disease. *J. Exp. Med.* **187**, 537-546 (1998).

28. Oppmann, B. *et al.* Novel p19 protein engages IL-12p40 to form a cytokine, IL-23, with biological activities similar as well as distinct from IL-12. *Immunity.* **13**, 715-725 (2000).

29. Weaver, C. T., Harrington, L. E., Mangan, P. R., Gavrieli, M. & Murphy, K. M. Th17: an effector CD4 T cell lineage with regulatory T cell ties. *Immunity.* **24**, 677-688 (2006).

30. Kobayashi, M. *et al.* Identification and purification of natural killer cell stimulatory factor (NKSF), a cytokine with multiple biologic effects on human lymphocytes. *J. Exp. Med.* **170**, 827-845 (1989).

31. Trinchieri, G. Interleukin-12 and the regulation of innate resistance and adaptive immunity. *Nat. Rev. Immunol.* **3**, 133-146 (2003).

32. Ma, X. *et al.* The interleukin 12 p40 gene promoter is primed by interferon gamma in monocytic cells. *J. Exp. Med.* **183**, 147-157 (1996).

33. Schulz, O. *et al.* CD40 triggering of heterodimeric IL-12 p70 production by dendritic cells in vivo requires a microbial priming signal. *Immunity.* **13**, 453-462 (2000).

34. Hunter, C. A. New IL-12-family members: IL-23 and IL-27, cytokines with divergent functions. *Nat. Rev. Immunol.* **5**, 521-531 (2005).

35. Wheelock, E. F. Interferon-like virus-inhibitor induced in human leukocytes by phytohemagglutinin. *Science* **149**, 310-311 (1965).

36. Schroder, K., Hertzog, P. J., Ravasi, T. & Hume, D. A. Interferon-gamma: an overview of signals, mechanisms and functions. *J. Leukoc. Biol.* **75**, 163-189 (2004).

37. Boehm, U., Klamp, T., Groot, M. & Howard, J. C. Cellular responses to interferon-gamma. *Annu. Rev. Immunol.* **15**, 749-795 (1997).

38. Pearl, J. E., Saunders, B., Ehlers, S., Orme, I. M. & Cooper, A. M. Inflammation and lymphocyte activation during mycobacterial infection in the interferon-gamma-deficient mouse. *Cell Immunol.* **211**, 43-50 (2001).

39. Wang, Z. E., Reiner, S. L., Zheng, S., Dalton, D. K. & Locksley, R. M. CD4+ effector cells default to the Th2 pathway in interferon gamma-deficient mice infected with Leishmania major. *J. Exp. Med.* **179**, 1367-1371 (1994).

40. Huang, S. *et al.* Immune response in mice that lack the interferon-gamma receptor. *Science* **259**, 1742-1745 (1993).

41. Fiorentino, D. F., Bond, M. W. & Mosmann, T. R. Two types of mouse T helper cell. IV. Th2 clones secrete a factor that inhibits cytokine production by Th1 clones. *J. Exp. Med.* **170**, 2081-2095 (1989).

42. Moore, K. W., de Waal, M. R., Coffman, R. L. & O'Garra, A. Interleukin-10 and the interleukin-10 receptor. *Annu. Rev. Immunol.* **19**, 683-765 (2001).

43. Jankovic, D. *et al.* Conventional T-bet(+)Foxp3(-) Th1 cells are the major source of host-protective regulatory IL-10 during intracellular protozoan infection. *J. Exp. Med.* **204**, 273-283 (2007).

44. Anderson, C. F., Oukka, M., Kuchroo, V. J. & Sacks, D. CD4(+)CD25(-)Foxp3(-) Th1 cells are the source of IL-10-mediated immune suppression in chronic cutaneous leishmaniasis. *J. Exp. Med.* **204**, 285-297 (2007).

45. O'Garra, A. & Vieira, P. Regulatory T cells and mechanisms of immune system control. *Nat. Med.* **10**, 801-805 (2004).

46. Berg, D. J. *et al.* Interleukin-10 is a central regulator of the response to LPS in murine models of endotoxic shock and the Shwartzman reaction but not endotoxin tolerance. *J. Clin. Invest* **96**, 2339-2347 (1995).

47. Rennick, D. M. & Fort, M. M. Lessons from genetically engineered animal models. XII. IL-10-deficient (IL-10(-/-) mice and intestinal inflammation. *Am. J. Physiol Gastrointest. Liver Physiol* **278**, G829-G833 (2000).

48. Kelly, J. P. & Bancroft, G. J. Administration of interleukin-10 abolishes innate resistance to Listeria monocytogenes. *Eur. J. Immunol.* **26**, 356-364 (1996).

49. Dai, W. J., Kohler, G. & Brombacher, F. Both innate and acquired immunity to Listeria monocytogenes infection are increased in IL-10-deficient mice. *J. Immunol.* **158**, 2259-2267 (1997).

50. van der, P. T., Marchant, A., Keogh, C. V., Goldman, M. & Lowry, S. F. Interleukin-10 impairs host defense in murine pneumococcal pneumonia. *J. Infect. Dis.* **174**, 994-1000 (1996).

51. Murray, P. J., Wang, L., Onufryk, C., Tepper, R. I. & Young, R. A. T cell-derived IL-10 antagonizes macrophage function in mycobacterial infection. *J. Immunol.* **158**, 315-321 (1997).

52. Murray, P. J. & Young, R. A. Increased antimycobacterial immunity in interleukin-10-deficient mice. *Infect. Immun.* **67**, 3087-3095 (1999).

53. Tonnetti, L. *et al.* Interleukin-4 and -10 exacerbate candidiasis in mice. *Eur. J. Immunol.* **25**, 1559-1565 (1995).

54. Romani, L. *et al.* Neutralization of IL-10 up-regulates nitric oxide production and protects susceptible mice from challenge with Candida albicans. *J. Immunol.* **152**, 3514-3521 (1994).

55. Kane, M. M. & Mosser, D. M. The role of IL-10 in promoting disease progression in leishmaniasis. *J. Immunol.* **166**, 1141-1147 (2001).

56. Miles, S. A., Conrad, S. M., Alves, R. G., Jeronimo, S. M. & Mosser, D. M. A role for IgG immune complexes during infection with the intracellular pathogen Leishmania. *J. Exp. Med.* **201**, 747-754 (2005).

57. Belkaid, Y., Piccirillo, C. A., Mendez, S., Shevach, E. M. & Sacks, D. L. CD4+CD25+ regulatory T cells control Leishmania major persistence and immunity. *Nature* **420**, 502-507 (2002).

58. Gordon, S. & Taylor, P. R. Monocyte and macrophage heterogeneity. *Nat. Rev. Immunol.* **5**, 953-964 (2005).

59. Conrad, S. M., Strauss-Ayali, D., Field, A. E., Mack, M. & Mosser, D. M. Leishmania-derived murine monocyte chemoattractant protein 1 enhances the recruitment of a restrictive population of CC chemokine receptor 2-positive macrophages. *Infect. Immun.* **75**, 653-665 (2007).

60. Qu, C. *et al.* Role of CCR8 and other chemokine pathways in the migration of monocyte-derived dendritic cells to lymph nodes. *J. Exp. Med.* **200**, 1231-1241 (2004).

61. Merad, M. *et al.* Langerhans cells renew in the skin throughout life under steady-state conditions. *Nat. Immunol.* **3**, 1135-1141 (2002).

62. Naito, M., Hasegawa, G. & Takahashi, K. Development, differentiation, and maturation of Kupffer cells. *Microsc. Res. Tech.* **39**, 350-364 (1997).

63. MACKANESS, G. B. THE IMMUNOLOGICAL BASIS OF ACQUIRED CELLULAR RESISTANCE. *J. Exp. Med.* **120**, 105-120 (1964).

64. Nathan, C. Mechanisms and modulation of macrophage activation. *Behring Inst. Mitt.* 200-207 (1991).

65. Mosser, D. M. The many faces of macrophage activation. *J. Leukoc. Biol.* **73**, 209-212 (2003).

66. Ma, Y. & Pope, R. M. The role of macrophages in rheumatoid arthritis. *Curr. Pharm. Des* **11**, 569-580 (2005).

67. Barnett, M. H., Henderson, A. P. & Prineas, J. W. The macrophage in MS: just a scavenger after all? Pathology and pathogenesis of the acute MS lesion. *Mult. Scler.* **12**, 121-132 (2006).

68. Grip, O., Janciauskiene, S. & Lindgren, S. Macrophages in inflammatory bowel disease. *Curr. Drug Targets. Inflamm. Allergy* **2**, 155-160 (2003).

69. Stein, M., Keshav, S., Harris, N. & Gordon, S. Interleukin 4 potently enhances murine macrophage mannose receptor activity: a marker of alternative immunologic macrophage activation. *J. Exp. Med.* **176**, 287-292 (1992).

70. Doyle, A. G. *et al.* Interleukin-13 alters the activation state of murine macrophages in vitro: comparison with interleukin-4 and interferon-gamma. *Eur. J. Immunol.* **24**, 1441-1445 (1994).

71. Pesce, J. *et al.* The IL-21 receptor augments Th2 effector function and alternative macrophage activation. *J. Clin. Invest* **116**, 2044-2055 (2006).

72. Herbert, D. R. *et al.* Alternative macrophage activation is essential for survival during schistosomiasis and downmodulates T helper 1 responses and immunopathology. *Immunity.* **20**, 623-635 (2004).

73. Anthony, R. M. *et al.* Memory T(H)2 cells induce alternatively activated macrophages to mediate protection against nematode parasites. *Nat. Med.* **12**, 955-960 (2006).

74. Reece, J. J., Siracusa, M. C. & Scott, A. L. Innate immune responses to lung-stage helminth infection induce alternatively activated alveolar macrophages. *Infect. Immun.* **74**, 4970-4981 (2006).

75. Rodriguez-Sosa, M. *et al.* Chronic helminth infection induces alternatively activated macrophages expressing high levels of CCR5 with low interleukin-12 production and Th2-biasing ability. *Infect. Immun.* **70**, 3656-3664 (2002).

76. Dzik, J. M., Golos, B., Jagielska, E., Zielinski, Z. & Walajtys-Rode, E. A non-classical type of alveolar macrophage response to Trichinella spiralis infection. *Parasite Immunol.* **26**, 197-205 (2004).

77. Donnelly, S., O'Neill, S. M., Sekiya, M., Mulcahy, G. & Dalton, J. P. Thioredoxin peroxidase secreted by Fasciola hepatica induces the alternative activation of macrophages. *Infect. Immun.* **73**, 166-173 (2005).

78. Oshiro, T. M., Macedo, M. S. & edo-Soares, M. F. Anti-inflammatory activity of PAS-1, a protein component of Ascaris suum. *Inflamm. Res.* **54**, 17-21 (2005).

79. Noel, W. *et al.* Infection stage-dependent modulation of macrophage activation in Trypanosoma congolense-resistant and -susceptible mice. *Infect. Immun.* **70**, 6180-6187 (2002).

80. Gordon, S. Alternative activation of macrophages. *Nat. Rev. Immunol.* **3**, 23-35 (2003).

81. Taylor, M. D., Harris, A., Nair, M. G., Maizels, R. M. & Allen, J. E. F4/80+ alternatively activated macrophages control CD4+ T cell hyporesponsiveness at sites peripheral to filarial infection. *J. Immunol.* **176**, 6918-6927 (2006).

82. Liang, S. C. *et al.* Regulation of PD-1, PD-L1, and PD-L2 expression during normal and autoimmune responses. *Eur. J. Immunol.* **33**, 2706-2716 (2003).

83. Wang, Y. *et al.* Ex vivo programmed macrophages ameliorate experimental chronic inflammatory renal disease. *Kidney Int.* **72**, 290-299 (2007).

84. Ponomarev, E. D., Maresz, K., Tan, Y. & Dittel, B. N. CNS-derived interleukin-4 is essential for the regulation of autoimmune inflammation and induces a state of alternative activation in microglial cells. *J. Neurosci.* **27**, 10714-10721 (2007).

85. Lumeng, C. N., Bodzin, J. L. & Saltiel, A. R. Obesity induces a phenotypic switch in adipose tissue macrophage polarization. *J. Clin. Invest* **117**, 175-184 (2007).

86. Kreider, T., Anthony, R. M., Urban, J. F., Jr. & Gause, W. C. Alternatively activated macrophages in helminth infections. *Curr. Opin. Immunol.* **19**, 448-453 (2007).

87. Muller, U. *et al.* IL-13 induces disease-promoting type 2 cytokines, alternatively activated macrophages and allergic inflammation during pulmonary infection of mice with Cryptococcus neoformans. *J. Immunol.* **179**, 5367-5377 (2007).

88. Weng, M. *et al.* Alternatively activated macrophages in intestinal helminth infection: effects on concurrent bacterial colitis. *J. Immunol.* **179**, 4721-4731 (2007).

89. Sutterwala, F. S. & Mosser, D. M. The taming of IL-12: suppressing the production of proinflammatory cytokines. *J. Leukoc. Biol.* **65**, 543-551 (1999).

90. Gerber, J. S. & Mosser, D. M. Reversing lipopolysaccharide toxicity by ligating the macrophage Fc gamma receptors. *J. Immunol.* **166**, 6861-6868 (2001).

91. Anderson, C. F. & Mosser, D. M. Cutting edge: biasing immune responses by directing antigen to macrophage Fc gamma receptors. *J. Immunol.* **168**, 3697-3701 (2002).

92. Anderson, C. F. & Mosser, D. M. A novel phenotype for an activated macrophage: the type 2 activated macrophage. *J. Leukoc. Biol.* **72**, 101-106 (2002).

93. Powell, M. J., Thompson, S. A., Tone, Y., Waldmann, H. & Tone, M. Posttranscriptional regulation of IL-10 gene expression through sequences in the 3'-untranslated region. *J. Immunol.* **165**, 292-296 (2000).

94. Brightbill, H. D., Plevy, S. E., Modlin, R. L. & Smale, S. T. A prominent role for Sp1 during lipopolysaccharide-mediated induction of the IL-10 promoter in macrophages. *J. Immunol.* **164**, 1940-1951 (2000).

95. Liu, Y. W., Tseng, H. P., Chen, L. C., Chen, B. K. & Chang, W. C. Functional cooperation of simian virus 40 promoter factor 1 and CCAAT/enhancer-binding protein beta and delta in lipopolysaccharide-induced gene activation of IL-10 in mouse macrophages. *J. Immunol.* **171**, 821-828 (2003).

96. Platzer, C., Meisel, C., Vogt, K., Platzer, M. & Volk, H. D. Up-regulation of monocytic IL-10 by tumor necrosis factor-alpha and cAMP elevating drugs. *Int. Immunol.* **7**, 517-523 (1995).

97. Benkhart, E. M., Siedlar, M., Wedel, A., Werner, T. & Ziegler-Heitbrock, H. W. Role of Stat3 in lipopolysaccharide-induced IL-10 gene expression. *J. Immunol.* **165**, 1612-1617 (2000).

98. Cao, S. *et al.* Differential regulation of IL-12 and IL-10 gene expression in macrophages by the basic leucine zipper transcription factor c-Maf fibrosarcoma. *J. Immunol.* **169**, 5715-5725 (2002).

99. Cao, S., Liu, J., Song, L. & Ma, X. The protooncogene c-Maf is an essential transcription factor for IL-10 gene expression in macrophages. *J. Immunol.* **174**, 3484-3492 (2005).

100. Ziegler-Heitbrock, L. *et al.* IFN-alpha induces the human IL-10 gene by recruiting both IFN regulatory factor 1 and Stat3. *J. Immunol.* **171**, 285-290 (2003).

101. Cao, S., Zhang, X., Edwards, J. P. & Mosser, D. M. NF-kappaB1 (p50) homodimers differentially regulate pro- and anti-inflammatory cytokines in macrophages. *J. Biol. Chem.* **281**, 26041-26050 (2006).

102. Jackson, S. P., MacDonald, J. J., Lees-Miller, S. & Tjian, R. GC box binding induces phosphorylation of Sp1 by a DNA-dependent protein kinase. *Cell* **63**, 155-165 (1990).

103. Ma, W. *et al.* The p38 mitogen-activated kinase pathway regulates the human interleukin-10 promoter via the activation of Sp1 transcription factor in lipopolysaccharide-stimulated human macrophages. *J. Biol. Chem.* **276**, 13664-13674 (2001).

104. Staples, K. J. *et al.* IL-10 induces IL-10 in primary human monocyte-derived macrophages via the transcription factor Stat3. *J. Immunol.* **178**, 4779-4785 (2007).

105. Zhang, X., Edwards, J. P. & Mosser, D. M. Dynamic and transient remodeling of the macrophage IL-10 promoter during transcription. *J. Immunol.* **177**, 1282-1288 (2006).

106. Lucas, M., Zhang, X., Prasanna, V. & Mosser, D. M. ERK activation following macrophage FcgammaR ligation leads to chromatin modifications at the IL-10 locus. *J. Immunol.* **175**, 469-477 (2005).

107. Matsukawa, A. *et al.* Aberrant inflammation and lethality to septic peritonitis in mice lacking STAT3 in macrophages and neutrophils. *J. Immunol.* **171**, 6198-6205 (2003).

108. Mori, N. & Prager, D. Activation of the interleukin-10 gene in the human T lymphoma line HuT 78: identification and characterization of NF-kappa B binding sites in the regulatory region of the interleukin-10 gene. *Eur. J. Haematol.* **59**, 162-170 (1997).

109. Shoemaker, J., Saraiva, M. & O'Garra, A. GATA-3 directly remodels the IL-10 locus independently of IL-4 in CD4+ T cells. *J. Immunol.* **176**, 3470-3479 (2006).

110. Im, S. H., Hueber, A., Monticelli, S., Kang, K. H. & Rao, A. Chromatin-level regulation of the IL10 gene in T cells. *J. Biol. Chem.* **279**, 46818-46825 (2004).

111. Clayton, A. L. & Mahadevan, L. C. MAP kinase-mediated phosphoacetylation of histone H3 and inducible gene regulation. *FEBS Lett.* **546**, 51-58 (2003).

112. Roux, P. P. & Blenis, J. ERK and p38 MAPK-activated protein kinases: a family of protein kinases with diverse biological functions. *Microbiol. Mol. Biol. Rev.* **68**, 320-344 (2004).

113. Sassone-Corsi, P. *et al.* Requirement of Rsk-2 for epidermal growth factor-activated phosphorylation of histone H3. *Science* **285**, 886-891 (1999).

114. Thomson, S. *et al.* The nucleosomal response associated with immediate-early gene induction is mediated via alternative MAP kinase cascades: MSK1 as a potential histone H3/HMG-14 kinase. *EMBO J.* **18**, 4779-4793 (1999).

115. Soloaga, A. *et al.* MSK2 and MSK1 mediate the mitogen- and stress-induced phosphorylation of histone H3 and HMG-14. *EMBO J.* **22**, 2788-2797 (2003).

116. Higashiyama, S., Abraham, J. A., Miller, J., Fiddes, J. C. & Klagsbrun, M. A heparin-binding growth factor secreted by macrophage-like cells that is related to EGF. *Science* **251**, 936-939 (1991).

117. Yang, Z., Mosser, D. M. & Zhang, X. Activation of the MAPK, ERK, following Leishmania amazonensis infection of macrophages. *J. Immunol.* **178**, 1077-1085 (2007).

118. Naglich, J. G., Metherall, J. E., Russell, D. W. & Eidels, L. Expression cloning of a diphtheria toxin receptor: identity with a heparin-binding EGF-like growth factor precursor. *Cell* **69**, 1051-1061 (1992).

119. Nishi, E. & Klagsbrun, M. Heparin-binding epidermal growth factor-like growth factor (HB-EGF) is a mediator of multiple physiological and pathological pathways. *Growth Factors* **22**, 253-260 (2004).

120. Nishi, E., Hiraoka, Y., Yoshida, K., Okawa, K. & Kita, T. Nardilysin enhances ectodomain shedding of heparin-binding epidermal growth factor-like growth factor through activation of tumor necrosis factor-alpha-converting enzyme. *J. Biol. Chem.* **281**, 31164-31172 (2006).

121. Nanba, D., Mammoto, A., Hashimoto, K. & Higashiyama, S. Proteolytic release of the carboxy-terminal fragment of proHB-EGF causes nuclear export of PLZF. *J. Cell Biol.* **163**, 489-502 (2003).

122. Kinugasa, Y., Hieda, M., Hori, M. & Higashiyama, S. The carboxyl-terminal fragment of pro-HB-EGF reverses Bcl6-mediated gene repression. *J. Biol. Chem.* **282**, 14797-14806 (2007).

123. Elenius, K., Paul, S., Allison, G., Sun, J. & Klagsbrun, M. Activation of HER4 by heparin-binding EGF-like growth factor stimulates chemotaxis but not proliferation. *EMBO J.* **16**, 1268-1278 (1997).

124. Iwamoto, R. *et al.* Heparin-binding EGF-like growth factor and ErbB signaling is essential for heart function. *Proc. Natl. Acad. Sci. U. S. A* **100**, 3221-3226 (2003).

125. Mine, N., Iwamoto, R. & Mekada, E. HB-EGF promotes epithelial cell migration in eyelid development. *Development* **132**, 4317-4326 (2005).

126. Shirakata, Y. *et al.* Heparin-binding EGF-like growth factor accelerates keratinocyte migration and skin wound healing. *J. Cell Sci.* **118**, 2363-2370 (2005).

127. Miyagawa, J. *et al.* Localization of heparin-binding EGF-like growth factor in the smooth muscle cells and macrophages of human atherosclerotic plaques. *J. Clin. Invest* **95**, 404-411 (1995).

128. Peoples, G. E. *et al.* T lymphocytes that infiltrate tumors and atherosclerotic plaques produce heparin-binding epidermal growth factor-like growth factor and basic fibroblast growth factor: a potential pathologic role. *Proc. Natl. Acad. Sci. U. S. A* **92**, 6547-6551 (1995).

129. Ouchi, N. *et al.* Role of membrane-anchored heparin-binding epidermal growth factor-like growth factor and CD9 on macrophages. *Biochem. J.* **328 (Pt 3)**, 923-928 (1997).

130. Ongusaha, P. P. *et al.* HB-EGF is a potent inducer of tumor growth and angiogenesis. *Cancer Res.* **64**, 5283-5290 (2004).

131. Mehta, V. B. & Besner, G. E. HB-EGF promotes angiogenesis in endothelial cells via PI3-kinase and MAPK signaling pathways. *Growth Factors* **25**, 253-263 (2007).

132. Tanaka, Y. *et al.* Clinical significance of heparin-binding epidermal growth factor-like growth factor and a disintegrin and metalloprotease 17 expression in human ovarian cancer. *Clin. Cancer Res.* **11**, 4783-4792 (2005).

133. Miyamoto, S., Yagi, H., Yotsumoto, F., Kawarabayashi, T. & Mekada, E. Heparin-binding epidermal growth factor-like growth factor as a novel targeting molecule for cancer therapy. *Cancer Sci.* **97**, 341-347 (2006).

134. Vinante, F., Rigo, A., Papini, E., Cassatella, M. A. & Pizzolo, G. Heparin-binding epidermal growth factor-like growth factor/diphtheria toxin receptor expression by acute myeloid leukemia cells. *Blood* **93**, 1715-1723 (1999).

135. Wang, F. *et al.* Heparin-binding EGF-like growth factor is an early response gene to chemotherapy and contributes to chemotherapy resistance. *Oncogene* **26**, 2006-2016 (2007).

136. Cheng, K., Xie, G. & Raufman, J. P. Matrix metalloproteinase-7-catalyzed release of HB-EGF mediates deoxycholyltaurine-induced proliferation of a human colon cancer cell line. *Biochem. Pharmacol.* **73**, 1001-1012 (2007).

137. Sorensen, B. S., Ornskov, D. & Nexo, E. The chemotherapeutic agent VP16 increases the stability of HB-EGF mRNA by a mechanism involving the 3'-UTR. *Exp. Cell Res.* **312**, 3651-3658 (2006).

138. Ornskov, D., Nexo, E. & Sorensen, B. S. Insulin induces a transcriptional activation of epiregulin, HB-EGF and amphiregulin, by a PI3K-dependent mechanism: identification of a specific insulin-responsive promoter element. *Biochem. Biophys. Res. Commun.* **354**, 885-891 (2007).

139. Ellis, P. D., Hadfield, K. M., Pascall, J. C. & Brown, K. D. Heparin-binding epidermal-growth-factor-like growth factor gene expression is induced by scrape-

wounding epithelial cell monolayers: involvement of mitogen-activated protein kinase cascades. *Biochem. J.* **354**, 99-106 (2001).

140. McCarthy, S. A. *et al.* Rapid phosphorylation of Ets-2 accompanies mitogen-activated protein kinase activation and the induction of heparin-binding epidermal growth factor gene expression by oncogenic Raf-1. *Mol. Cell Biol.* **17**, 2401-2412 (1997).

141. Uesaka, T., Lu, H., Katoh, O. & Watanabe, H. Heparin-binding EGF-like growth factor gene transcription regulated by Cdx2 in the intestinal epithelium. *Am. J. Physiol Gastrointest. Liver Physiol* **283**, G840-G847 (2002).

142. Chen, X. *et al.* Induction of heparin-binding EGF-like growth factor expression during myogenesis. Activation of the gene by MyoD and localization of the transmembrane form of the protein on the myotube surface. *J. Biol. Chem.* **270**, 18285-18294 (1995).

143. Biswas, S. K. *et al.* A distinct and unique transcriptional program expressed by tumor-associated macrophages (defective NF-kappaB and enhanced IRF-3/STAT1 activation). *Blood* **107**, 2112-2122 (2006).

144. Saccani, A. *et al.* p50 nuclear factor-kappaB overexpression in tumor-associated macrophages inhibits M1 inflammatory responses and antitumor resistance. *Cancer Res.* **66**, 11432-11440 (2006).

145. Lewis, C. E. & Pollard, J. W. Distinct role of macrophages in different tumor microenvironments. *Cancer Res.* **66**, 605-612 (2006).

146. Stuehr, D. J. & Nathan, C. F. Nitric oxide. A macrophage product responsible for cytostasis and respiratory inhibition in tumor target cells. *J. Exp. Med.* **169**, 1543-1555 (1989).

147. Corraliza, I. M., Campo, M. L., Soler, G. & Modolell, M. Determination of arginase activity in macrophages: a micromethod. *J. Immunol. Methods* **174**, 231-235 (1994).

148. Skeen, M. J., Miller, M. A., Shinnick, T. M. & Ziegler, H. K. Regulation of murine macrophage IL-12 production. Activation of macrophages in vivo, restimulation in vitro, and modulation by other cytokines. *J. Immunol.* **156**, 1196-1206 (1996).

149. Schebesch, C. *et al.* Alternatively activated macrophages actively inhibit proliferation of peripheral blood lymphocytes and CD4+ T cells in vitro. *Immunology* **92**, 478-486 (1997).

150. Kambayashi, T., Jacob, C. O. & Strassmann, G. IL-4 and IL-13 modulate IL-10 release in endotoxin-stimulated murine peritoneal mononuclear phagocytes. *Cell Immunol.* **171**, 153-158 (1996).

151. Stout, R. D. *et al.* Macrophages sequentially change their functional phenotype in response to changes in microenvironmental influences. *J. Immunol.* **175**, 342-349 (2005).

152. Modolell, M., Corraliza, I. M., Link, F., Soler, G. & Eichmann, K. Reciprocal regulation of the nitric oxide synthase/arginase balance in mouse bone marrow-

derived macrophages by TH1 and TH2 cytokines. *Eur. J. Immunol.* **25**, 1101-1104 (1995).

153. Raes, G. *et al.* FIZZ1 and Ym as tools to discriminate between differentially activated macrophages. *Dev. Immunol.* **9**, 151-159 (2002).

154. Holcomb, I. N. *et al.* FIZZ1, a novel cysteine-rich secreted protein associated with pulmonary inflammation, defines a new gene family. *EMBO J.* **19**, 4046-4055 (2000).

155. Kohama, T. *et al.* Molecular cloning and functional characterization of murine sphingosine kinase. *J. Biol. Chem.* **273**, 23722-23728 (1998).

156. Kihara, A., Anada, Y. & Igarashi, Y. Mouse sphingosine kinase isoforms SPHK1a and SPHK1b differ in enzymatic traits including stability, localization, modification, and oligomerization. *J. Biol. Chem.* **281**, 4532-4539 (2006).

157. Wu, W., Mosteller, R. D. & Broek, D. Sphingosine kinase protects lipopolysaccharide-activated macrophages from apoptosis. *Mol. Cell Biol.* **24**, 7359-7369 (2004).

158. Chao, C. C., Jensen, R. & Dailey, M. O. Mechanisms of L-selectin regulation by activated T cells. *The Journal of Immunology* **159**, 1686-1694 (1997).

159. Lowenthal, J. W., Zubler, R. H., Nabholz, M. & MacDonald, H. R. Similarities between interleukin-2 receptor number and affinity on activated B and T lymphocytes. *Nature* **315**, 669-672 (1985).

160. Yokoyama, W. M. *et al.* Characterization of a cell surface-expressed disulfide-linked dimer involved in murine T cell activation. *J. Immunol.* **141**, 369-376 (1988).

161. Raes, G. *et al.* Differential expression of FIZZ1 and Ym1 in alternatively versus classically activated macrophages. *J. Leukoc. Biol.* **71**, 597-602 (2002).

162. Nair, M. G. *et al.* Chitinase and Fizz family members are a generalized feature of nematode infection with selective upregulation of Ym1 and Fizz1 by antigen-presenting cells. *Infect. Immun.* **73**, 385-394 (2005).

163. Gratchev, A. *et al.* Alternatively activated macrophages differentially express fibronectin and its splice variants and the extracellular matrix protein betaIG-H3. *Scand. J. Immunol.* **53**, 386-392 (2001).

164. Kodelja, V. *et al.* Alternative macrophage activation-associated CC-chemokine-1, a novel structural homologue of macrophage inflammatory protein-1 alpha with a Th2-associated expression pattern. *J. Immunol.* **160**, 1411-1418 (1998).

165. Willment, J. A. *et al.* Dectin-1 expression and function are enhanced on alternatively activated and GM-CSF-treated macrophages and are negatively regulated by IL-10, dexamethasone, and lipopolysaccharide. *J. Immunol.* **171**, 4569-4573 (2003).

166. Albina, J. E., Mills, C. D., Henry, W. L., Jr. & Caldwell, M. D. Temporal expression of different pathways of l-arginine metabolism in healing wounds. *J. Immunol.* **144**, 3877-3880 (1990).

167. Scotton, C. J. *et al.* Transcriptional profiling reveals complex regulation of the monocyte IL-1 beta system by IL-13. *J. Immunol.* **174**, 834-845 (2005).

168. Brys, L. *et al.* Reactive oxygen species and 12/15-lipoxygenase contribute to the antiproliferative capacity of alternatively activated myeloid cells elicited during helminth infection. *J. Immunol.* **174**, 6095-6104 (2005).

169. Tamada, K. *et al.* LIGHT, a TNF-like molecule, costimulates T cell proliferation and is required for dendritic cell-mediated allogeneic T cell response. *J. Immunol.* **164**, 4105-4110 (2000).

170. Kwon, B. S. *et al.* A newly identified member of the tumor necrosis factor receptor superfamily with a wide tissue distribution and involvement in lymphocyte activation. *J. Biol. Chem.* **272**, 14272-14276 (1997).

171. Shi, G. *et al.* Mouse T cells receive costimulatory signals from LIGHT, a TNF family member. *Blood* **100**, 3279-3286 (2002).

172. Wan, X. *et al.* A TNF family member LIGHT transduces costimulatory signals into human T cells. *J. Immunol.* **169**, 6813-6821 (2002).

173. Melendez, A. J. & Ibrahim, F. B. Antisense knockdown of sphingosine kinase 1 in human macrophages inhibits C5a receptor-dependent signal transduction, Ca2+ signals, enzyme release, cytokine production, and chemotaxis. *J. Immunol.* **173**, 1596-1603 (2004).

174. Yang, J. *et al.* Sphingosine kinase 1 is a negative regulator of CD4+ Th1 cells. *J. Immunol.* **175**, 6580-6588 (2005).

175. Edwards, J. P., Zhang, X., Frauwirth, K. A. & Mosser, D. M. Biochemical and functional characterization of three activated macrophage populations. *J. Leukoc. Biol.* **80**, 1298-1307 (2006).

176. no, M., Raab, G., Lau, K., Abraham, J. A. & Klagsbrun, M. Purification and characterization of transmembrane forms of heparin-binding EGF-like growth factor. *J. Biol. Chem.* **269**, 31315-31321 (1994).

177. Matys, V. *et al.* TRANSFAC and its module TRANSCompel: transcriptional gene regulation in eukaryotes. *Nucleic Acids Res.* **34**, D108-D110 (2006).

178. Zhou, L., Nazarian, A. A. & Smale, S. T. Interleukin-10 inhibits interleukin-12 p40 gene transcription by targeting a late event in the activation pathway. *Mol. Cell Biol.* **24**, 2385-2396 (2004).

179. Sica, A. *et al.* Autocrine production of IL-10 mediates defective IL-12 production and NF-kappa B activation in tumor-associated macrophages. *J. Immunol.* **164**, 762-767 (2000).

180. Strassmann, G., Patil-Koota, V., Finkelman, F., Fong, M. & Kambayashi, T. Evidence for the involvement of interleukin 10 in the differential deactivation of murine peritoneal macrophages by prostaglandin E2. *J. Exp. Med.* **180**, 2365-2370 (1994).

181. Leemhuis, J., Boutillier, S., Schmidt, G. & Meyer, D. K. The protein kinase A inhibitor H89 acts on cell morphology by inhibiting Rho kinase. *J. Pharmacol. Exp. Ther.* **300**, 1000-1007 (2002).

182. Wiggin, G. R. *et al.* MSK1 and MSK2 are required for the mitogen- and stress-induced phosphorylation of CREB and ATF1 in fibroblasts. *Mol. Cell Biol.* **22**, 2871-2881 (2002).

183. Hetzer, C. *et al.* Recruitment and activation of RSK2 by HIV-1 Tat. *PLoS. ONE.* **2**, e151 (2007).

184. Li, J. C. & Lau, A. S. A role for mitogen-activated protein kinase and Ets-1 in the induction of interleukin-10 transcription by human immunodeficiency virus-1 Tat. *Immunology* **121**, 337-348 (2007).

185. Zaru, R., Ronkina, N., Gaestel, M., Arthur, J. S. & Watts, C. The MAPK-activated kinase Rsk controls an acute Toll-like receptor signaling response in dendritic cells and is activated through two distinct pathways. *Nat. Immunol.* **8**, 1227-1235 (2007).